Report No. FAA/RD-76/86

STEERABLE BEAM ARRAY ANTENNA FOR USE IN ATS-6 TEST PROGRAM

G.G. Sanford

Ball Brothers Research Corporation
P O Box 1062
Boulder Colorado 80302

AD A030661

DDC
OCT 13 1976

MAY 1976

Final Report

DOCUMENT IS AVAILABLE TO THE PUBLIC THROUGH THE NATIONAL TECHNICAL INFORMATION SERVICE, SPRINGFIELD, VIRGINIA 22161

U.S. DEPARTMENT OF TRANSPORTATION
FEDERAL AVIATION ADMINISTRATION
Systems Research and Development Service
Washington DC 20591

NOTICE

This document is disseminated under the sponsorship of the Department of Transportation in the interest of information exchange. The United States Government assumes no liability for its contents or use thereof.

NOTICE

The United States Government does not endorse products or manufacturers. Trade or manufacturers' names appear herein solely because they are considered essential to the object of this report.

(18) FAA/RD, (19) 76/86, FAA-76-12

Technical Report Documentation Page

1. Report No. FAA/RD - 76/86	2. Government Accession No.	3. Recipient's Catalog No.
4. Title and Subtitle (6) STEERABLE BEAM ARRAY ANTENNA FOR USE IN ATS-6 TEST PROGRAM		5. Report Date (11) May 1976
		6. Performing Organization Code (12) 139p.
7. Author(s) (10) G. G. Sanford		8. Performing Organization Report No. DOT-TSC-FAA-76-12
9. Performing Organization Name and Address Ball Brothers Research Corporation* P O Box 1062 Boulder CO 80302		10. Work Unit No. (TRAIS) FA511/R6129
		11. Contract or Grant No. (15) DOT-TSC-763 new
12. Sponsoring Agency Name and Address U. S. Department of Transportation Federal Aviation Administration Systems Research and Development Service Washington DC 20591		13. Type of Report and Period Covered (9) Final Report ~~Feb. 1974/May 1976~~ Feb 74 - May 76
		14. Sponsoring Agency Code

15. Supplementary Notes *Under Contract To: U. S. Department of Transportation Transportation Systems Center Kendall Square Cambridge MA 02142

16. Abstract

The design and development of an advanced L-Band microstrip phased array antenna for aircraft is described. The array is:

Electronically steerable in elevation
Conformal to the surface of an aircraft
0.20 inch thick
Low cost fabrication technique
Installed without cutting large holes in the aircraft
Capable of 12 dB gain relative to a right hand circular isotope

The development of the microstrip radiator, array configuration, diode phase shifter and the antenna control unit is described. The array design is considered in relation to the ground plane curvature, grating lobes, side lobes, beam shape and gain. Radiation pattern measurements of the full size antenna and scale model antennas on a scale model aircraft are presented. The design of simple loaded line and switched line phase shifters is reported. In addition, preliminary flight test performed from the ATS-6 satellite test program is presented.

17. Key Words Phased array, conformal array antenna, aircraft antenna, microstrip antenna, diode phase shifter, scale model testing, L-Band, satellite communicative, AEROSAT	18. Distribution Statement Document is available to the public through the National Technical Information Service, Springfield, Virginia 22161

19. Security Classif. (of this report)	20. Security Classif. (of this page)	21. No. of Pages	22. Price
Unclassified	Unclassified	142	

Form DOT F 1700.7 (8-72) Reproduction of completed page authorized

050 550

PREFACE

The design and fabrication of an eight-element phased array antenna was conducted as part of the international ATS-6 L-Band Experiment. The antenna provided conformal mounting to the exterior surface of a FAA KC-135 aircraft. The radiation pattern of the antenna was nominally 15-degree elevation by 80-degree azimuth. The radiation pattern could be electroni ally steered in elevation through nine beam positions. The angle of the radiation (beam position) is controlled by a control box inside the aircraft. The controller can be programed for a fixed beam or for time scanning of the antenna to track the satellite. Final flight testing of the antenna was accomplished on an FAA KC-135 under coordination of Federal Aviation Administration/ National Aviation Facilities Experimental Center (NAFEC).

This antenna program was conducted by DOT/Transportation Systems Center supported by Ball Brothers Research Corporation under contract DOT-TSC-763.

The principal DOT/TSC contributing personnel are L. Klein and R. Bland.

The antenna was installed at the FAA Center Oklahoma City with the assistance provided by FAA supervisors Jerry Searcy and Bob Greybill.

The KC-135 flight operations were managed by Mr. Francis W. Jefferson who also provided auxiliary support at the FAA/National Aviation Facilities Experimental Center, Atlantic City, New Jersey.

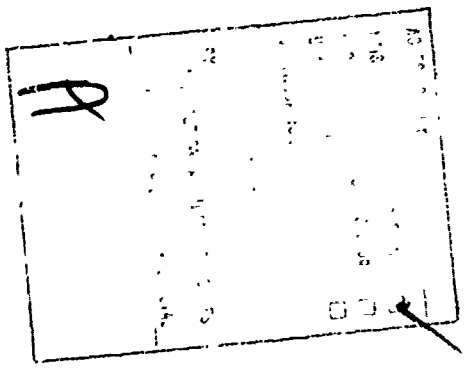

METRIC CONVERSION FACTORS

Approximate Conversions to Metric Measures

Symbol	When You Know	Multiply by	To Find	Symbol
		LENGTH		
in	inches	*2.5	centimeters	cm
ft	feet	30	centimeters	cm
yd	yards	0.9	meters	m
mi	miles	1.6	kilometers	km
		AREA		
in^2	square inches	6.5	square centimeters	cm^2
ft^2	square feet	0.09	square meters	m^2
yd^2	square yards	0.8	square meters	m^2
mi^2	square miles	2.6	square kilometers	km^2
	acres	0.4	hectares	ha
		MASS (weight)		
oz	ounces	28	grams	g
lb	pounds	0.45	kilograms	kg
	short tons (2000 lb)	0.9	tonnes	t
		VOLUME		
tsp	teaspoons	5	milliliters	ml
Tbsp	tablespoons	15	milliliters	ml
fl oz	fluid ounces	30	milliliters	ml
c	cups	0.24	liters	l
pt	pints	0.47	liters	l
qt	quarts	0.95	liters	l
gal	gallons	3.8	liters	l
ft^3	cubic feet	0.03	cubic meters	m^3
yd^3	cubic yards	0.76	cubic meters	m^3
		TEMPERATURE (exact)		
°F	Fahrenheit temperature	5/9 (after subtracting 32)	Celsius temperature	°C

*1 in = 2.54 (exactly). For other exact conversions and more detailed tables, see NBS Misc. Publ. 286, Units of Weights and Measures, Price $2.25, SD Catalog No. C13.10:286

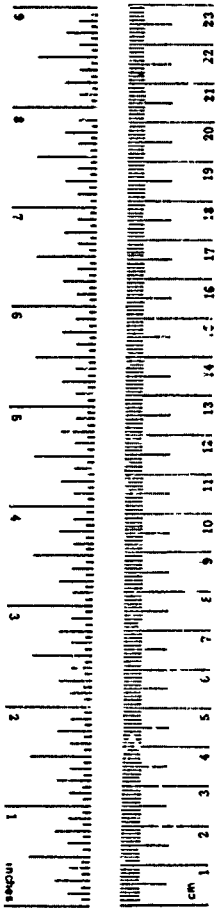

Approximate Conversions from Metric Measures

Symbol	When You Know	Multiply by	To Find	Symbol
		LENGTH		
mm	millimeters	0.04	inches	in
cm	centimeters	0.4	inches	in
m	meters	3.3	feet	ft
m	meters	1.1	yards	yd
km	kilometers	0.6	miles	mi
		AREA		
cm^2	square centimeters	0.16	square inches	in^2
m^2	square meters	1.2	square yards	yd^2
km^2	square kilometers	0.4	square miles	mi^2
ha	hectares (10,000 m^2)	2.5	acres	
		MASS (weight)		
g	grams	0.035	ounces	oz
kg	kilograms	2.2	pounds	lb
t	tonnes (1000 kg)	1.1	short tons	
		VOLUME		
ml	milliliters	0.03	fluid ounces	fl oz
l	liters	2.1	pints	pt
l	liters	1.06	quarts	qt
l	liters	0.26	gallons	gal
m^3	cubic meters	35	cubic feet	ft^3
m^3	cubic meters	1.3	cubic yards	yd^3
		TEMPERATURE (exact)		
°C	Celsius temperature	9/5 (then add 32)	Fahrenheit temperature	°F

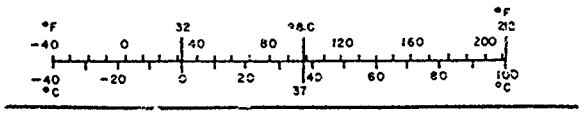

TABLE OF CONTENTS

Section			Page
	SUMMARY		x
1	GENERAL SYSTEM DESCRIPTION		1-1
	1.1	System Function	1-1
	1.2	System Design Approach	1-3
	1.3	System Analysis	1-7
2	MICROSTRIP RADIATING ELEMENT		2-1
3	ARRAY DESIGN AND FABRICATION		3-1
	3.1	Physical Description	3-1
	3.2	Electrical Design	3-4
	3.3	Fabrication and Assembly	3-14
4	ARRAY CONTROLLER DESIGN AND CONSTRUCTION		4-1
	4.1	Physical Description	4-1
	4.2	Functional Description	4-1
	4.3	Controller Operating Procedure	4-3
5	LABORATORY SYSTEMS TESTS		5-1
	5.1	Performance Tests - Full Scale Array	5-1
	5.2	Environmental Test Program	5-52
	5.3	Scale Model Testing	5-58
6	FIELD INSTALLATION		6-1
7	REFERENCES		7-1

APPENDIXES

Appendix		Page
A	CONFORMAL MICROSTRIP AIRBORNE PHASED ARRAY TEST	A-1
B	REPORT OF INVENTIONS	B-1

LIST OF TABLES

Table		Page
3-1	EFFECTIVE THIRTY-DEGREE PHASE RESOLUTION USING THREE BIT PHASE SHIFTERS	3-11
4-1	CONTROLLER READOUT FOR BEAM POSITIONS	4-14
5-1	FULL SCALE PATTERN TESTS	5-2
5-2	VIBRATION TEST FOR STEERABLE ARRAY ANTENNA	5-54
5-3	VIBRATION TEST FOR STEERABLE ARRAY CONTROLLER	5-54
A-1	JANUARY 1975 ANTENNA FLIGHT TEST SUMMARY	A-3
A-2	ANTENNA TEST DATA DERIVED FROM REAL-TIME MEASUREMENTS	A-6
A-3	COMPUTER ANALYZED ANTENNA TEST DATA	A-7

LIST OF ILLUSTRATIONS

Figure		Page
S-1	Project Schedule	xii
1-1	Steerable Beam Antenna Test Flight Installation on KC135A	1-2
1-2	Phased Array Mechanical Design	1-4
1-3	Phased Array Installation on Aircraft	1-4
1-4	Steerable Beam Antenna Control Unit	1-5
1-5	Antenna Boresight Orientation on Aircraft	1-8
1-6	Elevation Beam Positions	1-9
1-7	Calculated Multipath Rejection	1-10
2-1	Linearly Polarized Microstrip Element	2-2
2-2	Electric Field in Vicinity of Microstrip Element	2-3
2-3	E-Plane Radiation Pattern of Linearly Polarized Microstrip Element	2-3
2-4	Circularly Polarized Element With Two-Point Feed	2-4
2-5	Circularly Polarized Patch Antenna With Quadrature Hybrid Feed	2-4
2-6	Circularly Polarized Element With Single-Point Feed	2-5

List of Illustrations (Continued)

Figure		Page
3-1	First Delivered Phased Array	3-2
3-2	Second Delivered Phased Array	3-2
3-3	Printed Circuit	3-3
3-4	Beam Position Number 1, Calculated Antenna Response	3-7
3-5	Beam Position Number 5, Calculated Antenna Response	3-7
3-6	Beam Position Number 9, Calculated Antenna Response	3-8
3-7	Loaded Line Phase Shifter	3-12
3-8	Switched Line Phase Shifter	3-13
4-1	Steerable Beam Array Antenna	4-2
4-2	Steerable Beam-Array Antenna Controller	4-4
4-3	Schematic Steerable-Beam Array Antenna Controller	4-5
4-4	Schematic Diagram Steerable Beam Array Antenna Control Panel and Power Supply	4-11
4-5	Controller Program Time Line	4-14
4-6	Switching Between Automatic Sequencing and Manual Position	4-15
5-1	Antenna Mounted on 4- x 4-Foot Ground Plane	5-3
5-2	Elevation Pattern Beam Position 1 S/N 001	5-4
5-3	Azimuth Pattern Beam Position 1 S/N 001	5-5
5-4	Azimuth Pattern Beam Position 2 S/N 001	5-6
5-5	Azimuth Pattern Beam Position 2 S/N 001	5-7
5-6	Elevation Pattern Beam Position 3 S/N 001	5-8
5-7	Azimuth Pattern Beam Position 3 S/N 001	5-9
5-8	Elevation Pattern Beam Position 4 S/N 001	5-10
5-9	Azimuth Pattern Beam Position 4 S/N 001	5-11
5-10	Elevation Pattern Beam Position 5 S/N 001	5-12

List of Illustrations (Continued)

Figure		Page
5-11	Azimuth Pattern Beam Position 5 S/N 001	5-13
5-12	Elevation Pattern Beam Position 6 S/N 001	5-14
5-13	Azimuth Pattern Beam Position 6 S/N 001	5-15
5-14	Elevation Pattern Beam Position 7 S/N 001	5-16
5-15	Azimuth Pattern Beam Position 7 S/N 001	5-17
5-16	Elevation Pattern Beam Position 8 S/N 001	5-18
5-17	Azimuth Pattern Beam Position 8 S/N 001	5-19
5-18	Elevation Pattern Beam Position 9 S/N 001	5-20
5-19	Azimuth Pattern Beam Position 9 S/N 001	5-21
5-20	Elevation Pattern Beam Position 1 S/N 002	5-22
5-21	Elevation Pattern Beam Position 2 S/N 002	5-23
5-22	Elevation Pattern Beam Position 3 S/N 002	5-24
5-23	Elevation Pattern Beam Position 4 S/N 002	5-25
5-24	Elevation Pattern Beam Position 5 S/N 002	5-26
5-25	Elevation Pattern Beam Position 6 S/N 002	5-27
5-26	Elevation Pattern Beam Position 7 S/N 002	5-28
5-27	Elevation Pattern Beam Position 8 S/N 002	5-29
5-28	Elevation Pattern Beam Position 9 S/N 002	5-30
5-29	-10° Conical Cut Beam Position 1 S/N 002	5-31
5-30	+0° Conical Cut Beam Position 1 S/N 002	5-32
5-31	+5° Conical Cut Beam Position 1 S/N 002	5-33
5-32	+9° Conical Cut Beam Position 1 S/N 002	5-34
5-33	+15° Conical Cut Beam Position 1 S/N 002	5-35
5-34	+20° Conical Cut Beam Position 1 S/N 002	5-36
5-35	+6° Conical Cut Beam Position 2 S/N 002	5-37
5-36	+19° Conical Cut Beam Position 2 S/N 002	5-38
5-37	+23° Conical Cut Beam Position 2 S/N 002	5-39
5-38	+30° Conical Cut Beam Position 2 S/N 002	5-40
5-39	+35° Conical Cut Beam Position 2 S/N 002	5-41
5-40	+20° Conical Cut Beam Position 4 S/N 002	5-42

List of Illustrations (Continued)

Figure		Page
5-41	+30° Conical Cut Beam Position 4 S/N 002	5-43
5-42	+35° Conical Cut Beam Position 4 S/N 002	5-44
5-43	+38° Conical Cut Beam Position 4 S/N 002	5-45
5-44	+40° Conical Cut Beam Position 4 S/N 002	5-46
5-45	+45° Conical Cut Beam Position 4 S/N 002	5-47
5-46	+55° Conical Cut Beam Position 4 S/N 002	5-48
5-47	Composite Impedance Plot for Nine Beam Positions Antenna S/N 001	5-50
5-48	Composite Impedance Plot for Nine Beam Positions Antenna S/N 002	5-51
5-49	Test Plan of DOT/TSC Steerable Beam Antenna	5-53
5-50	Vibration Levels - Steerable Array Antenna (Group 8, Category A, D-16046)	5-55
5-51	Vibration Levels - Steerable Array Controller (Group 9, Category A, D-16046)	5-56
5-52	Post-environmental Elevation-Pattern Antenna S/N 001 Beam Position 1	5-57
5-53	Completed Model Antennas	5-59
5-54	Coordinate System--1/10-Scale-Model Aircraft--Pattern Tests	5-59
5-55	Tenth-Scale Model on Model Aircraft and Eight-Element Phased-Array Azimuth Pattern Beam Position 1	5-61
5-56	Tenth-Scale Model on Model Aircraft and Eight-Element Phased-Array Elevation Pattern Beam Position 1	5-62
5-57	Tenth Scale Model on Model Aircraft and Eight-Element Phased-Array Elevation Pattern Beam Position 2	5-63
5-58	Tenth-Scale Model on Model Aircraft and Eight-Element Phased-Array Elevation Pattern Beam Position 4	5-64
A-1	KC-135 Antenna Locations	A-2
A-2	Simplified Typical R-F Test Configuration	A-4

SUMMARY

The successful development of an L-band microstrip phased array for aircraft-satellite communications is described. The array has the following characteristics:

Electronically steerable in elevation.

Conformal to the surface of an aircraft.

0.20-inch thick.

Inherently low-cost fabrication method.

Installed without cutting large holes in the aircraft.

Capable of 12 dB gain relative to right-hand circular isotrope.

The phased array system actually includes three components: the antenna unit, a separate control unit and the connecting cables. The antenna is an etched circuit on Teflon fiberglass with a thin dielectric cover. The control unit selects the desired beam positions according to a predetermined schedule and applies the appropriate voltage or current to each PIN diode in the array.

Primarily as a result of multipath considerations, the array was designed in a 1 by 8 configuration mounting circumferentially on the aircraft. Nine different beam positions could be chosen. Microstrip elements were selected for the radiating structures. A dual microstrip feed was designed for each element to provide circular polarization. The array design was considered in relation to ground plane curvature, grating lobes, side lobes, beam shape and gain. A technique for obtaining 30-degree phase resolution from 3-bit phase shifters was developed. Loaded line

and switched line phase shifters were designed with special emphasis on reducing insertion loss.

The control unit was designed for rack mounting in the aircraft. It includes all the logic circuits, timer circuits and drivers to operate the system automatically from take-off to completion of test.

The performance of the array was measured before, during and after environmental testing. A complete set of radiation patterns and impedance data was recorded for all beam positions. Environmental tests included vibration, thermal and rain tests. Tenth scale model tests of selected beam positions were also made using scale models of the array and of a Convair 880 aircraft.

The antenna was installed on the aircraft without difficulty. Minor problems discovered in the control unit after installation were corrected. After installation the array operated over a wide, rapidly changing temperature range during the KC-135 test program which extended over an eight-month period, with no indication of failure or degradation in electrical performance or mechanical integrity.

Figure S-1 shows the project schedule.

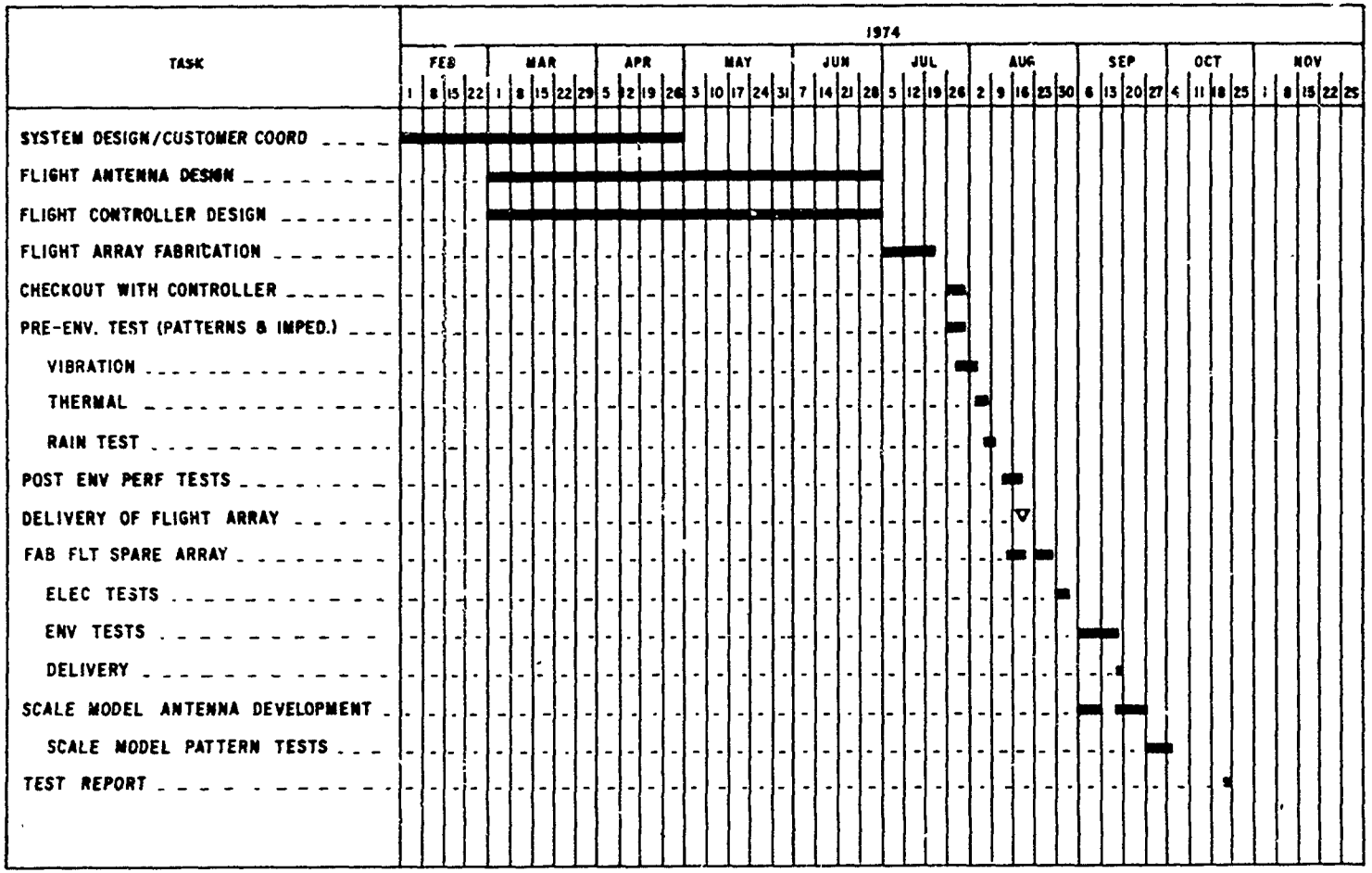

Figure S-1 Project Schedule

1. GENERAL SYSTEM DESCRIPTION

1.1 SYSTEM FUNCTION

One of the primary experiments planned for the ATS-6 satellite was an aircraft location and communication experiment. This was part of an extensive engineering and development effort for a system of geostationary communication satellites to be used by transoceanic commercial aircraft. The system, called Aerosat, will provide reliable high quality communication channels capable of voice, data and independent surveillance transmissions between aircraft and ground.

The U. S. Aeronautical Experiment Program using the ATS-6 Satellite included channel multipath measurements, modem evaluations and antenna tests utilizing aircraft and ships of several countries. Two different antennas were tested and compared. One was a low-gain, wide beam antenna, and the other was a medium-gain, steerable beam phased array. The antennas were mounted on an FAA owned KC135 for the test flights. The antenna tests compared performance in terms of antenna gain, measured by the received carrier to noise density ratio (C/No), and multipath rejection, measured by the received signal to interference ratio (S/I).

The development of an electronically scanned phased array was undertaken for the purposes of the test and to demonstrate the use of advanced technology in making a phased array practical for a commercial application. A single phased array mounted on one side of the aircraft, as shown in Figure 1-1, was determined to be sufficient for the test. A further simplification was the decision to use the antenna in the receive mode only. Therefore, there was no power handling requirement, although it was recognized

that the phased array design approach must be adaptable to high power operation. Similarly, the only bandwidth requirement was the 1543.5 MHz to 1558.5 MHz Aerosat receive band, but the design must be adaptable to operation on both the receive and transmit bands assigned to the satellite-aircraft service.

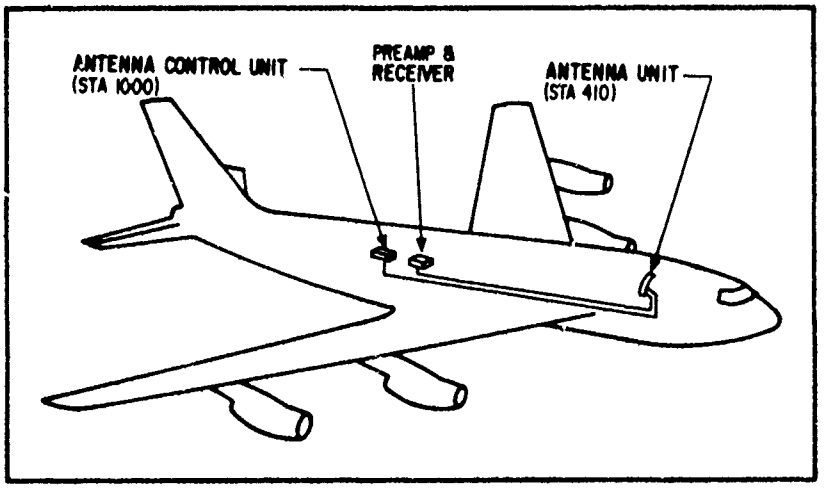

Figure 1-1 Steerable Beam Antenna Test Flight Installation on KC135A

Requirements for the array are listed below:

Operation from 1543.5 to 1558.5 MHz.

VSWR <2:1 referenced to 50 ohms.

Fan shaped beam, narrow in elevation plane and wide in azimuth plane.

Beam steering in the elevation plane.

12 dBi right-hand circular gain.

Right-hand circular polarization with 3 dB maximum axial ratio.

Side lobes minimized in ocean multipath direction.

3-bit digital phase shifter resolution.

Aircraft operation at temperatures between +50°C and -50°C, altitudes to 50,000 feet, humidity to 100 percent relative and vibration levels characteristic of the mounting area.

In order to make the array practical for commercial application it must conform to four qualitative requirements:

Inherently low-cost fabrication.

Void of any significant effect on the aircraft structural or aerodynamic characteristics.

Easy to install and replace on the aircraft.

Inexpensive to operate and maintain.

These requirements have been satisfied in a minimu ost phased array development program which is described in the ollowing paragraphs.

1.2 SYSTEM DESIGN APPROACH

The phased array system concept includes three components: an antenna unit, a separate control unit located within the aircraft and connecting cables. The antenna unit is an all-microstrip design. This means that the microstrip radiating elements, matching networks, phase shifters, distribution lines, power dividers and the dc bias control lines are all etched from the copper laminate on one side of a Teflon fiberglass substrate. This is all accomplished in a single manufacturing step; the assembly is then completed with the installation of connectors, diodes and a thin dielectric cover. The cover is all dielectric so that, unlike stripline antennas, there is no problem in aligning the second layer or maintaining good short circuits

between the two surfaces of the antenna. Microstrip technology is well suited to the development of phased arrays, and the inherent features of the thin, single-piece, lightweight, structurally self-sufficient conformal design are particularly beneficial in aircraft applications. Although the radiating aperture of the array is about 3 inches by 31 inches, the complete printed circuit board is 14 inches in width by 35 inches in length. This allows sufficient board area for all variations in phase shifter design and distribution network layout that have been required during the development. This also increases the border area around the connectors required to achieve better structural design of the antenna. Figure 1-2 illustrates the basic design approach and the mechanical configuration. Figure 1-3 shows how the antenna is installed on the aircraft.

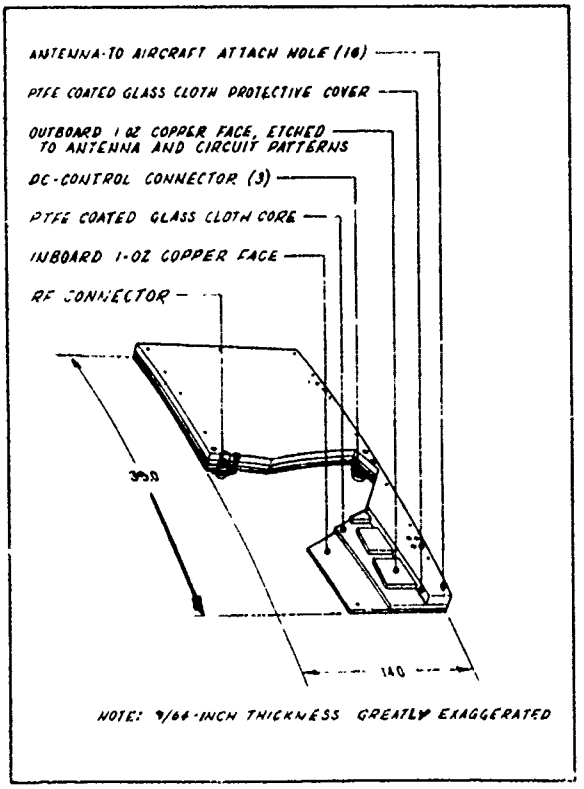

Figure 1-2 Phased-Array Mechanical Design

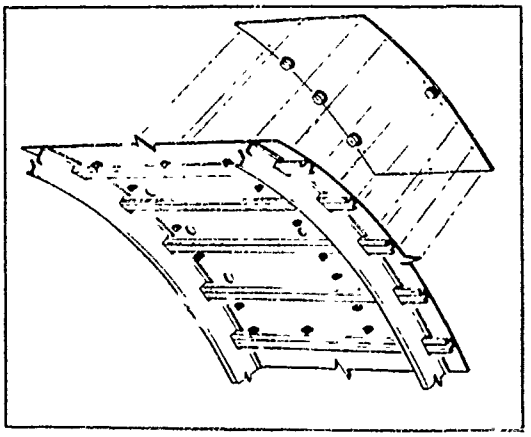

Figure 1-3 Phased Array Installation on Aircraft

Because of the difficulty of replacing faulty diodes in the array assembly, it was determined that it would be prudent to fabricate, and have available, a spare array assembly to use in case of failure in the prime unit.

The control unit, Figure 1-4, selects predetermined beam positions at appropriate times according to the flight test plan. The beam position information is translated into a set of diode states for that particular beam position. This controls the diode drivers which operate the phase shifters on the antenna.

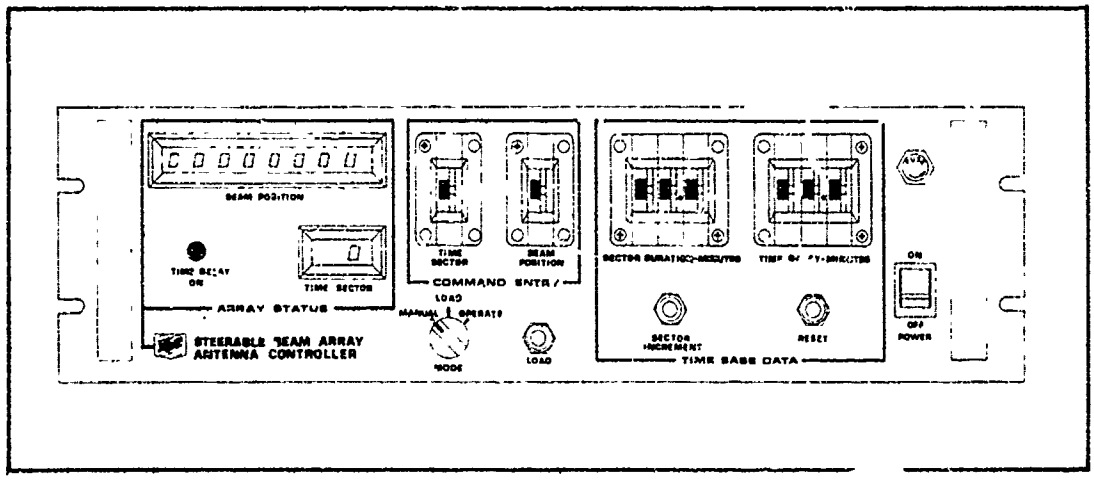

Figure 1-4 Steerable Beam Antenna Control Unit

In an alternative system concept considered during the preliminary design phase, the diode drivers and some of the logic circuits were located on the antenna circuit board. The reason for this

was that it minimized the number of control wires between the control unit and the antenna. Control information would be sequentially transmitted to the antenna where it would be decoded to operate the driver circuits. The problem that developed with this arrangement was the packaging of the driver components. A removable cover over these components was suggested to simplify the packaging and to enable removal and repair. However, the initial layout indicated that printed circuit subassemblies would be required to accommodate the driver transistors and associated passive elements because of the complexity of interconnecting printed circuit wiring. This increased complexity in the array design exceeded that originally contemplated, wherein the components would be imbedded directly in the laminated printed circuit board. There was no way to reduce the complexity of this circuitry using readily available components, and the only alternative was to locate the drivers in the control unit, and run a single conductor for each of the 48 pairs of diodes to the antenna assembly. This would also reduce the risk of damaging the logic components during the cover lamination process. The alternative was approved during a design review meeting with TSC. It was recognized during the meeting that the alternative had the additional advantage of providing convenient checkout and replacement of all active components except the PIN diodes on the array itself.

The cabling between the control unit and the array thus consisted of one low loss coaxial transmission line, 48 dc control wires and 6 dc ground return wires. Approximately 70 feet of cable was required to connect the antenna at station 450 to the equipment mounted near the aft end of the aircraft. A preliminary cabling layout was made indicating a tentative choice of RG-217/U coaxial cable for the RF circuits. This layout was subsequently reviewed and the cable was changed to a low-loss Andrews Cable type HJ5-50. This is a low loss air articulated cable with outside diameter of about 1-1/16-inch. A short length of standard coaxial cable was

used at the antenna end to enable connection of the antenna to the relatively stiff low-loss cable.

1.3 SYSTEM ANALYSIS

System parameters such as aperture configuration and beam steering angles were determined as a result of computer analysis. The computer was programed to find the complex sum of the radiated amplitudes of each element. The data was plotted in one degree increments from +90° to -90° with respect to the antenna boresight. The program was designed to permit location of elements anywhere in the plane of the pattern being calculated. This feature allows the curvature of the aircraft surface (ground plane) to be included in the simulation.

The derived pattern data was used to predict multipath rejection for the array. If the array center is mounted at an angle θ above the horizon as in Figure 1-5, then θ becomes the boresight angle for the array. With the satellite at angle α above the horizon, the direction of the multipath signal is $-\alpha$. The antenna "sees" the satellite at an angle $\theta-\alpha$ from its boresight and "sees" the multipath signal at an angle $\theta+\alpha$ from its boresight. The ratio of the calculated antenna directivities in these two directions is then plotted to indicate multipath rejection. This, of course, does not include the additional attenuation of the multipath signal due to the surface reflection coefficient and the polarization reversal at the ocean surface.

The analysis showed that eight elements arrayed linearly provided superior multipath rejection compared to a two-by-four array. Nine beam positions were determined to be sufficient and the angle θ in Figure 1-5 was set at 41 degrees. The implementation of the analysis is discussed in the section on Array Design and

Fabrication. Figure 1-6 shows the nine beam center positions in the airplane coordinates and Figure 1-7 shows the final multipath rejection plot for the one-by-eight array.

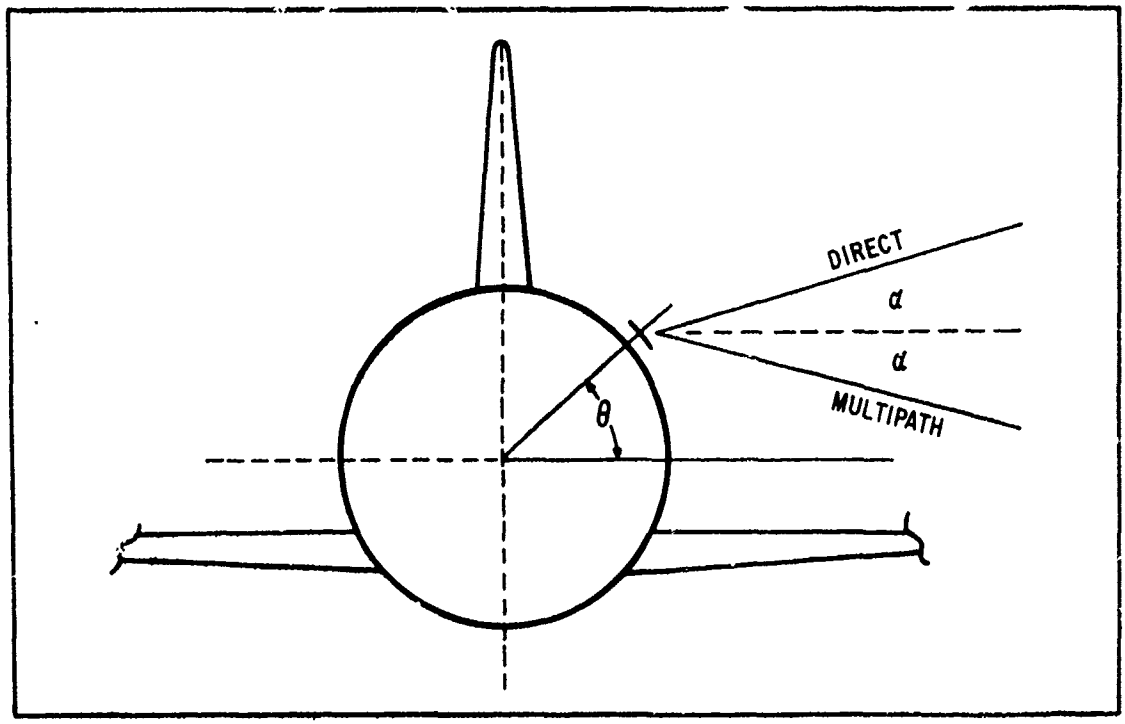

Figure 1-5 Antenna Boresight Orientation on Aircraft

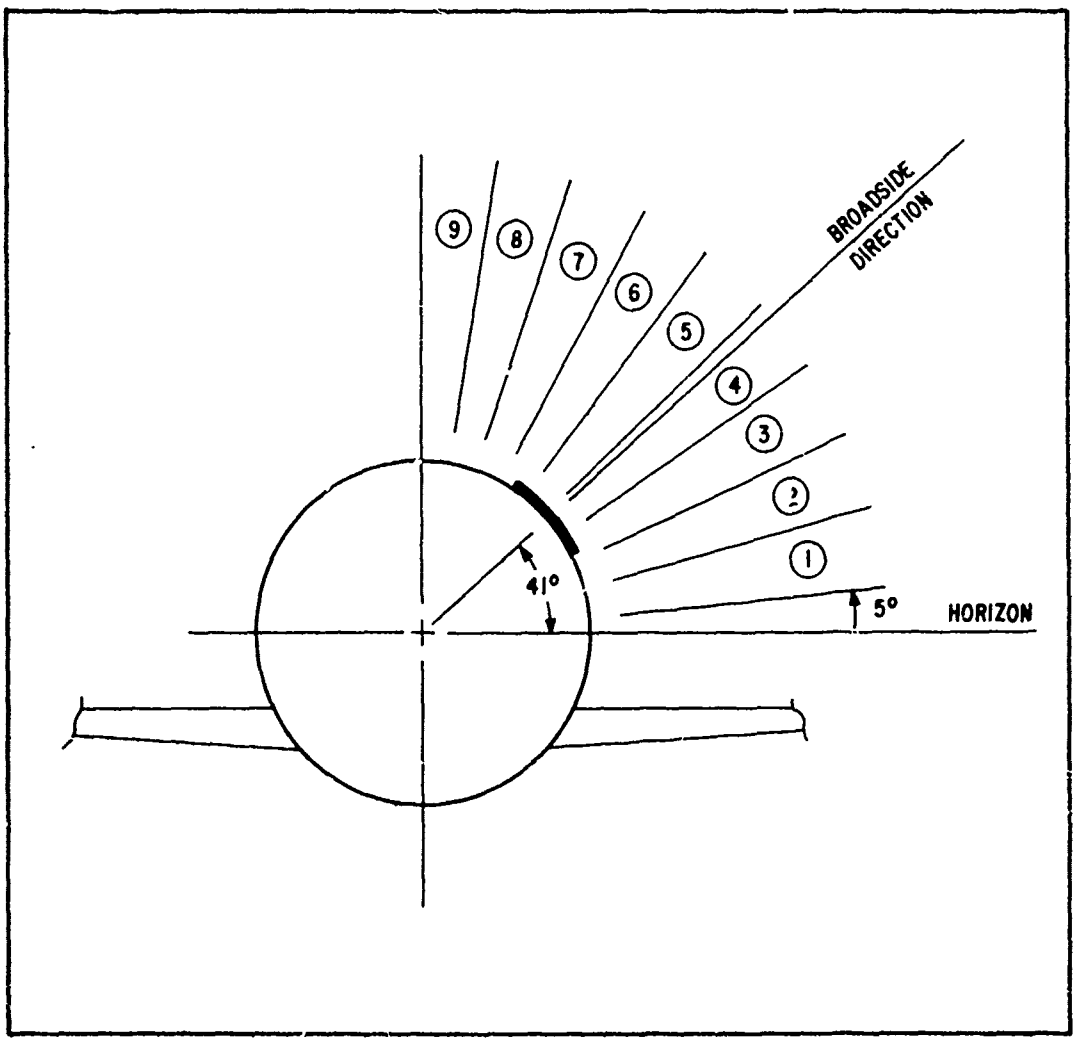

Figure 1-6 Elevation Beam Positions

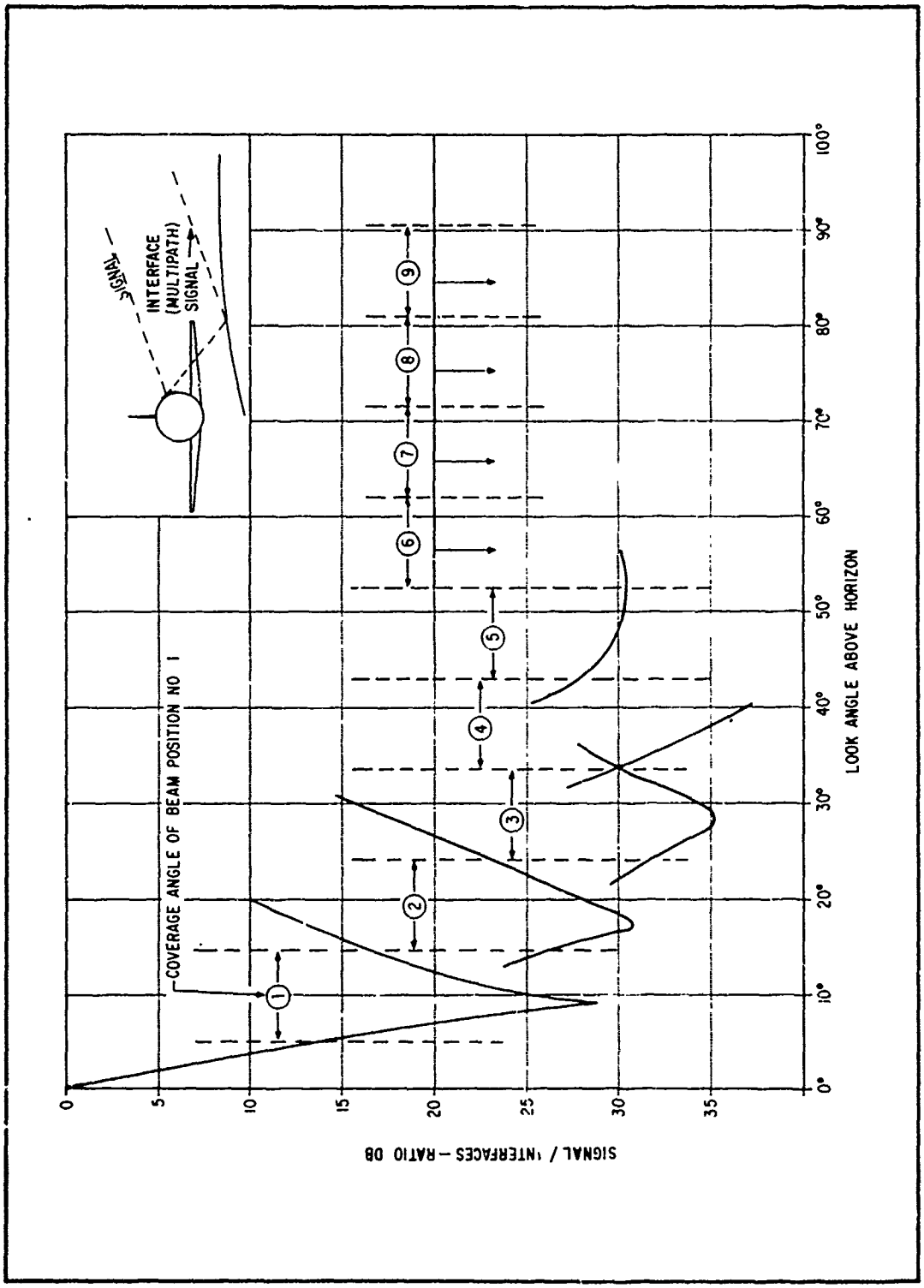

Figure 1-7 Calculated Multipath Rejection

2. MICROSTRIP RADIATING ELEMENT

A primary consideration in designing a low cost array is the choice of the basic radiating element. The microstrip element should be compared with crossed dipoles, crossed slots and slot dipoles. The microstrip element is simply a resonant patch of metal etched on a Teflon-fiberglass substrate. It is an efficient low profile radiator with a broad radiation pattern. Since it is manufactured with the same techniques used to produce printed circuit boards, it is a very reliable, low cost device. In its simplest form it is a narrow-band device, but bandwidth is sufficient for the present receive-only application which requires about a 1 percent bandwidth.

Crossed dipoles can also be etched from metal foil on dielectric substrate, but the dipoles must be supported at one quarter wavelength above the ground plane with baluns carefully positioned between the dipole and the feed line on the ground plane. This is expensive to manufacture and can be rather fragile. Crossed slots can be made more rugged, but the cavity behind the slots is expensive to manufacture and is large compared to a microstrip radiator. The slot dipole has the same disadvantages as the slot and the dipole with the additional complexity of having to adjust the dipole and the slot to obtain circular polarization.

At this point it is useful to explain the basis of operation (See Table of References, p. 7-1) of a microstrip radiating element. First, consider the linearly-polarized microstrip element which is basically a two-slot radiator, Figure 2-1. The two slots are separated by a length of very low impedance transmission line. The length of this line can be made just short of a half wavelength so that the complex admittance G_s of Slot A is transformed to G_s at Slot B where it is added in

parallel with the admittance G_S of Slot B. The result is a real admittance corresponding to the radiation admittance of the antenna plus a small loss component. Losses depend on the loss tangent and thickness of the dielectric material and the conductivity of the conducting surfaces. In practice, efficiencies as high as 95 percent have been obtained; 80 percent is common.

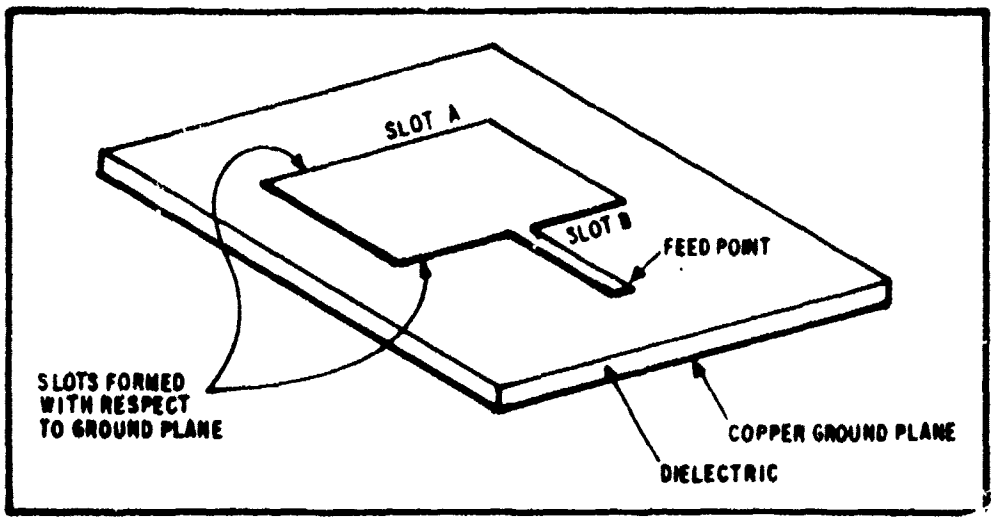

Figure 2-1 Linearly Polarized Microstrip Element

Figure 2-2 is a sectional representation of the electric field in the vicinity of a microstrip radiator. Since the element is about a half wavelength long in the dielectric, the field at one end of the microstrip cavity is reversed from that at the other end of the cavity. However, the radiated fields are in phase and tend to add in the broadside direction. Figure 2-3 shows a typical E-plane pattern attributable to these fields.

To obtain circular polarization from the microstrip element it must be made resonant in two orthogonal dimensions. The two orthogonal modes must be excited equally, in phase quadrature.

This may be done simply by dividing the input power and inserting a 90-degree phase shift in one feed line as shown in Figure 2-4. A quadrature hybrid (Figure 2-5) can be used to provide the phase shift and power division. Impedance mismatch reflection would be absorbed in the loaded post. The system impedance bandwidth would be increased; however, this would be caused by the increased loss in the loaded post. Another way to feed a circularly polarized microstrip element is shown in Figure 2-6. Here the impedance of one orthogonal mode is made slightly capacitive, and the impedance of the other slightly inductive. Equal power division and phase quadrature result when the element is fed at the corner. The radiated power is circularly polarized over a limited bandwidth. Although this technique has several advantages, it seems to be somewhat more difficult to etch repeatably, and the Figure 2-4 technique was chosen.

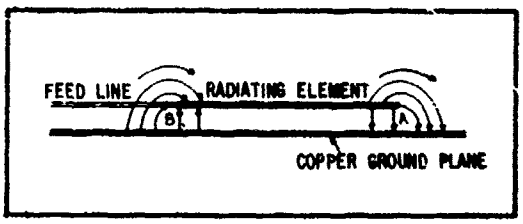

Figure 2-2 Electric Field in Vicinity of Microstrip Element

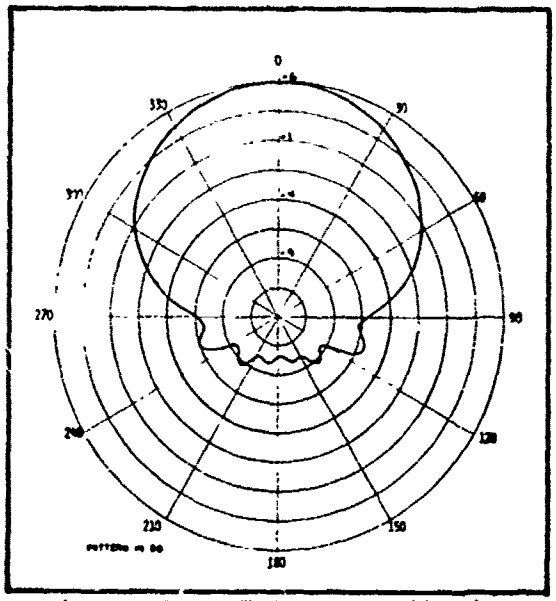

Figure 2-3 E-Plane Radiation Pattern of Linearly Polarized Microstrip Element

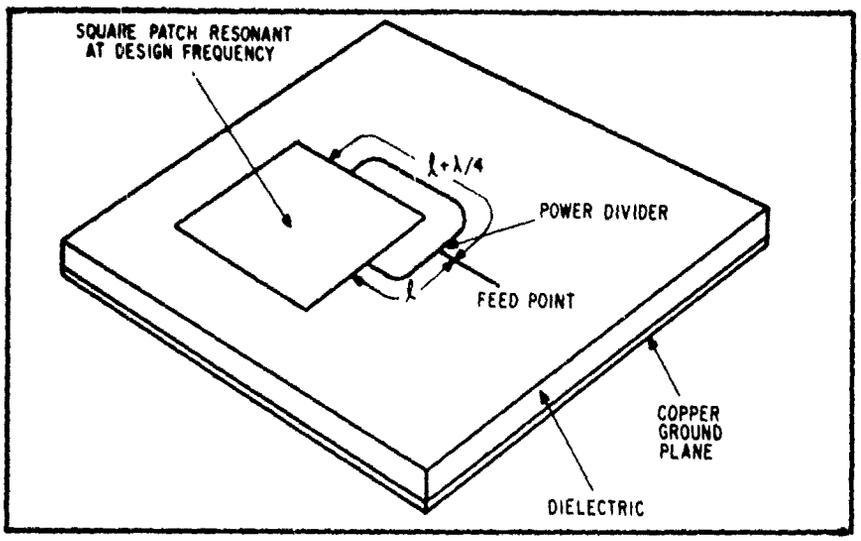

Figure 2-4 Circularly Polarized Element With Two-Point Feed

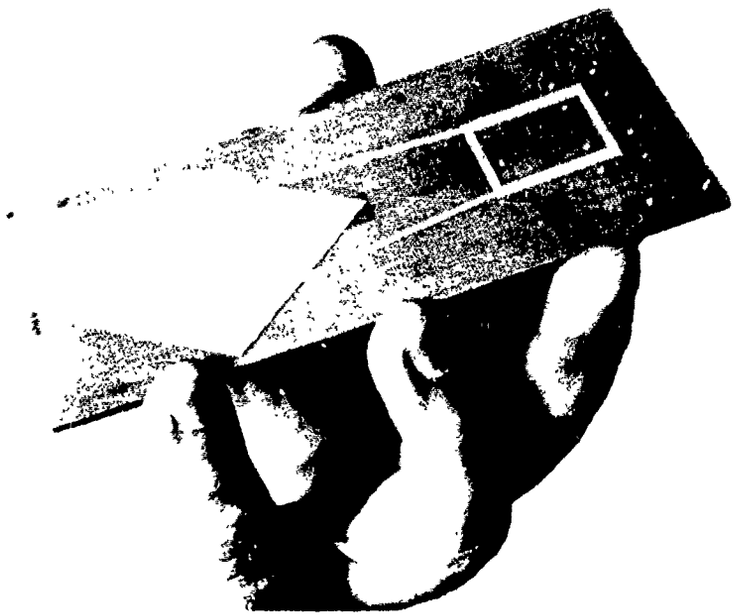

Figure 2-5 Circularly Polarized Patch Antenna With Quadrature Hybrid Feed

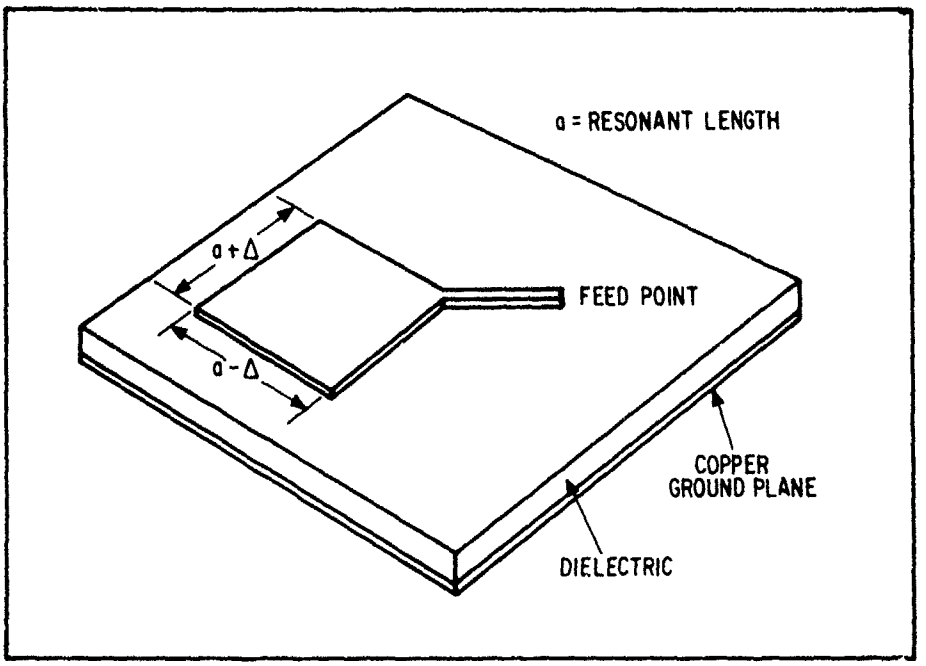

Figure 2-6 Circularly Polarized Element With Single-Point Feed

During the development a question was raised as to whether it would be an advantage to use the hybrid feed, in view of a future need to operate on both transmit and receive frequencies simultaneously. Since the frequencies would be quite wide-spread more modification would be required to the patch to make it resonant at two frequencies than just the addition of a hybrid, and since this was divergent from the original intent of this development, the decision was made to stay with the two-point feed with 90-degree offset as shown schematically in Figure 2-4.

3. ARRAY DESIGN AND FABRICATION

3.1 PHYSICAL DESCRIPTION

The basic array, as distinguished from other components of the phased array system, is a 1/8-inch Teflon fiberglass printed circuit board 14-inches by 35-inches. The first delivered array unit had a pure Teflon adhesive-backed cover with an aluminum frame around the border (Figure 3-1). The frame was riveted to the assembly to prevent the moving air from catching the cover and pulling it off. The second delivered unit (Figure 3-2) had a laminated Teflon fiberglass cover. No additional frame was required since the laminating bond on the Teflon fiberglass had sufficient adhesion to hold it in place.

The printed circuit under the cover, shown in Figure 3-3, includes the radiating elements, element feed networks, matching transformers, phase shifters, power dividers and dc bias lines. PIN diodes for the phase shifters are recessed into the circuit board, but the solder connections to the printed circuit stand high enough to make small lumps in the cover. The dc bias lines and ground are brought together in three groups where they are fed to three connectors, each having 18 terminals. Three connectors were used, instead of one large connector, to minimize the size of the holes required in the skin of the aircraft. The maximum diameter of the connector with its extension is one inch. A Type N coaxial connector is used for the RF connection.

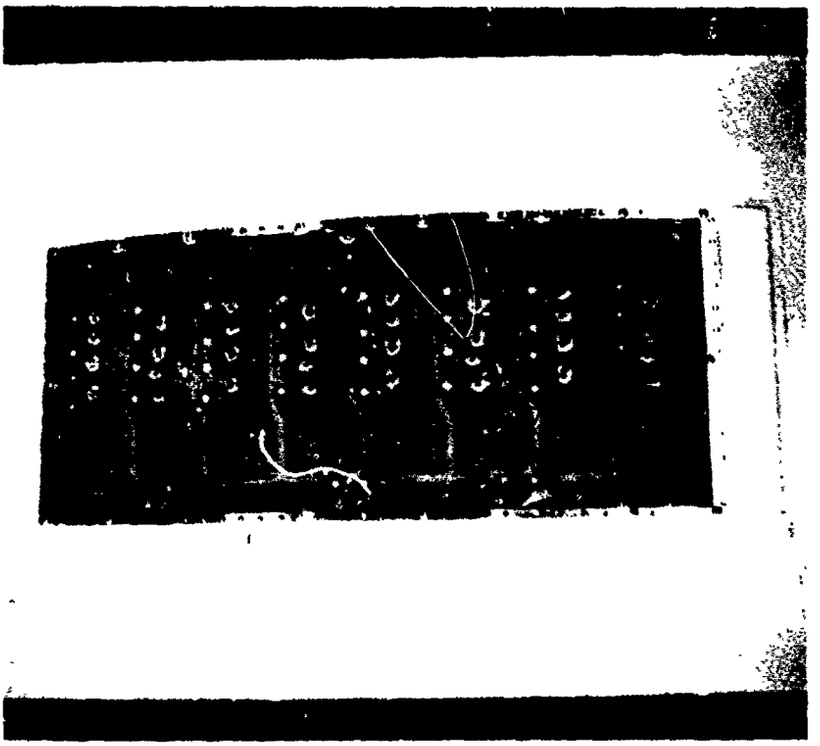

Figure 3-1 First Delivered Phased Array

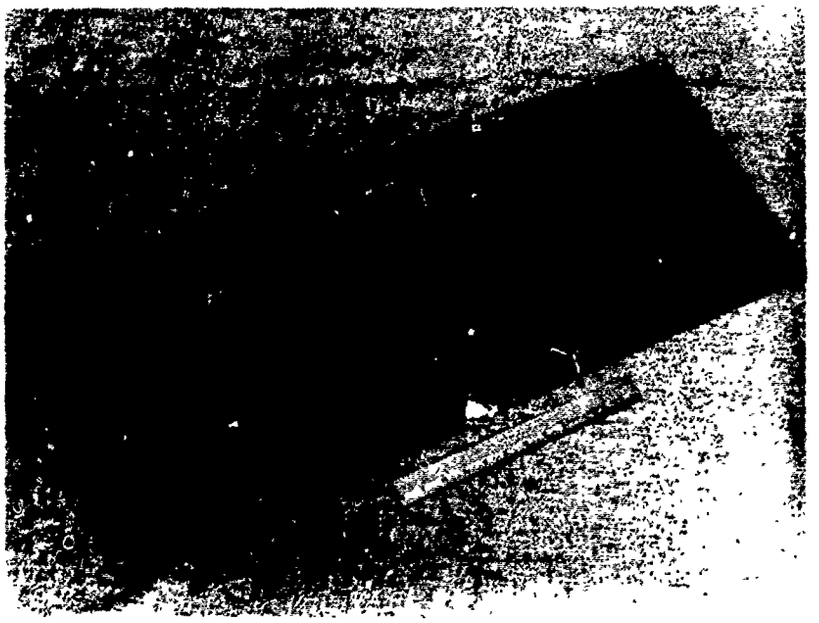

Figure 3-2 Second Delivered Phased Array

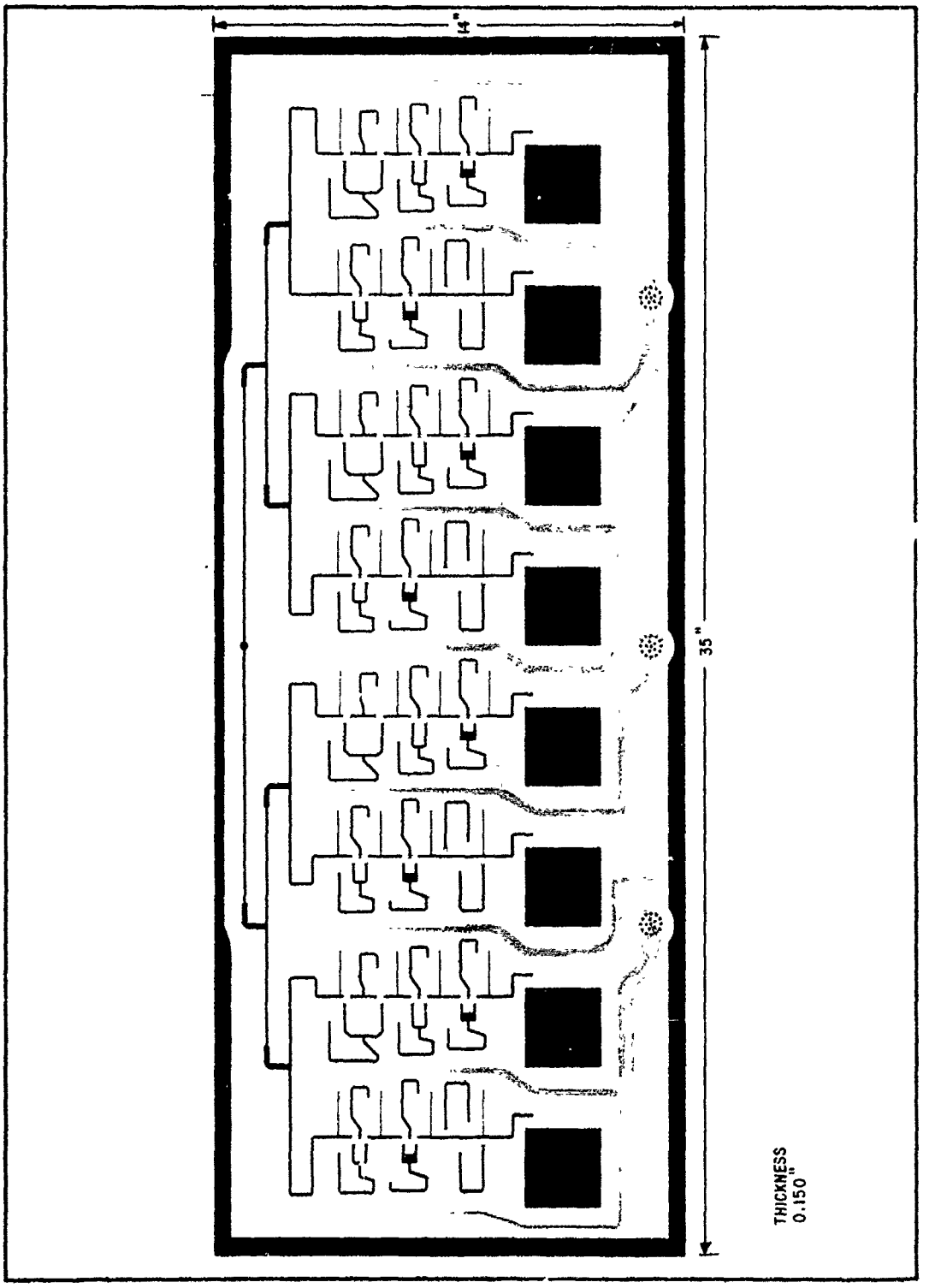

Figure 3-3 Printed Circuit

3.2 ELECTRICAL DESIGN

3.2.1 Element and Feed

As previously explained, the element chosen for the array is a square microstrip element fed on two adjacent sides as shown schematically in Figure 2-4. The input impedance at each of the two feed points is on the order of 200 ohms; this impedance is transformed through a quarter wavelength of 140 ohm microstrip line to 100 ohms. The design impedance of the 90-degree differential phase line is 100 ohms so that the impedance looking into the differential phase line is the same as the impedance looking into the line without the differential phase. This ensures that the power will be split equally when the two lines are connected and fed together. It is important to correctly locate the line with the differential phase shift relative to the other line. The configuration sketched in Figure 2-4 is correct for right-hand circular polarization and the mirror image would radiate left-hand circular polarization. When the two lines are connected the two 100 ohm impedances are combined in parallel to yield 50 ohms. Since all the phase shifters and distribution network are designed for 100 ohms, the 50 ohm combined feed is transformed through a 70 ohm line to 100 ohms. In order to minimize feed line losses and assure repeatable feed line impedances when etched, the feed line impedances used are normally 50 to 150 ohms.

3.2.2 Array Design

The radiating elements must be arrayed and phased to provide the desired beam shape and gain. In addition, the curvature of the ground plane must be considered. Each element is pointed in a slightly different direction and has an inherent phase error relative to the two center elements. A digital computer was used

to determine how the design parameters actually affect the performance of the array.

Normally the design of a phased array would include an extensive analysis of the mutual coupling problem. However, microstrip elements have relatively little mutual coupling. The array has some minor beam shape distortions that might be attributable to mutual coupling, but they are insignificant.

Spacing of the array elements must be greater than 0.32 wavelength (in free space) because the physical size of the radiating element on Teflon fiberglass requires this space. As the spacing is increased from 0.32 wavelength, the total array aperture for a given number of elements is also increased. This reduces the beamwidth and increases the gain. However, a limit is reached when grating lobes begin to form. The spacing required to prevent the formation of grating lobes is given by:

$$D \leq \lambda/(1 + \sin \theta) \qquad (1)$$

where

D is the separation

λ is the wavelength

θ is the maximum beam steering angle.

For a 50-degree maximum steering angle the spacing must be less than 0.57 wavelength. A spacing slightly less than this, 0.52 wavelength, was chosen for the array.

The required number of elements is a function of the desired gain and the element spacing. The desired peak gain is at least 12 dBi right-hand circular, but an additional 2 dB must be allowed for

phase shifter losses and array losses. Thus, 14 dB gain is used to determine the required aperture area.

$$G = 10 \log_{10} 4\pi A \qquad (2)$$

where

G is the gain of the array in dB

and

A is the area of the array in square wavelengths.

Therefore

$$14 = 10 \log_{10} 4\pi A$$

and

A = 2 square wavelengths.

Since each element occupies an effective area of about (0.5 wavelength)^2, eight elements are required for the array. Eight is a good number because experience in designing microstrip arrays has shown that RF power division can be controlled more precisely when the number of elements is an integer power of two.

The elements can be arranged in 2 by 4 array (55-degree by 30-degree beam) or a 1 by 8 array (80-degree by 15-degree beam). The former would be steered in the plane of the four elements as well as the plane of the two elements. The latter would be steered in the plane of the eight elements only. Ultimately the choice of the 1 by 8 configuration was based on the requirement for multipath rejection. Figures 3-4, 3-5 and 3-6 show three of the calculated patterns for the 1 by 8 array.

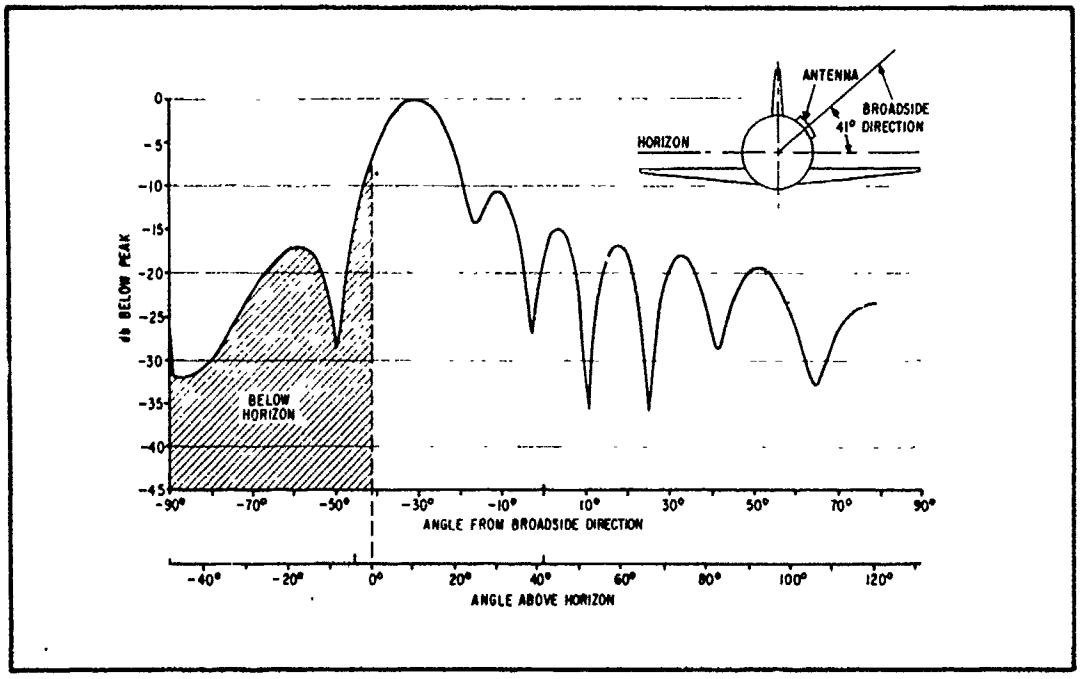

Figure 3-4 Beam Position Number 1, Calculated Antenna Response

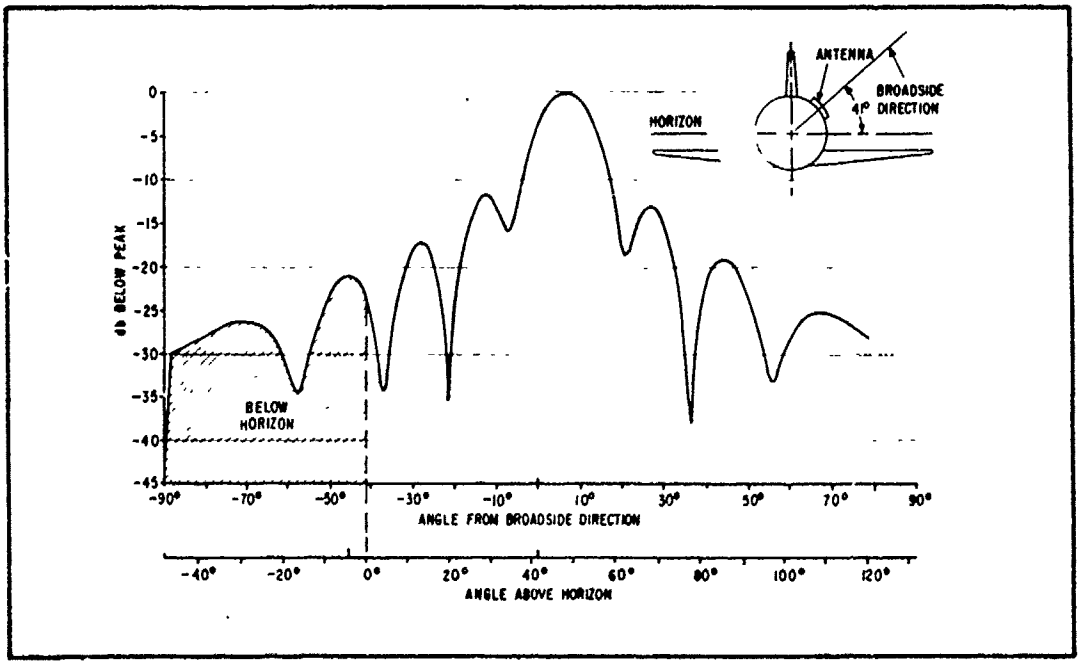

Figure 3-5 Beam Position Number 5, Calculated Antenna Response

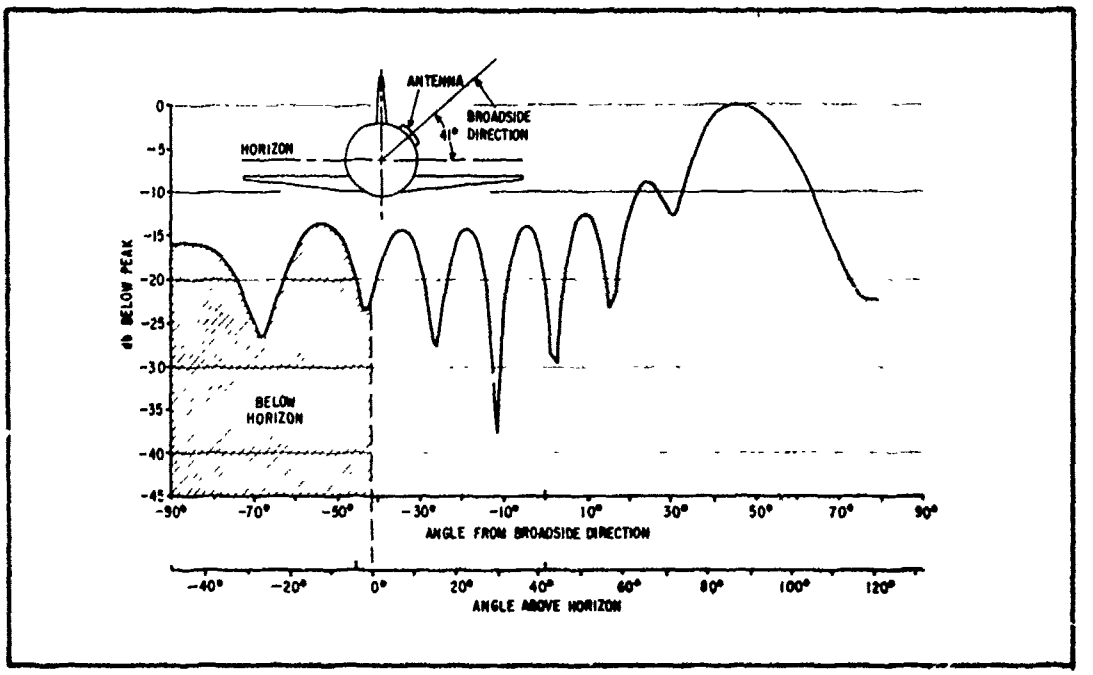

Figure 3-6 Beam Position Number 9, Calculated Antenna Response

3.2.3 Multipath Rejection

Multipath rejection was defined by the equation:

$$R = G_{\alpha} - G_{-\alpha}$$

where

R is multipath rejection in dB

G_{α} is antenna gain on the aircraft in dB at an angle α from the horizon

$G_{-\alpha}$ is antenna gain on the aircraft in dB at an angle $-\alpha$ from the horizon

α is the elevation angle of the satellite above the horizon

Computer plots of the elevation beam patterns were calculated for both the 1 by 8 and the 2 by 4 configurations to determine G_{α} and $G_{-\alpha}$. The multipath rejection of the 1 by 8 array was at least 10 dB better at critical angles of α (10 degrees to 30 degrees above horizon of wing) than the rejection of the 2 by 4 array.

With the nominal 15-degree beamwidths specified by the choice of the 1 by 8 array, it was determined that there should be nine beam positions. The beams would be centered at intervals of 9-1/2 degrees in the elevation plane to allow a 5-1/2-degree overlap.

Further multipath improvement was accomplished in two ways. First it was noted that the offending side lobes were better controlled for smaller scan angles. It was reasoned that the maximum scan toward the horizon could be reduced by moving the array down on the aircraft and increasing the maximum scan toward the zenith. In this way the side lobes for beams near the horizon could be improved at the expense of the non-critical beams near the zenith. Figure 1-6 shows the position of the antenna on the aircraft relative to the nine beam positions.

In addition to adjusting the antenna position to improve multipath rejection, the use of non-linear element phase tapers was also considered. It is possible to reduce side lobes on one side of the main beam while increasing them on the other side by imposing certain phase distortions. A simple distortion that accomplishes this advantageously for a scanned beam is the phase error resulting from the ground plane curvature. Therefore, the array was designed with only a small compensation for the curvature. The calculated multipath rejection for the final array design is plotted in Figure 1-7 as a function of α, the elevation angle of the satellite above the horizon.

3.2.4 Phase Shifter Design

To maintain good control of the beam shape in a small phased array it is desirable to phase the array aperture with a constant phase progression, overlooking the phase distortion of the curved ground plane. Constant phase progression with 9-1/2-degree steering increments and 0.52 wavelength spacing between elements requires phase shifter resolution of 30 degrees or less. Normally, four-bit phase shifters would be required to do this; however, with the eight-element array it is possible to select three bits for each element that will provide the desired phase progression. The phase shifter for each element has three of the following bits: 30 degrees, 60 degrees, 120 degrees and 180 degrees. The arrangement of these bits and the resulting phase progression for each beam position are shown in Table 3-1. The reason that this technique works is because in general there is always one element in a phased array which need not be phased at all. Since all the elements in this array have controlled phases, the extra logic capability may be used to obtain the 30-degree resolution.

Digital phase shifters can be designed with either series PIN diodes or shunt diodes. The advantage of the series configuration is that two or more bits can be combined without having to use dc blocks. The advantages of the shunt configuration include better heat sinking for high power applications and easier compensation for the capacitance of the back-biased diode. Since dc blocks seemed to add unnecessary complexity to this array, phase shifters with series diodes were used.

The phase shifter circuits were designed with a 100-ohm characteristic impedance for three reasons. It reduced insertion loss of the phase shifters by reducing the ratio of diode resistance to characteristic impedance. It was convenient for the design of the power divider network. Also it kept the transmission line widths at a reasonable dimension.

Table 3-1

EFFECTIVE THIRTY-DEGREE PHASE RESOLUTION USING THREE BIT PHASE SHIFTERS

Element Number	Phase Bit Required	Beam Position 1	Beam Position 2	Beam Position 3	Beam Position 4	Beam Position 5	Beam Position 6	Beam Position 7	Beam Position 8	Beam Position 9
1	60, 120, 180	120	120	240	0	0	240	0	120	0
2	(30, 60, 120) +180*	240	210	300	30	0	210	300	30	240
3	60, 120, 180	0	300	0	60	0	180	240	300	120
4	30, 60, 120	120	30	60	90	0	150	180	210	0
5	60, 120, 180	240	120	120	120	0	120	120	120	240
6	30, 60, 120	0	210	180	150	0	90	60	30	120
7	60, 120, 180	120	300	240	180	0	60	0	300	0
8	(30, 60, 120) +180*	240	30	300	210	0	30	300	210	240

*Fixed 180° phase shift.

Considerations in selecting phase shifter circuits included simplicity, compactness and insertion loss. For the 30-degree bit a loaded line phase shifter was chosen. This circuit, shown in Figure 3-7 consists of two switchable stubs spaced a quarter wavelength apart. The effective length of the stubs determines the phase shift, and the spacing between the stubs allows the impedance effects of the stubs to cancel. The additional phase shift due to the capacitance of the back biased diodes was compensated by adjusting the stub lengths empirically.

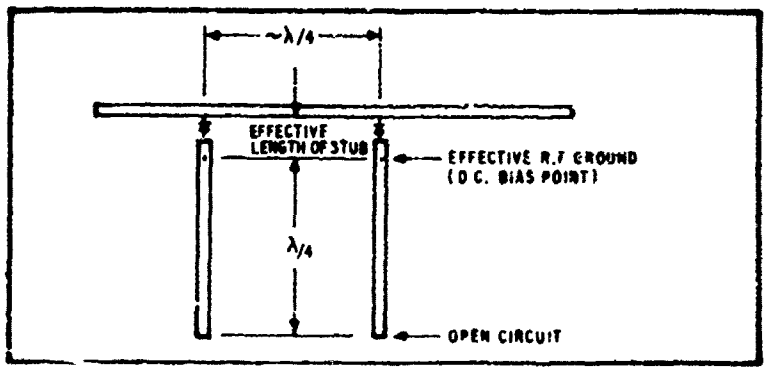

Figure 3-7 Loaded Line Phase Shifter

The stubs of the loaded line phase shifter may be lengthened to make a 60-degree bit. However, it is difficult to avoid locating the diodes at a high current point in the standing wave pattern. The result is a much larger I^2R loss for the diodes in their forward bias state. To avoid this problem and maintain the simplicity of the design, switched line phase shifters were used for the 60-degree, 120-degree and 180-degree bits. This circuit requires two SPDT switches (four diodes) for switching between two different lengths of transmission line as shown in Figure 3-8. The phase

shift then is proportional to the difference between L_1 and L_2. Although the operation of this circuit is straightforward, the capacitance of the back-biased diodes precludes the possibility of either L_1 or L_2 being completely out of the circuit. As a result, the wrong choice of L_1 will introduce phase errors and high insertion losses. The problem is analyzed using an expression for the transmission S parameter of this two path network. The analysis was performed using a digital computer. Phase shift and insertion loss for the 60-degree, 120-degree and 180-degree bits were calculated as functions of diode forward bias resistance, diode reverse bias capacitance and length L_1. The computed data suggested that L_1 should be as short as possible for the 60-degree and 120-degree bits. Length L_1 for the 180-degree bit is less critical, but it was found that the mismatch due to the diode capacitance could be more easily corrected if L_1 was about 0.2 wavelength. Stubs were used to correct the capacitive mismatches.

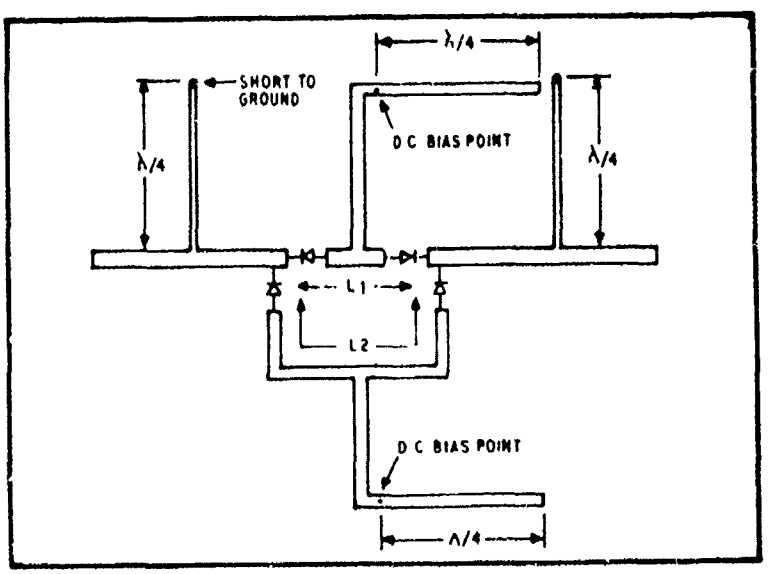

Figure 3-8 Switched Line Phase Shifter

Unitrode IN5767 diodes were initially selected for the phase shifters because of their low resistance and mechanical strength. Several iterations were made on the phase shifter layouts. The principal efforts were directed toward lowering the insertion loss and improving the impedance characteristic of the shifter. The distance between the junctions of the phase shifter switches was adjusted as suggested by the computer analysis and the total insertion loss for the three bits was lowered to 2.0 dB. The analysis also showed that if the diode resistance could be further reduced without increasing the shunt capacitance, the losses could be further minimized. Because of this analysis, Microwave Associates Type MA 47054 diodes which have lower diode resistance than the Unitrode IN5767 were selected and the measured insertion loss was reduced to 1.0 dB. The Unitrode IN5767 diodes were replaced with Microwave Associates Type MA 47054 diodes and the measured insertion loss was decreased to 1.0 dB.

Further adjustments on the phase shifter were made using a simulated lamination cover consisting of plastic tape, which afforded an expedient way of performing developmental testing without producing a completely laminated phase shifter.

3.3 FABRICATION AND ASSEMBLY

The original assembly concept was quite simple and considerable effort was required to retain this simplicity in the flight antenna. Originally, the antenna including phase shifter and logic circuits was to be etched, the active components were to be soldered in place in recesses in the circuit board and then the cover was to be bonded in place under high pressure and temperature. Preliminary information from the manufacturers of the active components indicated that the components would survive the lamination process. However, several lamination tests were performed which introduced serious doubts into the fabrication process.

The first change that was made as a result of this problem and the problem of circuit complexity was moving all logic circuits back into the control unit. This increased the number of wires in the control cable from 10 to 54 which was considered acceptable in view of the potential reliability risk. The decision was made with the understanding that, in the future, as confidence increases in the assembly of microstrip phased arrays, it will be important to reconsider the location of the logic circuits.

The PIN diodes for the phase shifters could not be removed from the array surface, and therefore a fabrication problem still existed. Three alternatives were proposed for solving the problem.

a. Provide openings in the lamination cover in the vicinity of the diodes through which the diodes could be installed after lamination, and potted with a weather-proof material. An antenna was actually built using this approach, but there were doubts remaining about the sealant and integrity of the laminate near the diode cut-outs. A small leak could cause a failure that would invalidate data from an expensive one-time-only flight test.

b. A radome standing 1/4-inch to 3/4-inch off the antenna was considered. This radome would have mechanical fasteners around its border and standoff fasteners located as required across the surface of the antenna. The radome concept provided convenient access to active components on the antenna, but the added complexity of the radome design problem was significant. Standoff height sufficient to preclude any effect on the antenna would have to be determined. There was no knowledge of how much movement in the radome could be tolerated. The relationship of

radome flexure to radome material, thickness and number of standoffs was not known. Furthermore, the whole concept seemed to add excessive complexity to an antenna that was intended to be simple.

c. A room-temperature adhesive turned out to be the best alternative. Candidate adhesives were (a) low dielectric constant polyurethane, (b) high dielectric constant polyurethane, (c) epoxy, and (d) Teflon adhesive sheet. The first three adhesives would be used to bond Teflon fiberglass to the antenna, whereas the Teflon adhesive sheet provided its own Teflon cover layer. Sample phase shifter circuits were assembled including covers bonded with the candidate adhesives. Both electrical and mechanical tests of each sample were made to determine the best adhesive. The low dielectric constant polyurethane and the Teflon adhesive sheet were determined to be most acceptable. The latter was used on the first delivered unit. As a precaution against the air stream catching a corner of the sheet and pulling it completely off, an aluminum border frame was riveted to the antenna. Although this proved to be quite satisfactory in actual flight tests, it was decided to use the polyurethane on the second antenna because its higher peel strength eliminated the need for a border frame.

While the flexibility of the 1/8-inch Teflon fiberglass eased the curving of the antenna to the aircraft radius, it made problems for some of the diodes. All diodes were mounted with a strain relief bend in the leads, but even so the MA 47054 diodes showed a tendency to crack when the antenna was flexed. This was the primary reason for using the higher loss IN5767 diodes on the first delivered antenna. The IN5767 diodes are manufactured in

a way that makes them virtually indestructible in this application. The second antenna did use the MA 47054 diodes, but a special fixture was attached to the antenna to ensure that it would not be flexed when it was off the ground plane. The problem could have been further alleviated by arranging all diodes parallel with the axis of the airplane since there is no flexure of the antenna along these lines.

4. ARRAY CONTROLLER DESIGN AND CONSTRUCTION

4.1 PHYSICAL DESCRIPTION

The control unit is contained in a box 5.25 inches high by 19.0 inches wide by 11.25 inches deep. It is designed for rack mounting in the aircraft and requires somewhat more than 11.25 inches of rack depth to allow room for cable connections. Figure 4-1 is a reduced drawing of the control unit. The assembly consists principally of a wire wrap circuit board into which welded sub-modules and integrated circuit components plug. There are 24 welded modular assemblies each containing two diode drivers. The interconnecting wiring to the control panel and power supplies is conventional harness wiring. A Jones test strip across the chassis provides access to each of the diode driver lines running to the antenna. This access is for troubleshooting or confirmation checks on the functioning of the control unit and the health of each pair of diodes.

The power supplies for the beam steering control unit are self-contained and through the driver logic supply about 35 milliamperes to each of the diodes in the array in the on-state.

4.2 FUNCTIONAL DESCRIPTION

The initial concept of the control unit was modified from that presented in the original proposal to simplify the setup of the beam steering positions by the operator. The modified design enables the operator to select a beam position by setting a single beam position switch rather than a sequence of commands for each programmable beam position. The control unit was also modified to enable locating the control unit at some distance from the antenna array.

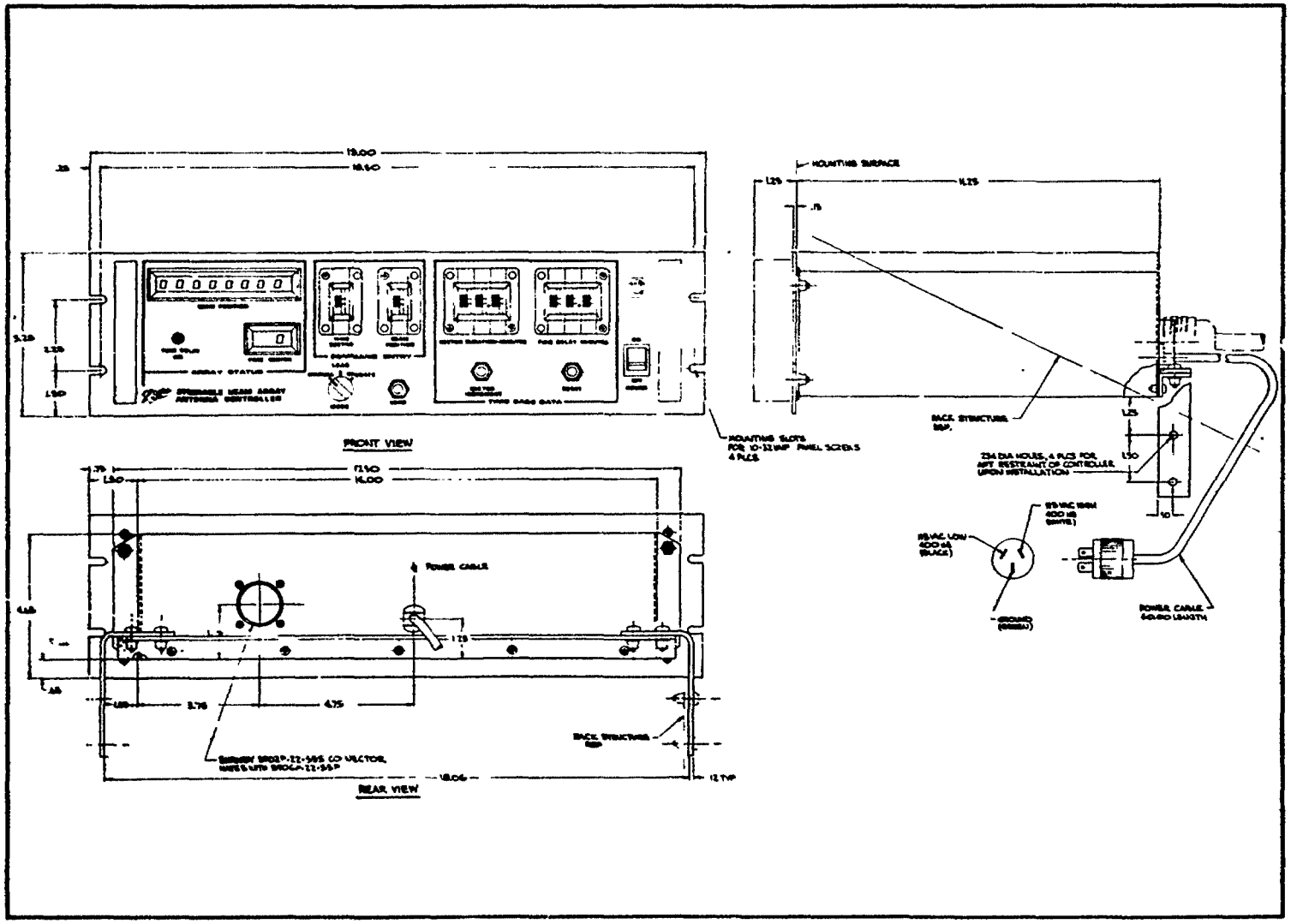

Figure 4-1 Steerable Beam Array Antennna

The function of each circuit in the control unit is shown in a block diagram, Figure 4-2. The actual circuitry is drawn in schematic diagrams, Figures 4-3 and 4-4.

4.3 CONTROLLER OPERATING PROCEDURE

The controller has three operating modes -- load, operate and manual. The manual mode is used to obtain a fixed beam position. The beam position can be manually switched to any of the nine positions. When the flight path of the satellite in relation to the aircraft is known, the controller can be programed to switch through four beam positions hesitating the specified time in each beam positions such as to track the satellite. The beam positions and time intervals are programed into the controller during the load mode. An initial time delay may also be programed into the controller. The time delay would allow the controller to be actuated on the ground before the aircraft starts and the controller will automatically start sequencing at a later time. After the beam positions and times have been programed into the controller, the controller is switched to operate for automatic sequencing.

The scanning of four beam positions provides a scan field of view of approximately 49 degrees. This capability is entirely sufficient for normal flight operation and therefore it was not necessary to expand the controller cost and size for the capability of a nine position scan.

The operation procedure for the three modes is as follows.

1) LOAD

Place the MODE SWITCH in the LOAD position.

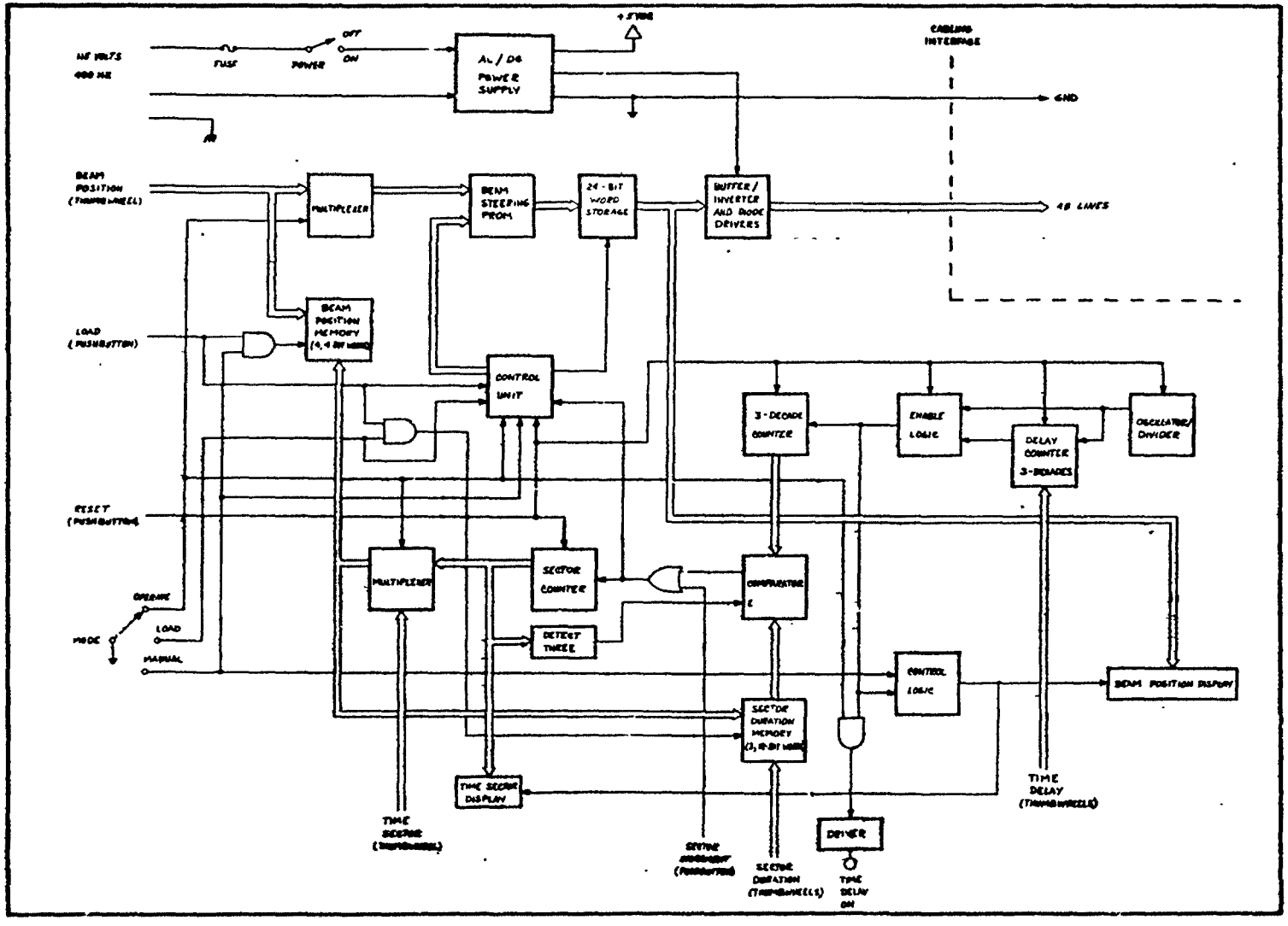

Figure 4-2 Steerable Beam-Array Antenna Controller

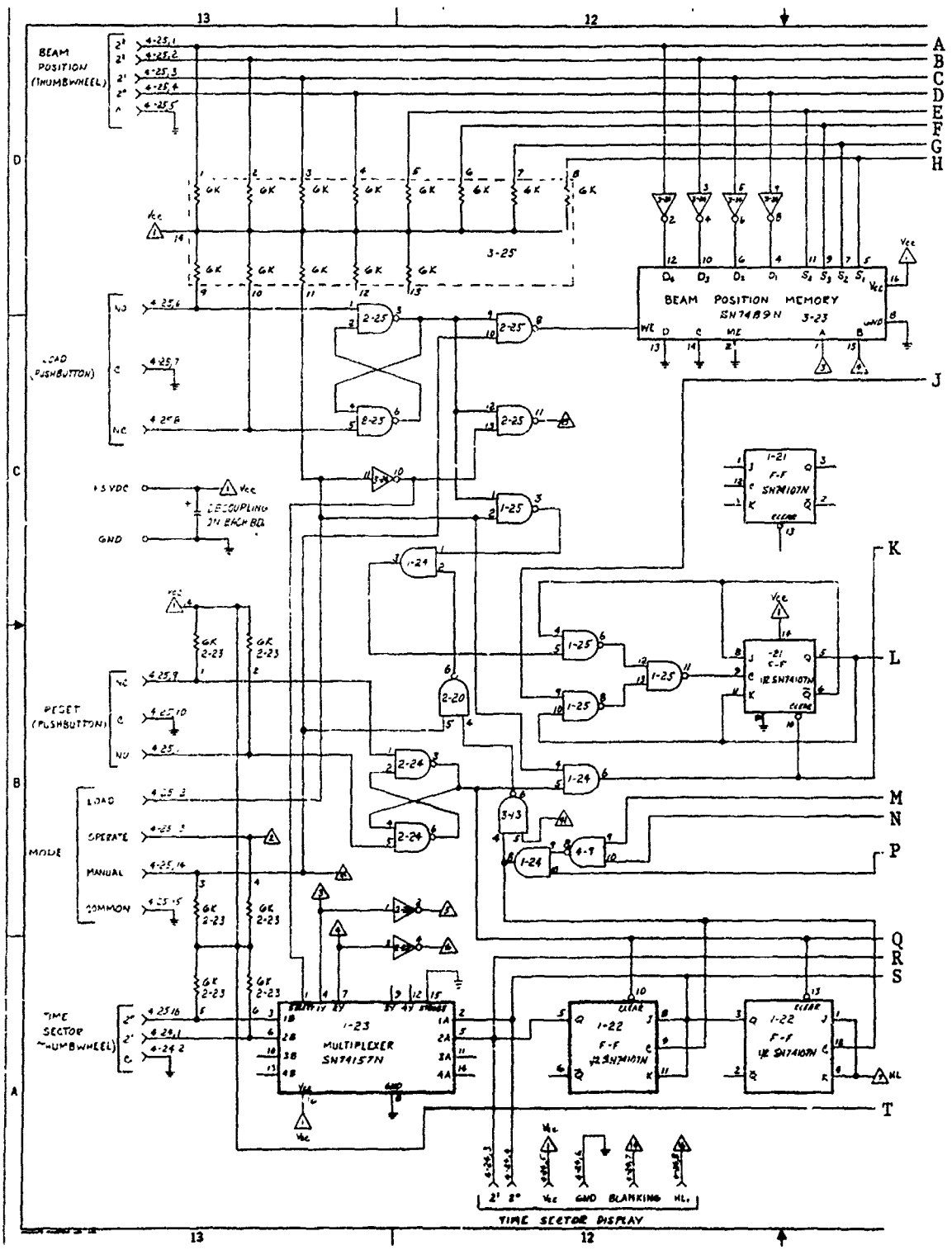

Figure 4-3 Schematic Steerable-Beam Array Antenna Controller

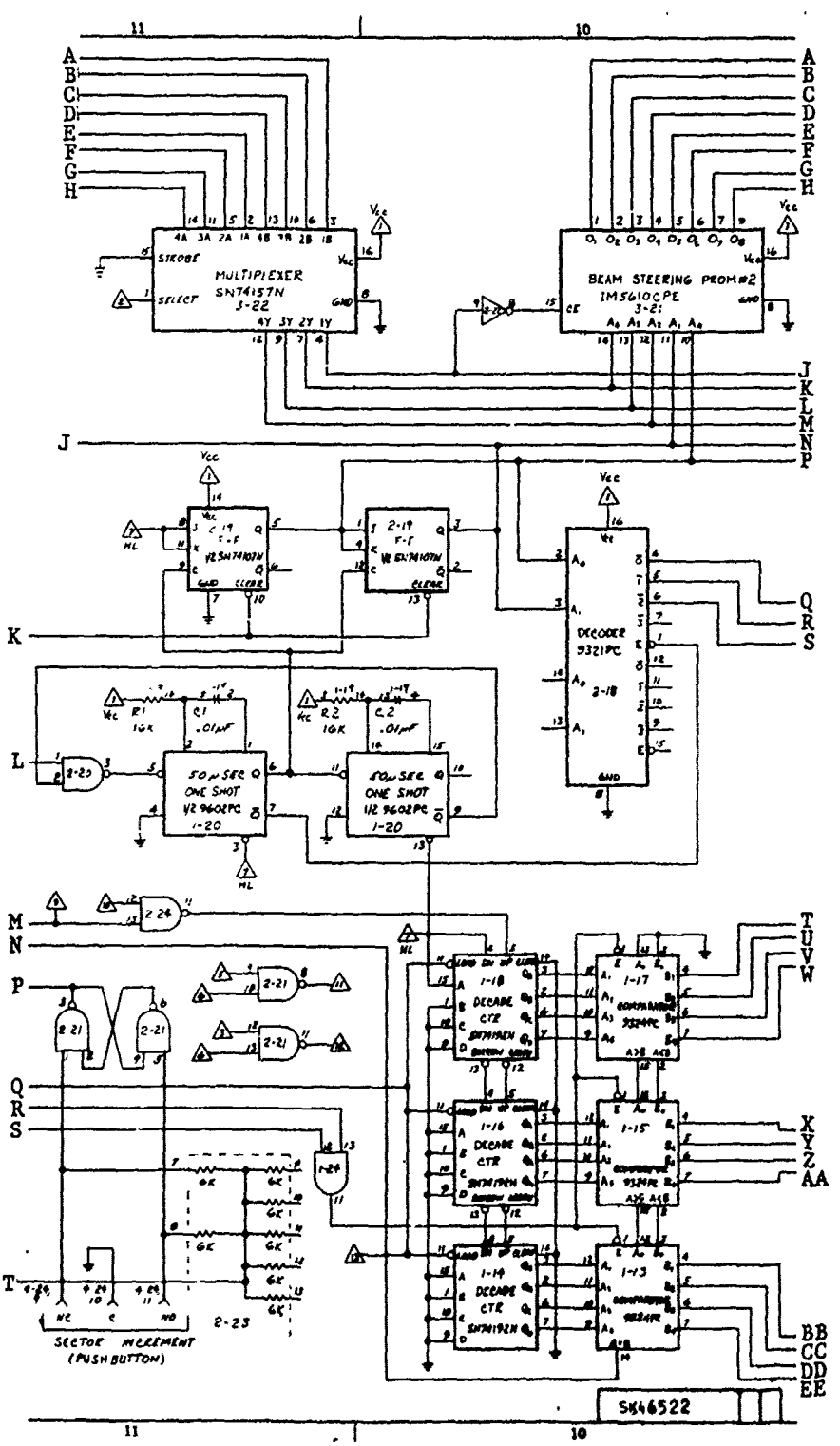

Figure 4-3 Schematic Steerable-Beam Array Antenna Controller (Con't)

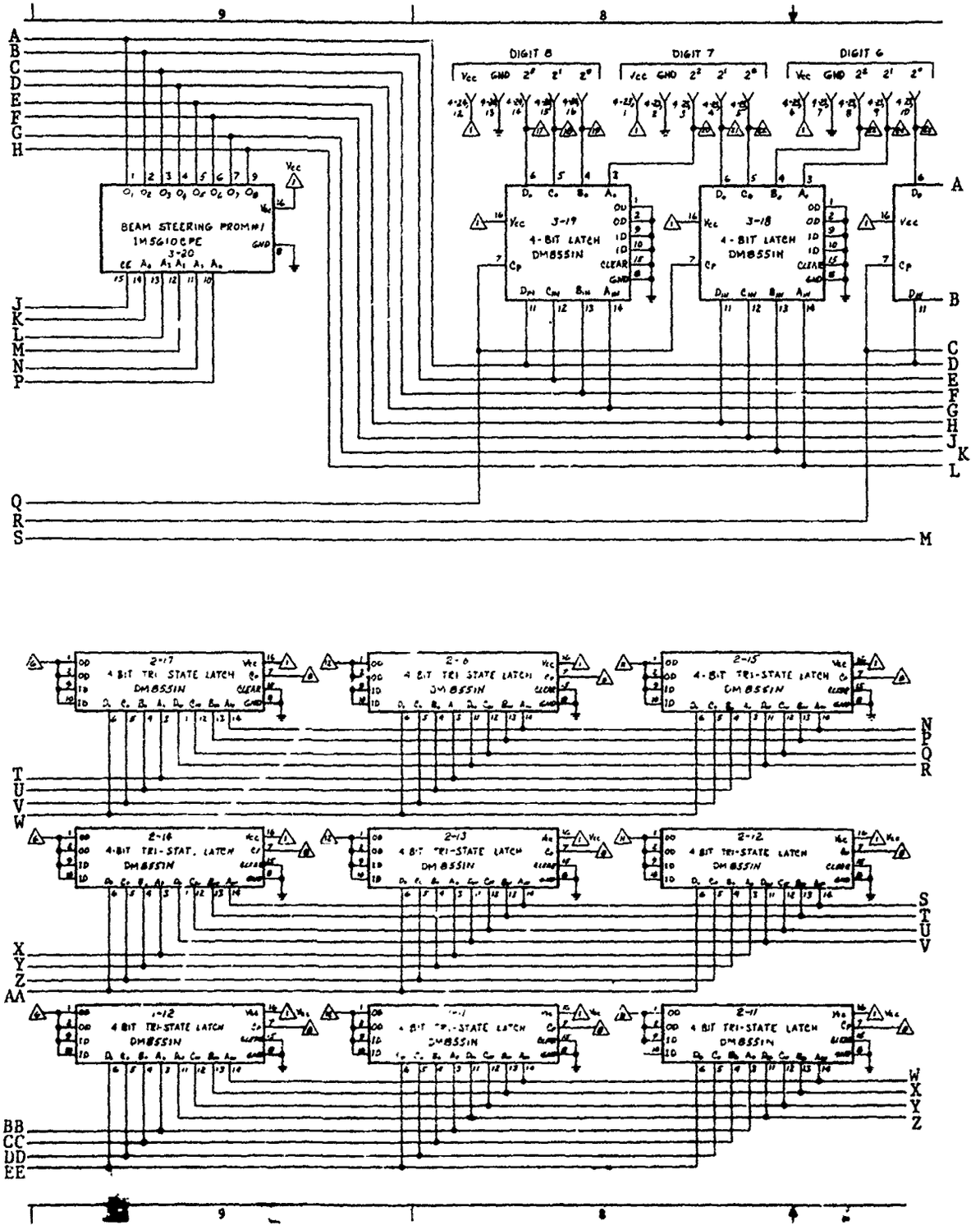

Figure 4-3 Schematic Steerable-Beam Array Antenna Controller (Con't)

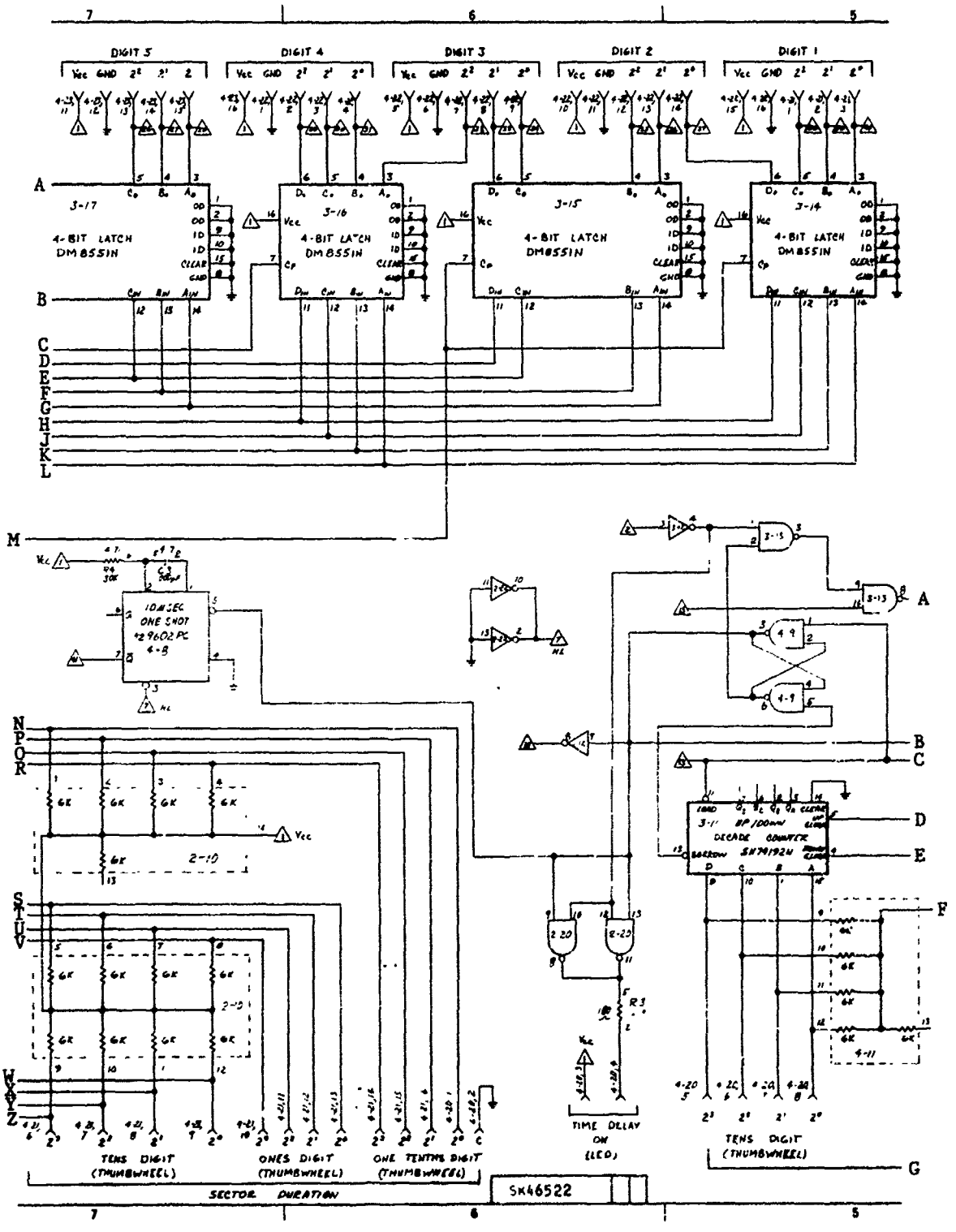

Figure 4-3 Schematic Steerable-Beam Array Antenna Controller (Con't)

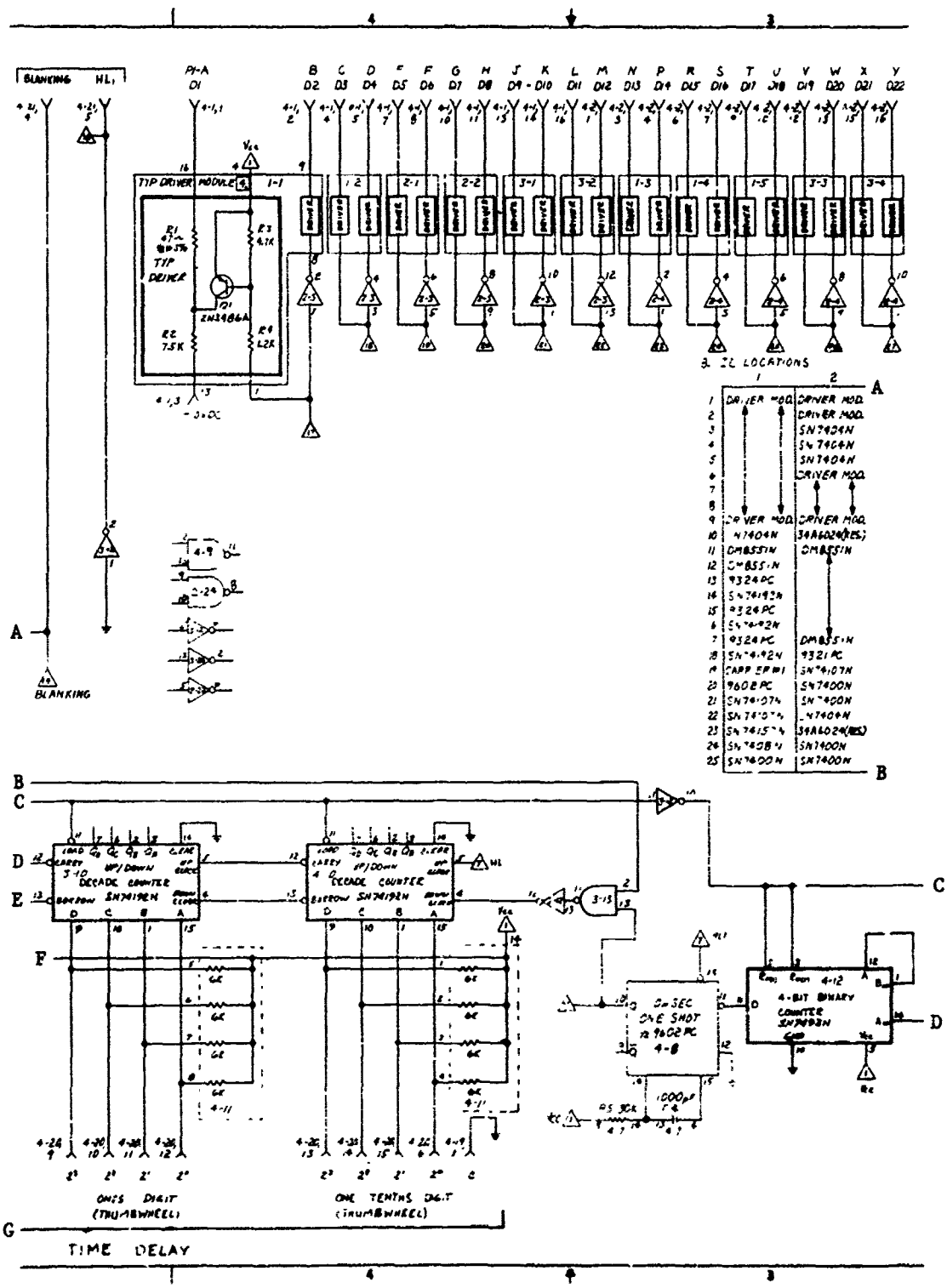

Figure 4-3 Schematic Steerable-Beam Array Antenna Controller (Con't)

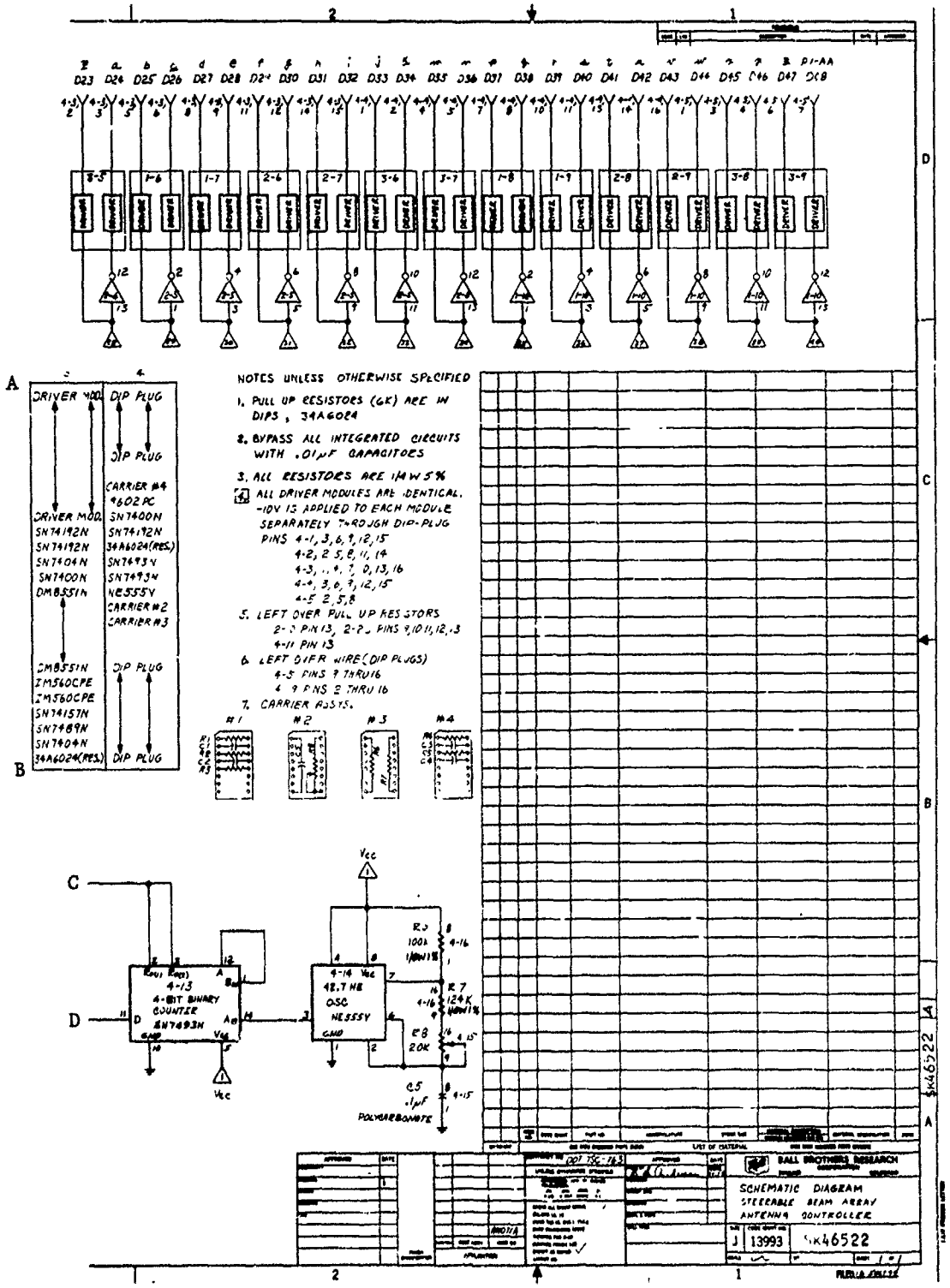

Figure 4-3 Schematic Steerable-Beam Array Antenna Controller (Con't)

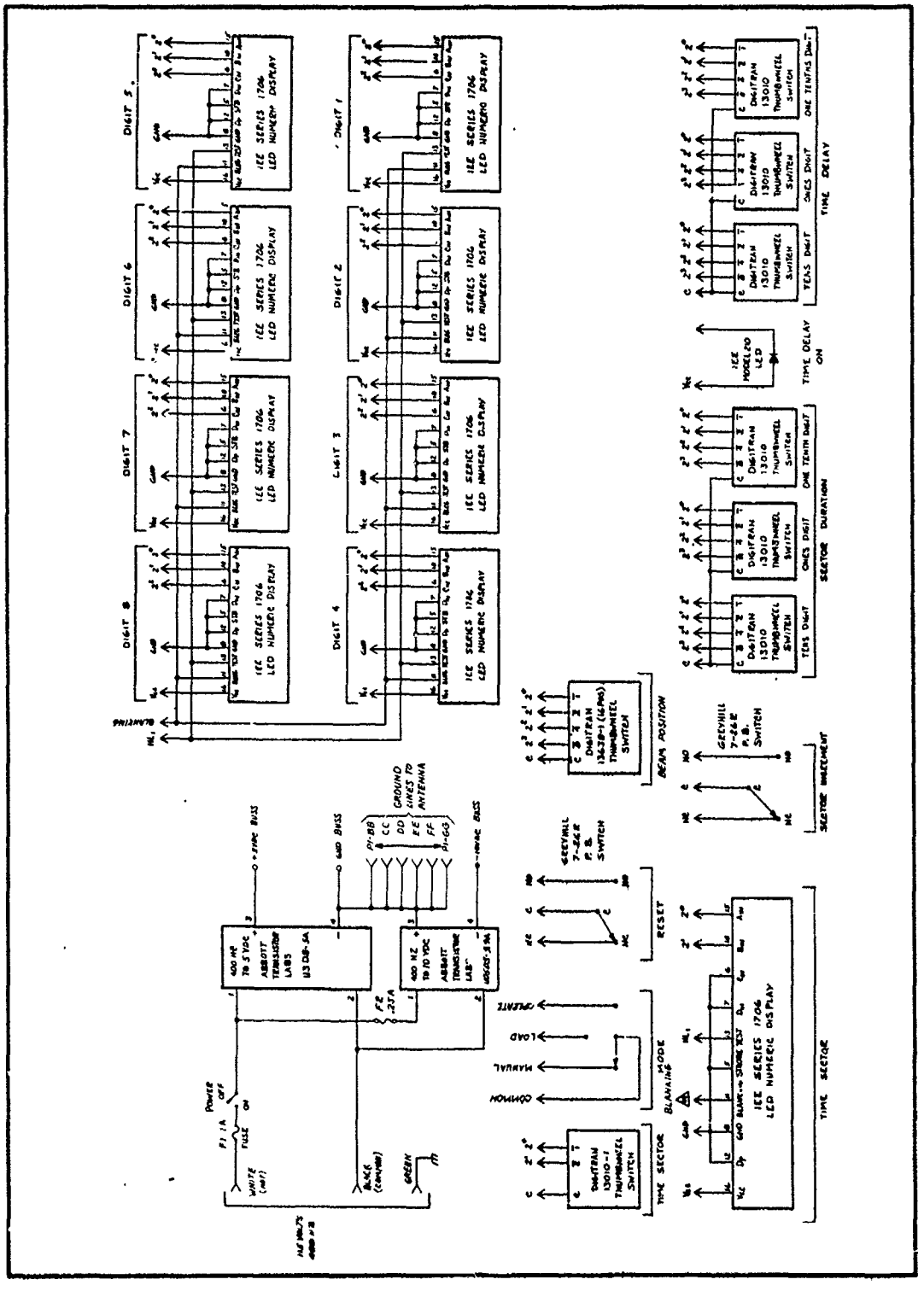

Figure 4-4 Schematic Diagram Steerable Beam Array Antenna Control Panel and Power Supply

Set the TIME SECTOR thumb wheel to 0.

Set the BEAM POSITION switch to the position corresponding to the first desired steering angle.

Set the SECTOR DURATION switches to the desired sector time (0.2 minute minimum).

Depress and release the LOAD pushbutton.

Set the TIME SECTOR thumb wheel to 1.

Set the BEAM POSITION switch to the number corresponding to the second desired steering angle.

*Set the SECTOR DURATION switches to the desired sector time.

Depress and release the LOAD pushbutton.

Set the TIME SECTOR thumb wheel to 2.

Set the BEAM POSITION switch to the number corresponding to the third desired steering angle.

*Set the SECTOR DURATION switches to the desired sector time.

Depress and release the LOAD pushbutton.

Set the TIME SECTOR thumb wheel to 3.

Set the BEAM POSITION switch to the number corresponding to the fourth desired steering angle.

---

*These sector durations are referenced to the beginning of sector 0 (see time line, Figure 4-5).

Depress and release the LOAD pushbutton.

A TIME DURATION is not required since this beam position is held until reset is activated.

Set the TIME DELAY switches to the desired time delay.

2) OPERATE

Place the MODE SWITCH in the OPERATE position.

Depress and release the RESET pushbutton.

The time delay will begin when the RESET pushbutton is released. The TIME DELAY on lamp will be on and the TIME SECTOR display will be off. At the end of the time delay the TIME DELAY on lamp will turn off and TIME SECTOR display will indicate sector zero. The readouts will display beam steering and sector as time progresses, as shown in Table 4-1. The array antenna will be steered to the indicated position.

3) MANUAL

Place the MODE SWITCH in the MANUAL position.

Set the BEAM POSITION switch to the number corresponding to the desired steering angle.

Depress and release the LOAD pushbutton. The selected beam position will be displayed and the array antenna will be steered to the indicated position.

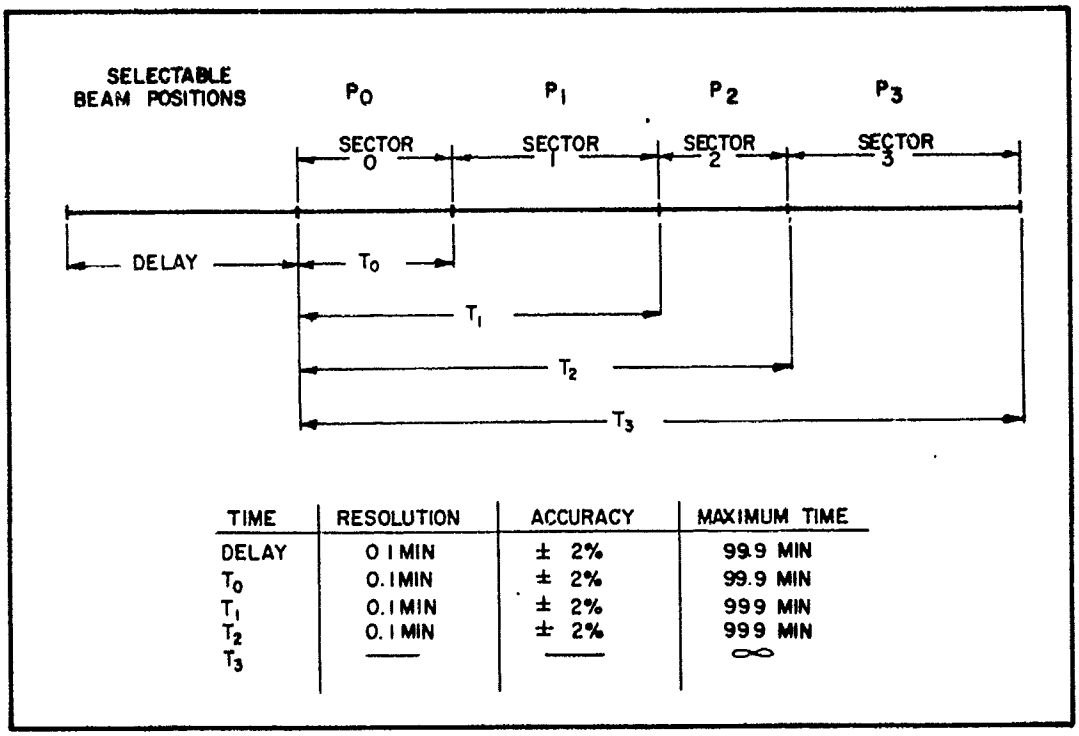

TIME	RESOLUTION	ACCURACY	MAXIMUM TIME
DELAY	0.1 MIN	± 2%	99.9 MIN
T_0	0.1 MIN	± 2%	99.9 MIN
T_1	0.1 MIN	± 2%	999 MIN
T_2	0.1 MIN	± 2%	999 MIN
T_3	——	——	∞

Figure 4-5 Controller Program Time Line

Table 4-1

CONTROLLER READOUT FOR BEAM POSITIONS

BEAM POSITION	DISPLAY							
1	2	6	0	5	5	4	2	6
2	2	0	3	0	2	3	3	3
3	5	5	0	6	2	7	5	5
4	0	3	4	2	2	1	1	0
5	0	7	0	4	0	4	0	7
6	5	0	1	1	2	2	4	3
7	0	5	5	7	2	6	0	5
8	2	3	3	3	2	0	3	0
9	0	6	2	4	5	5	0	6
CHECK POSITIONS								
14	0	0	0	0	0	0	0	0
15	7	7	7	7	7	7	7	7

If the controller was in the operate mode before the manual mode was selected, returning to the operate mode will cause the controller to pick up at the next time sector and continue with the automatic sequence. The beam position will remain in the manually selected position until a pulse from the time sequencer switches the antenna to the time sector beam position. Note, that since the automatic sequences run continuously, when the time durations are short more than one sector may be crossed while in the manual mode. This sequencing is illustrated in Figure 4-6.

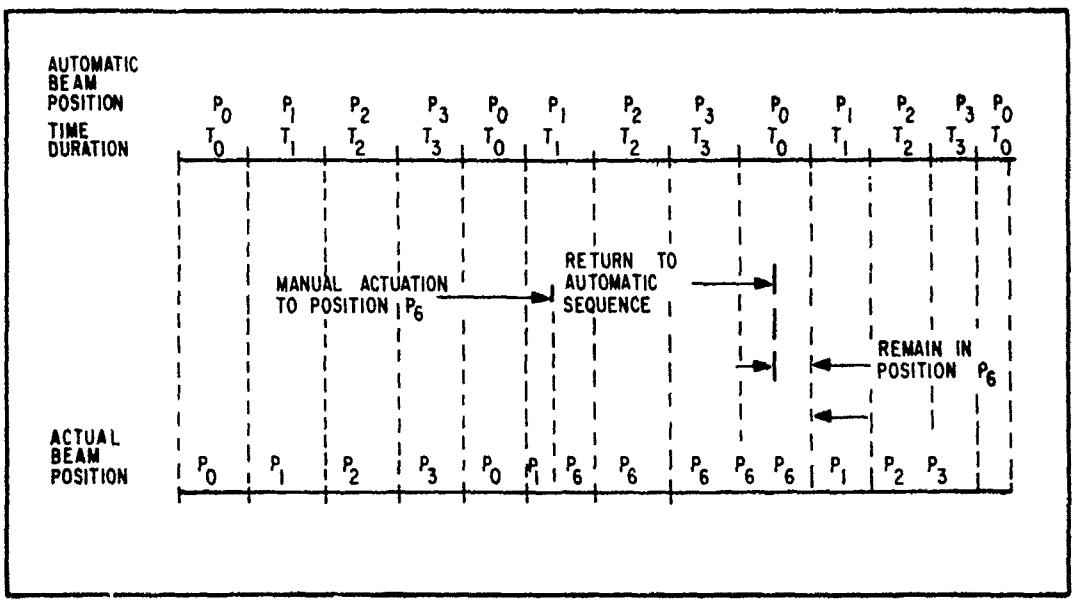

Figure 4-6 Switching Between Automatic Sequencing and Manual Position

If the controller was in the operate mode before the manual mode was selected, returning to the operate mode will cause the controller to pick up at the next time sector and continue with the automatic sequence. Note, when the time durations are short more than one sector may be crossed while in the manual mode.

5. LABORATORY SYSTEMS TESTS

The series of tests described below were conducted on the array assembly and control console to verify their electrical performance and capability to survive the environment to be encountered during flight operations of the KC-135A.

Scale model antenna tests were also conducted using a one-tenth scale model of the Convair 880 which approximates the structure of the KC-135A. The results of these scale model tests can be used to evaluate effects of the presence of aircraft structure on the patterns of the full scale antennas when mounted on the aircraft.

5.1 PERFORMANCE TESTS - FULL SCALE ARRAY

5.1.1 Patterns

Performance of the steerable array assembly was verified prior to the commencement of environmental testing by running pattern tests as shown in Table 5-1. The principal plane patterns were taken on the antenna mounted on a 4 by 4 foot ground plane, as shown in Figure 5-1. As each beam position was selected, the ground plane was adjusted so that the principal cut orthogonal to the elevation cut passed through the peak of the main lobe of the selected beam position. Elevation cuts were taken to show the side lobe structure as well as the characteristics of the main beam. Data was recorded in polar form and is included in this report as indicated in the table.

Three beam positions were selected for comparison with the tenth scale antenna models. The conical patterns taken for these positions are shown in the second part of Table 5-1. Patterns were taken

Table 5-1

FULL SCALE PATTERN TESTS

PRINCIPAL-PLANE CUTS -- Full Scale (Flight) Antennas -- 4-Foot by 4-Foot Ground Plane:

Beam Position	Aircraft Azimuth	Coordinates Elevation (Degrees)	S/N 001	S/N 002
1	0	Var	Figure 5-2	Figure 5-20
	Var	9.7	Figure 5-3	
2	0	Var	Figure 5-4	Figure 5-21
	Var	19.2	Figure 5-5	
3	0	Var	Figure 5-6	Figure 5-22
	Var	28.6	Figure 5-7	
4	0	Var	Figure 5-8	Figure 5-23
	Var	38.1	Figure 5-9	
5	0	Var	Figure 5-10	Figure 5-24
	Var	47.5	Figure 5-11	
6	0	Var	Figure 5-12	Figure 5-25
	Var	56.9	Figure 5-13	
7	0	Var	Figure 5-14	Figure 5-26
	Var	66.4	Figure 5-15	
8	0	Var	Figure 5-16	Figure 5-27
	Var	75.8	Figure 5-17	
9	0	Var	Figure 5-18	Figure 5-28
	Var	85.3	Figure 5-19	

CONICAL CUTS -- Full Scale Antenna -- 4-Foot by 4-Foot Ground Plane:

Beam Position	Azimuth	Elevation (Degrees)	S/N 002
1	Var	-10 to 20	Figure 5-29 to 5-34
2	Var	6 to 35	Figure 5-35 to 5-39
4	Var	20 to 55	Figure 5-40 to 5-46

with the ground plane adaptor set at an angle which brought the coordinate system of the antenna coincident with that existing after installation on the aircraft. The table may again be used as a guide to data included in this report.

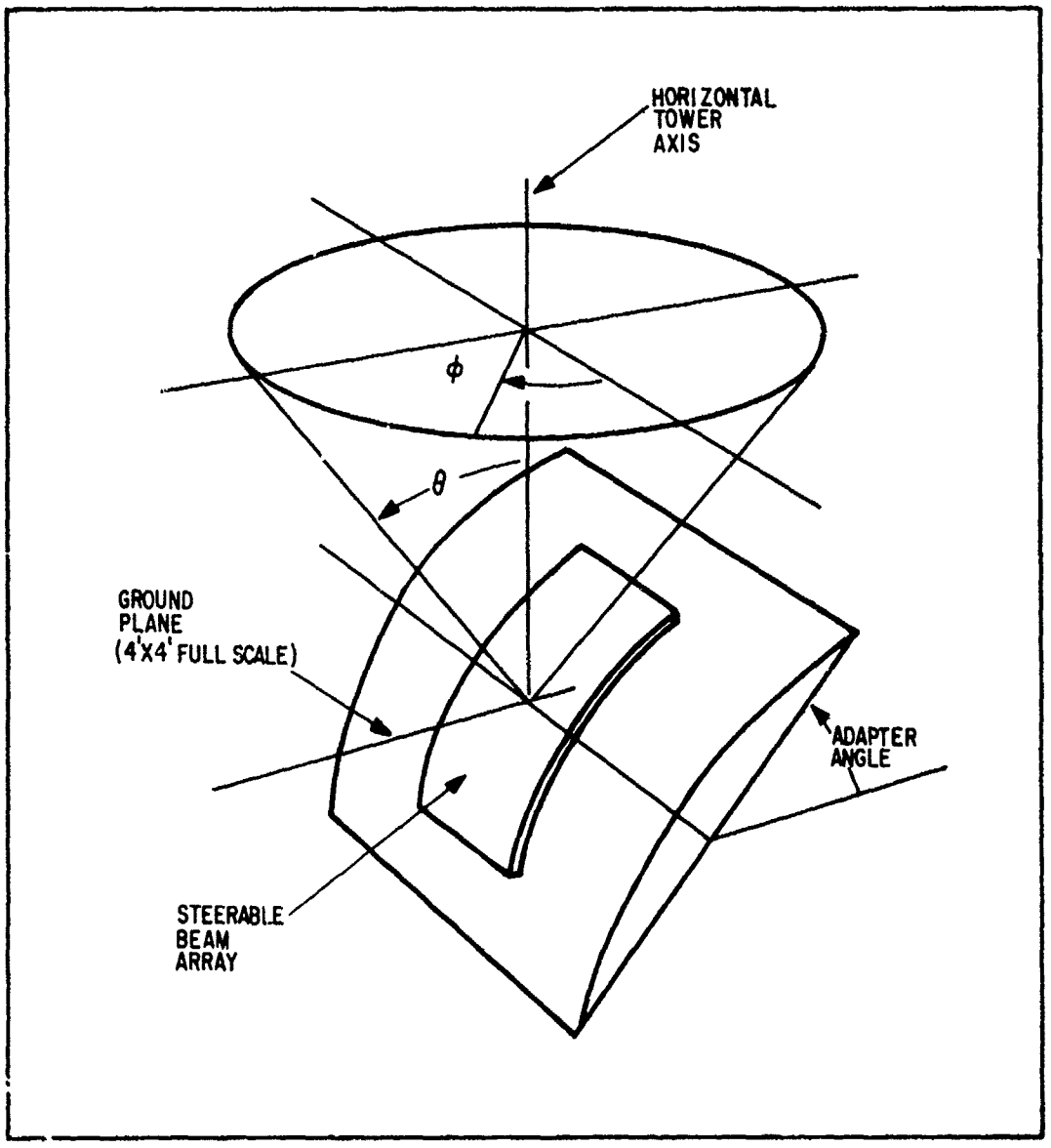

Figure 5-1 Antenna Mounted on 4- x 4-Foot Ground Plane

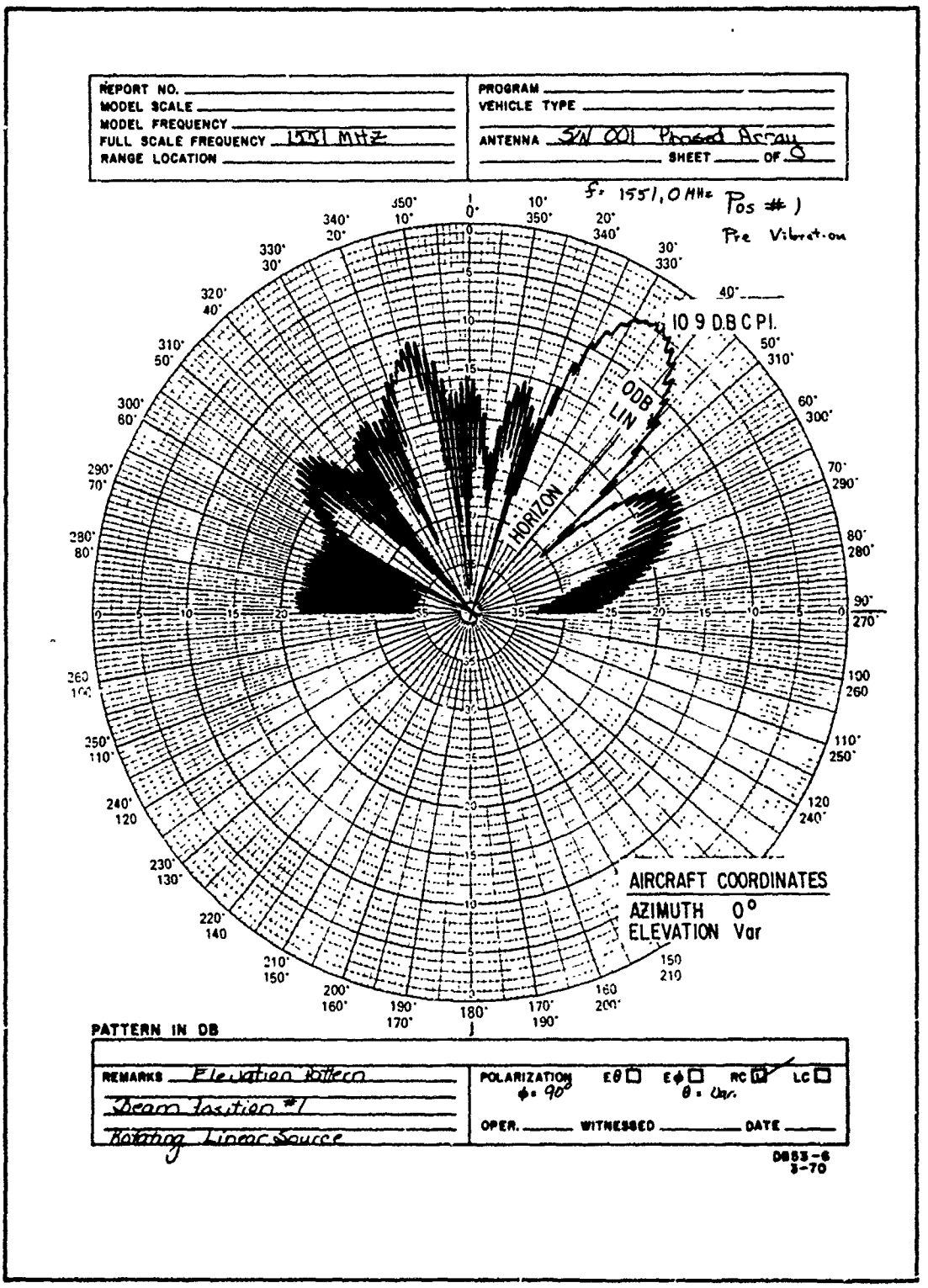

Figure 5-2 Elevation Pattern Beam Position 1 S/N 001

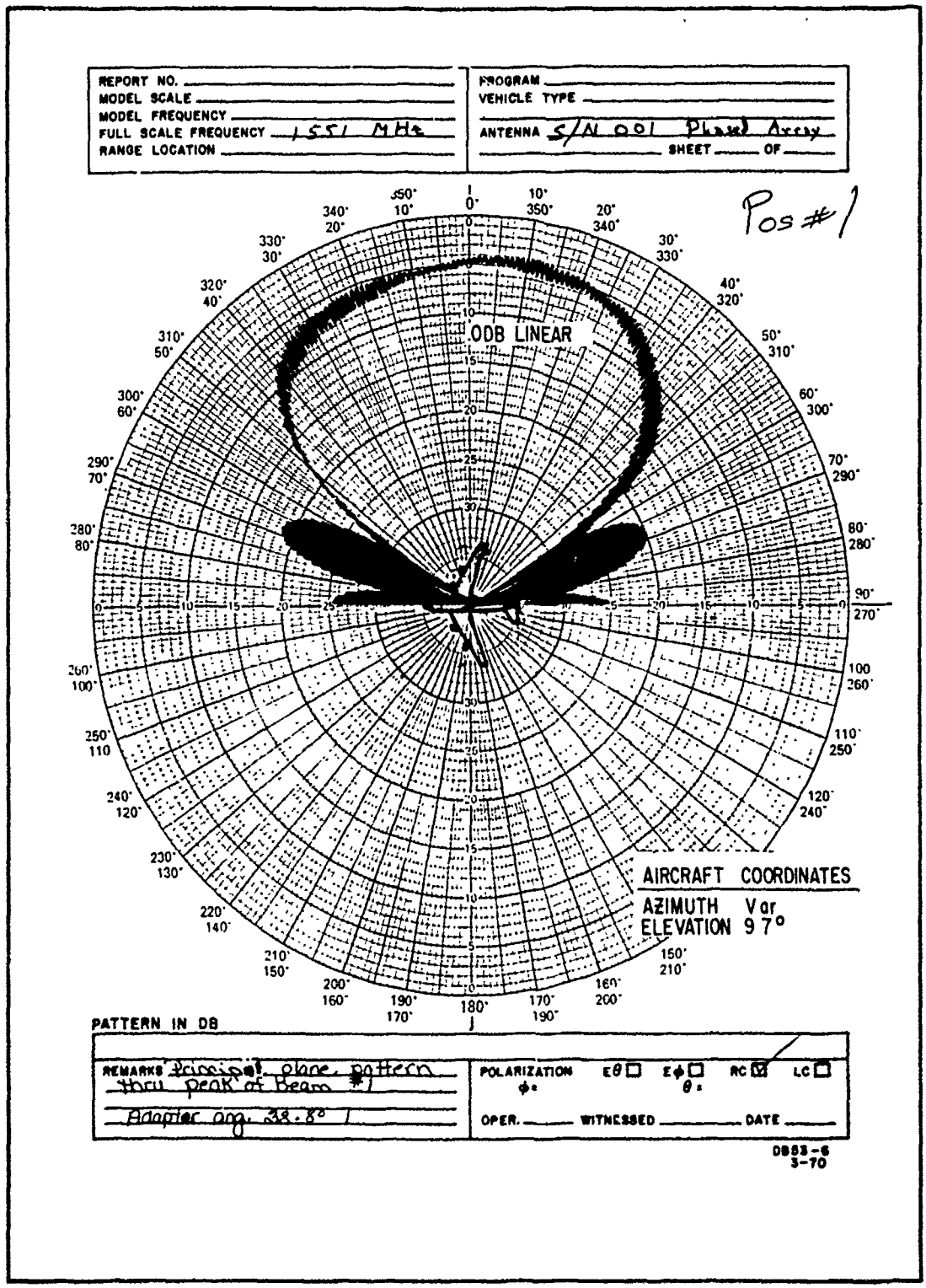

Figure 5-3 Azimuth Pattern Beam Position 1 S/N 001

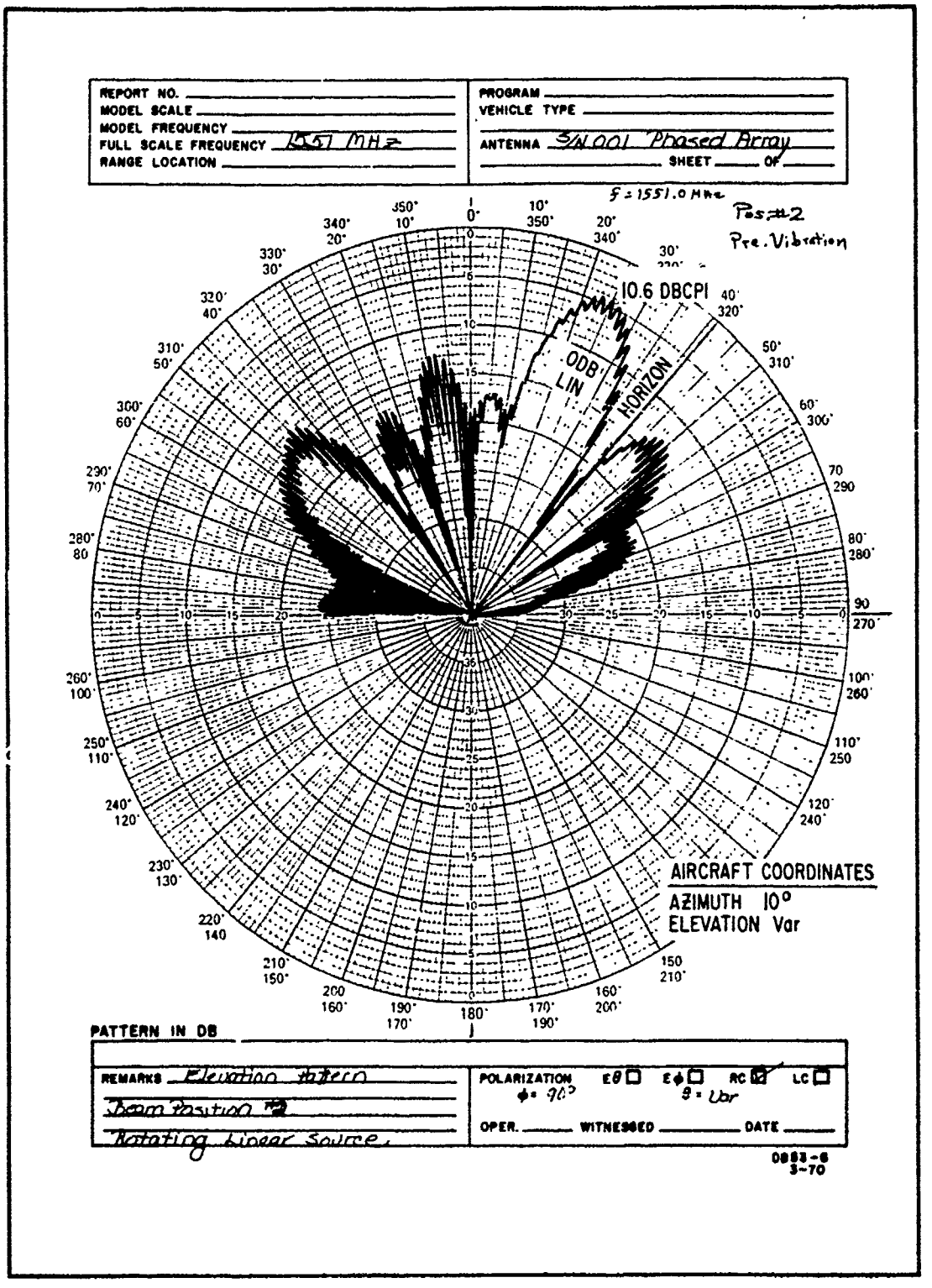

Figure 5-4 Azimuth Pattern Beam Position 2 S/N 001

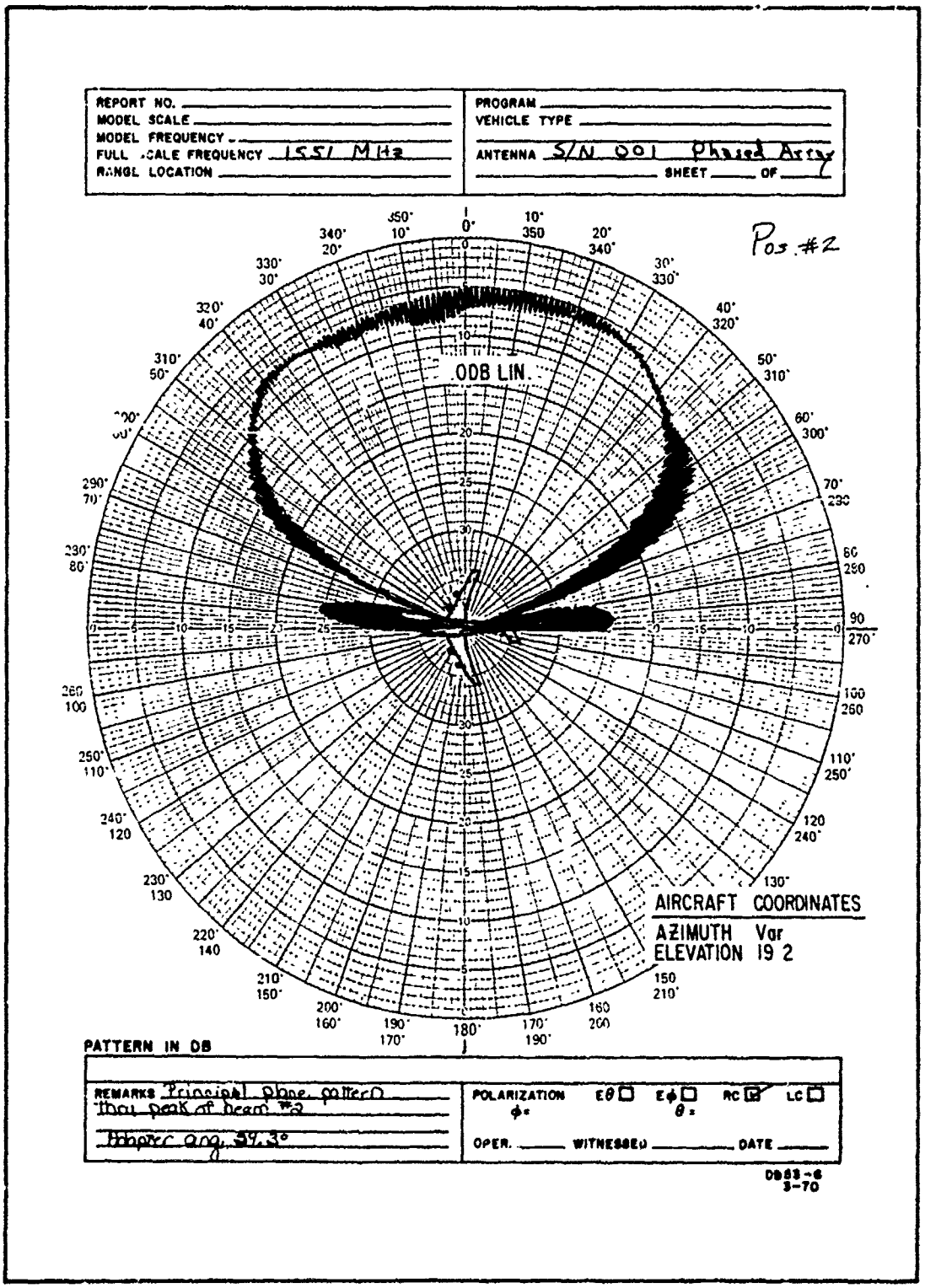

Figure 5-5 Azimuth Pattern Beam Position 2 S/N 001

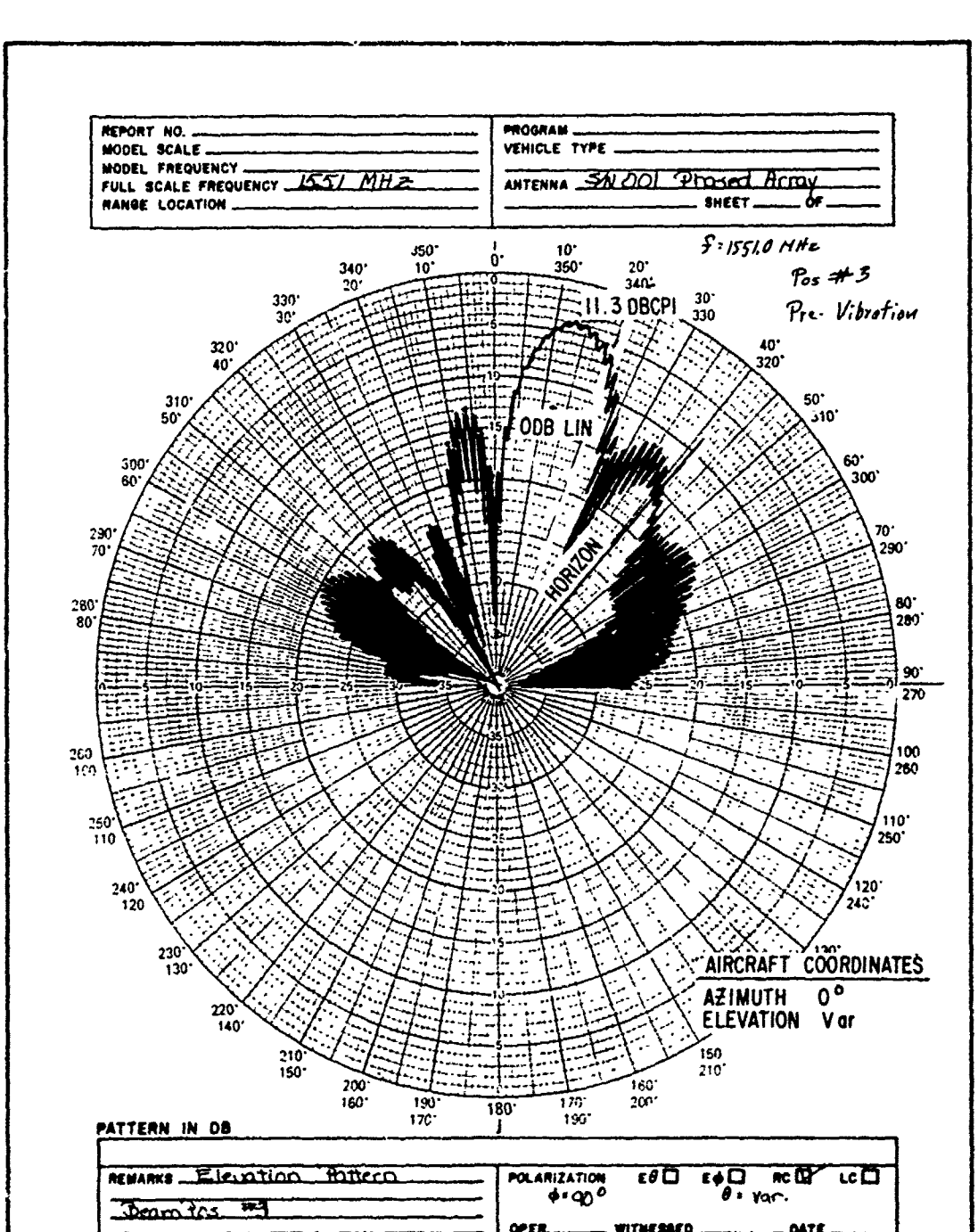

Figure 5-6 Elevation Pattern Beam Position 3 S/N 001

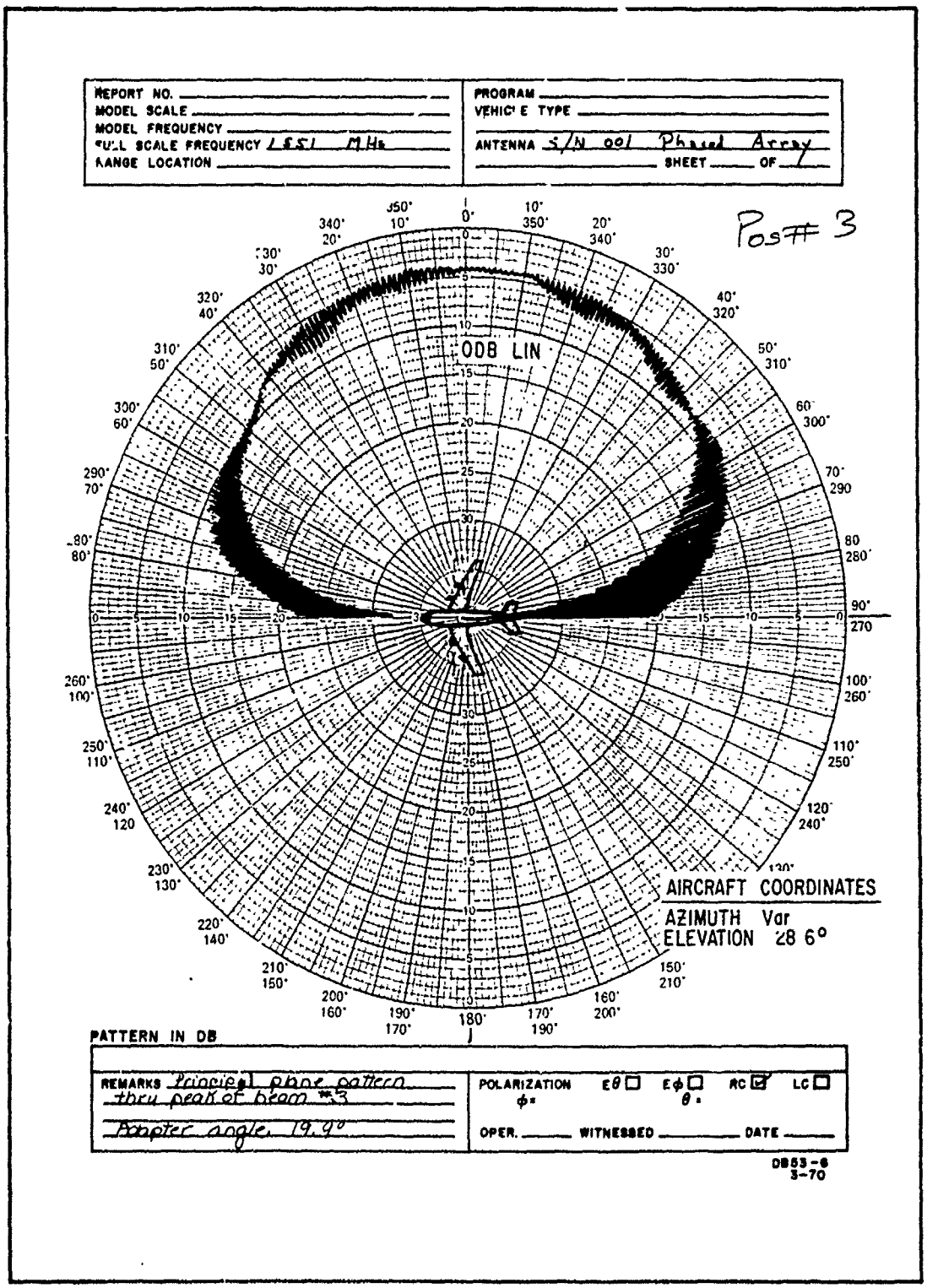

Figure 5-7 Azimuth Pattern Beam Position 3 S/N 001

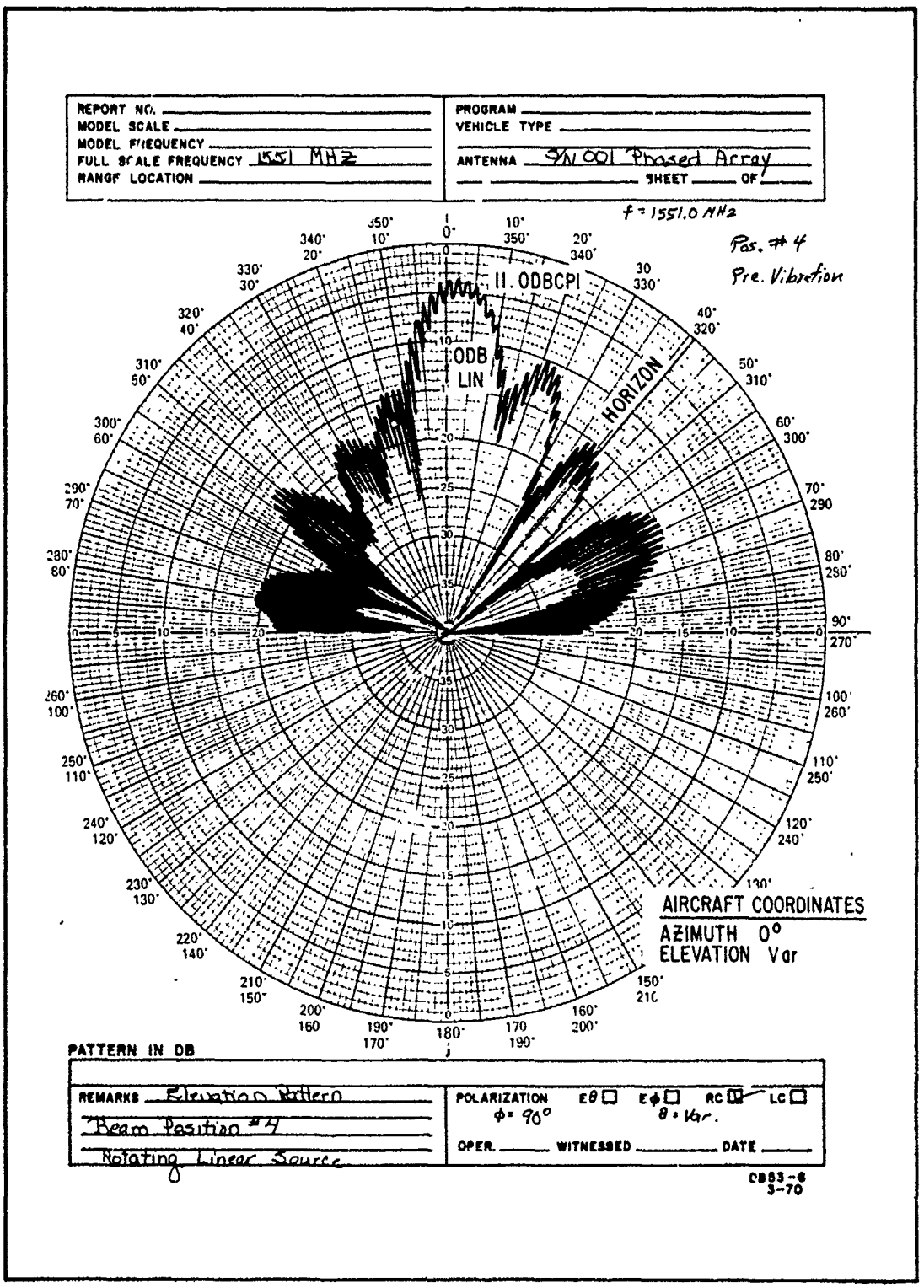

Figure 5-8 Elevation Pattern Beam Position 4 S/N 001

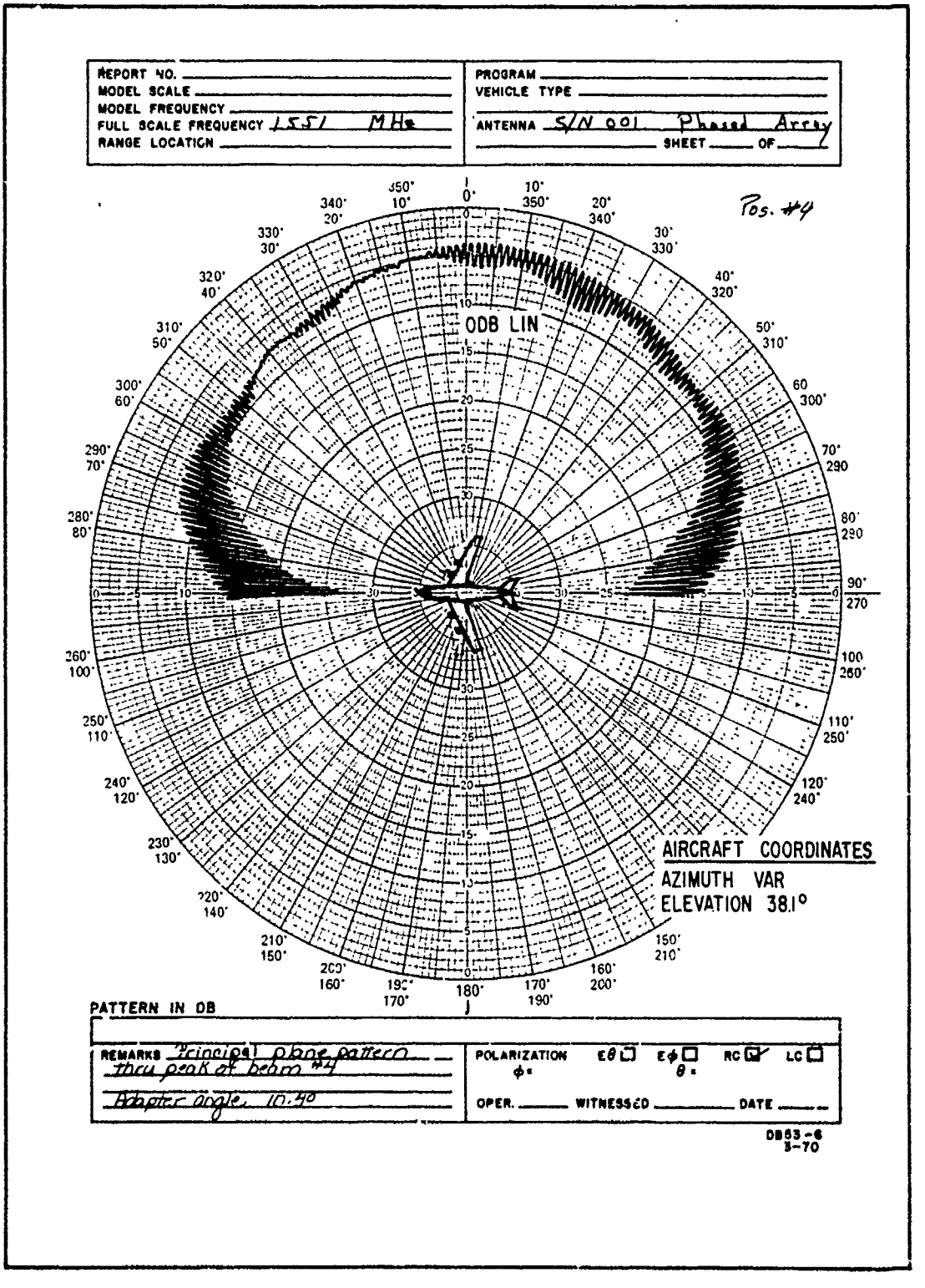

Figure 5-9 Azimuth Pattern Beam Position 4 S/N 001

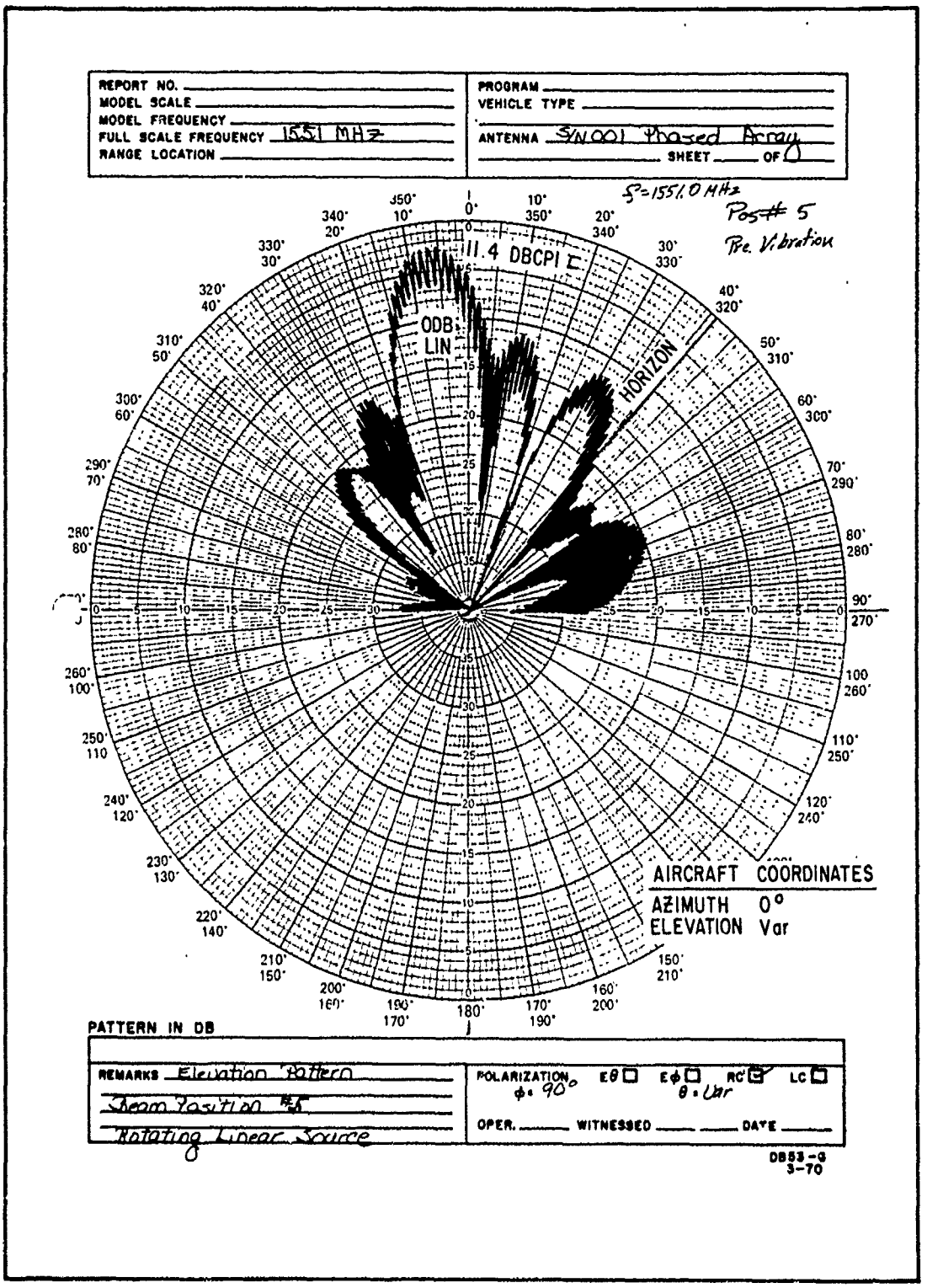

Figure 5-10 Elevation Pattern Beam Position 5 S/N 001

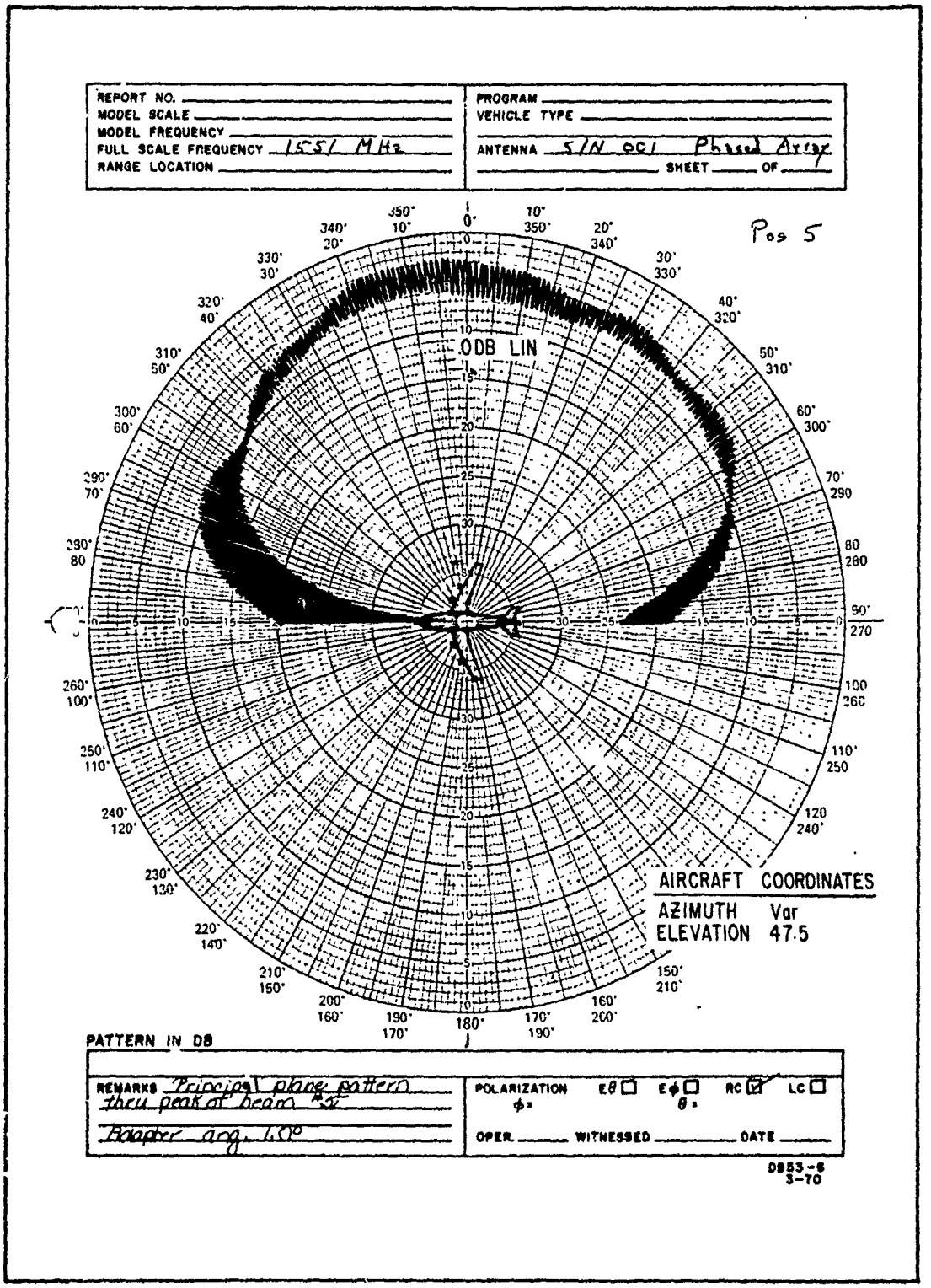

Figure 5-11 Azimuth Pattern. Beam Position 5 S/N 001

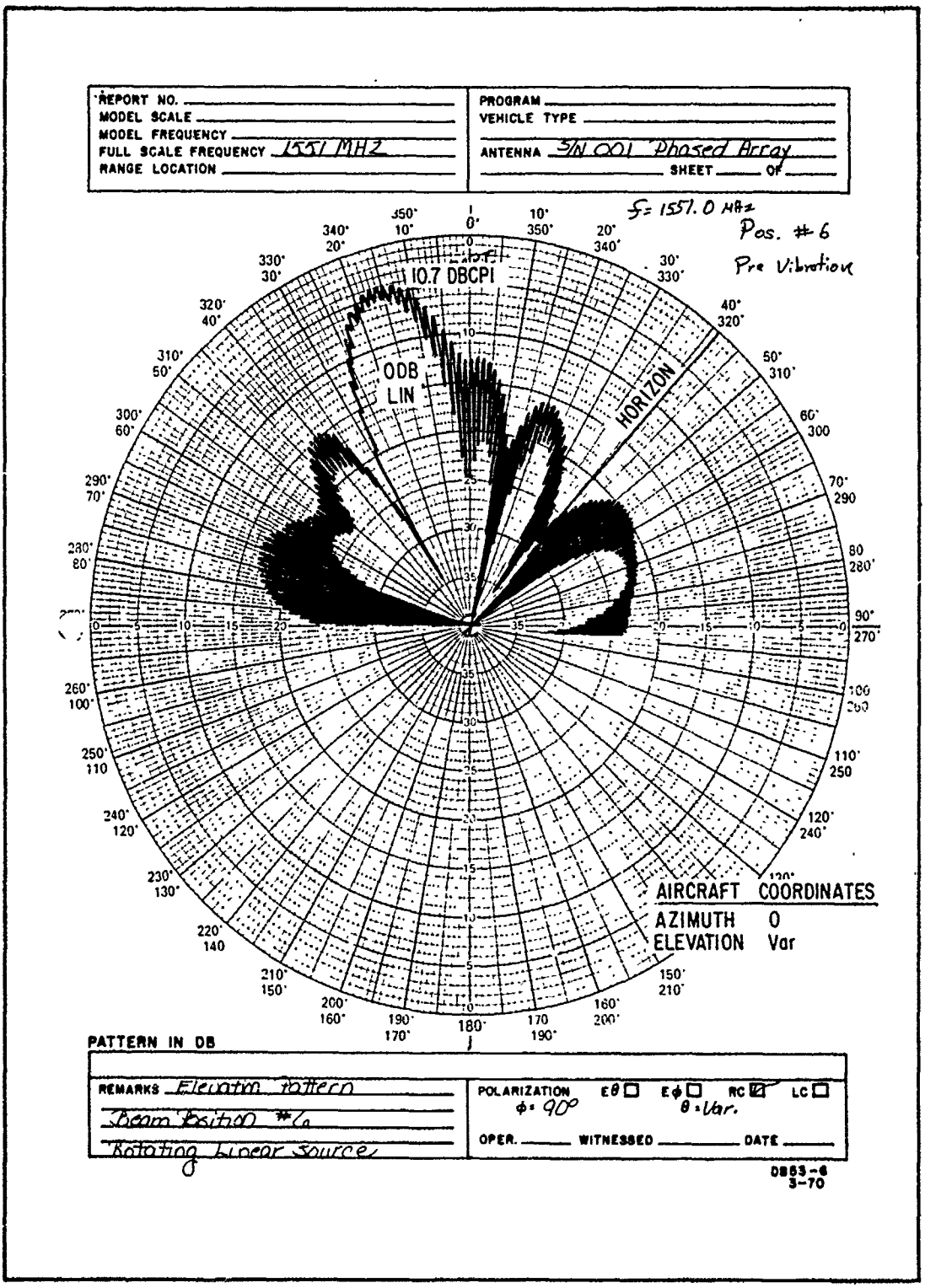

Figure 5-12 Elevation Pattern Beam Position 6 S/N 001

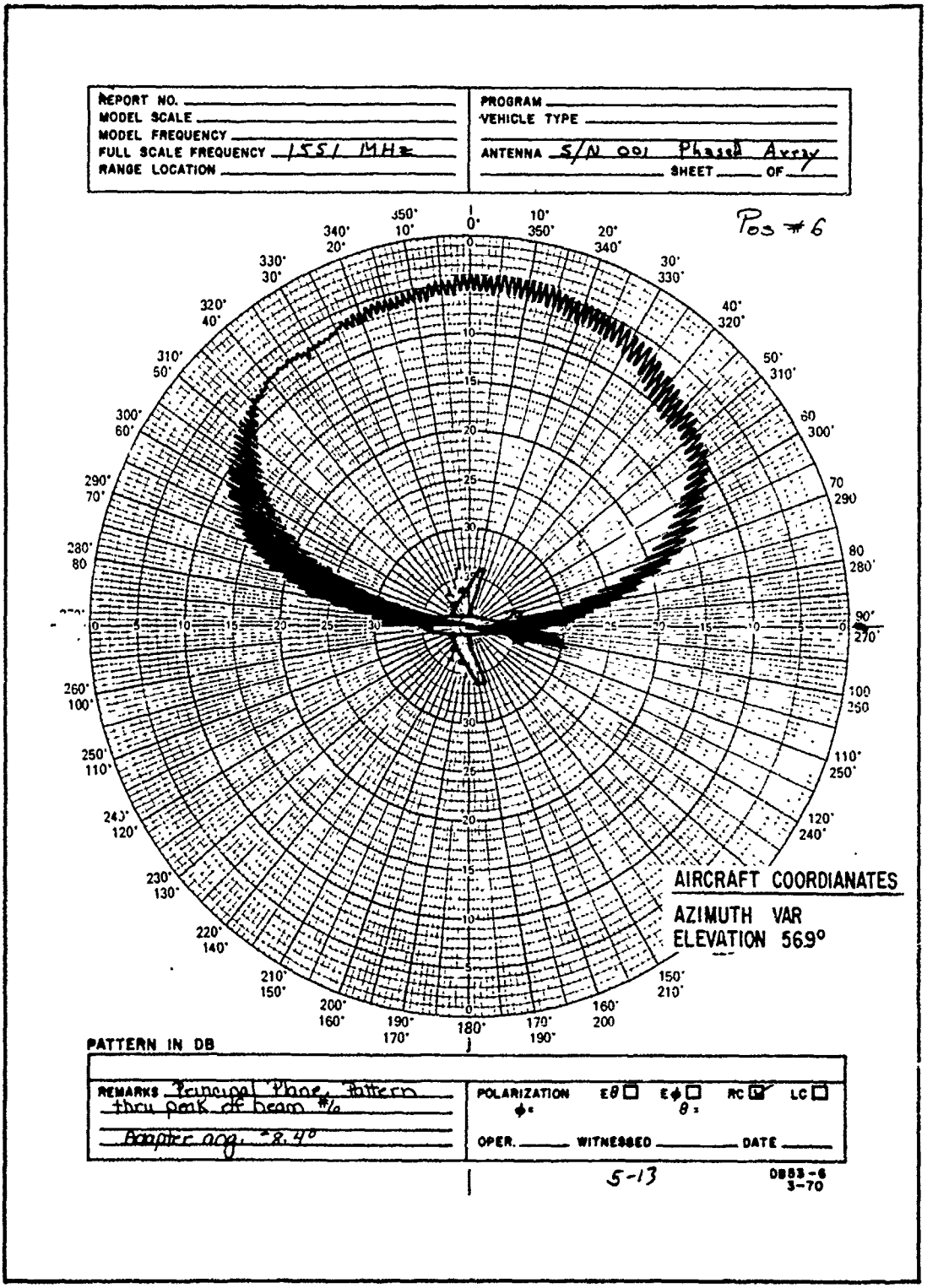

Figure 5-13 Azimuth Pattern Beam Position 6 S/N 001

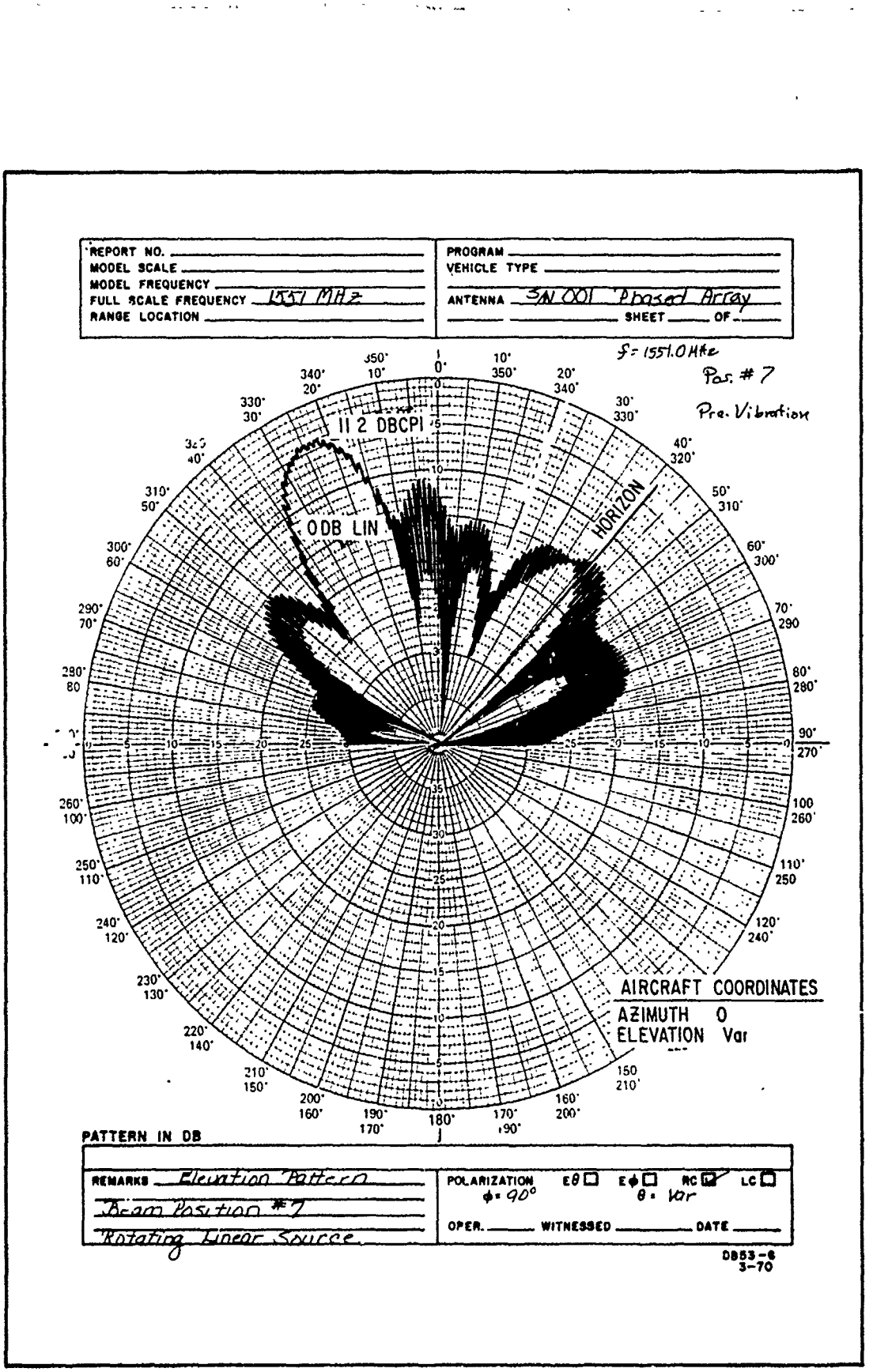

Figure 5-14 Elevation Pattern Beam Position 7 S/N 001

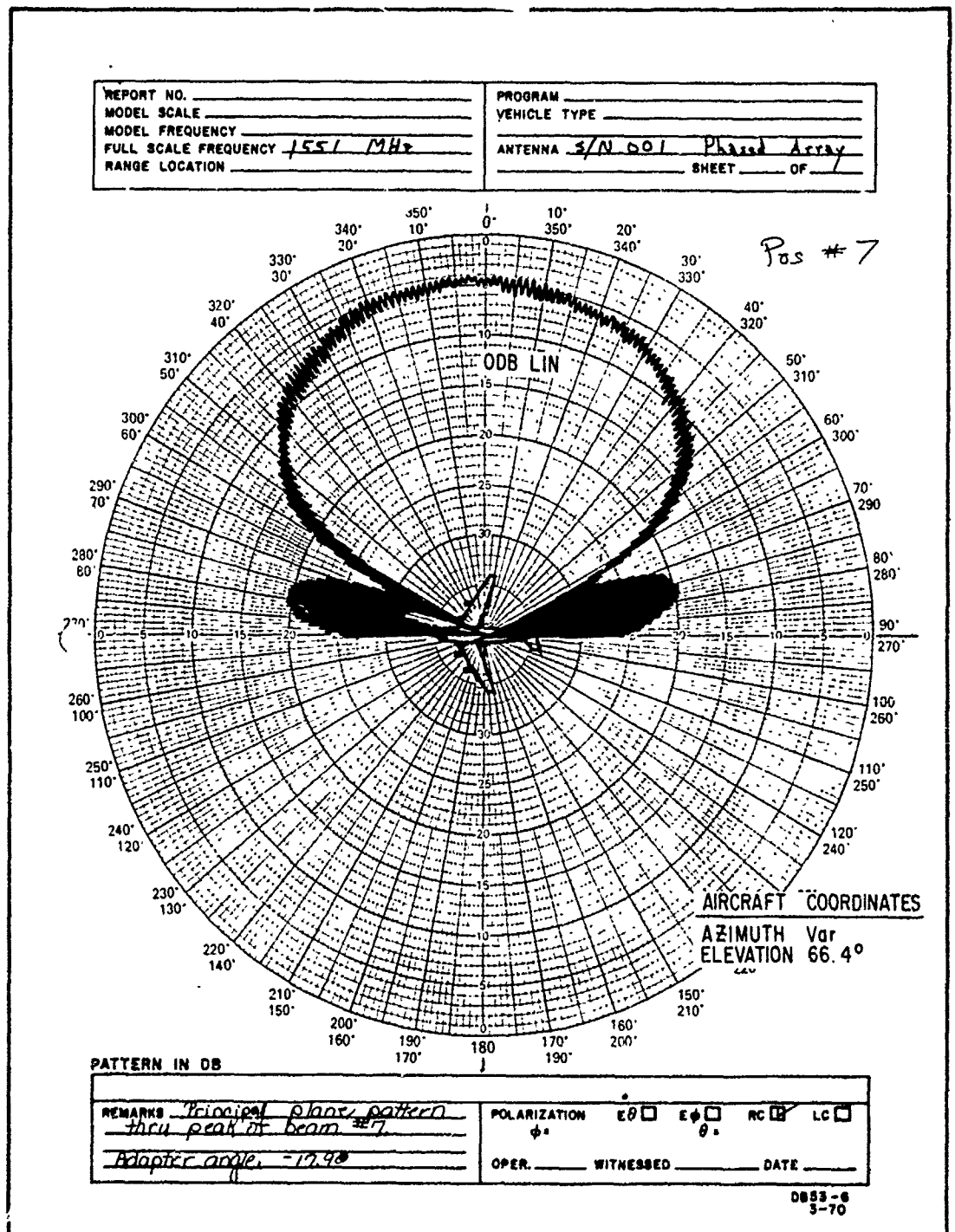

Figure 5-15 Azimuth Pattern Beam Position 7 S/N 001

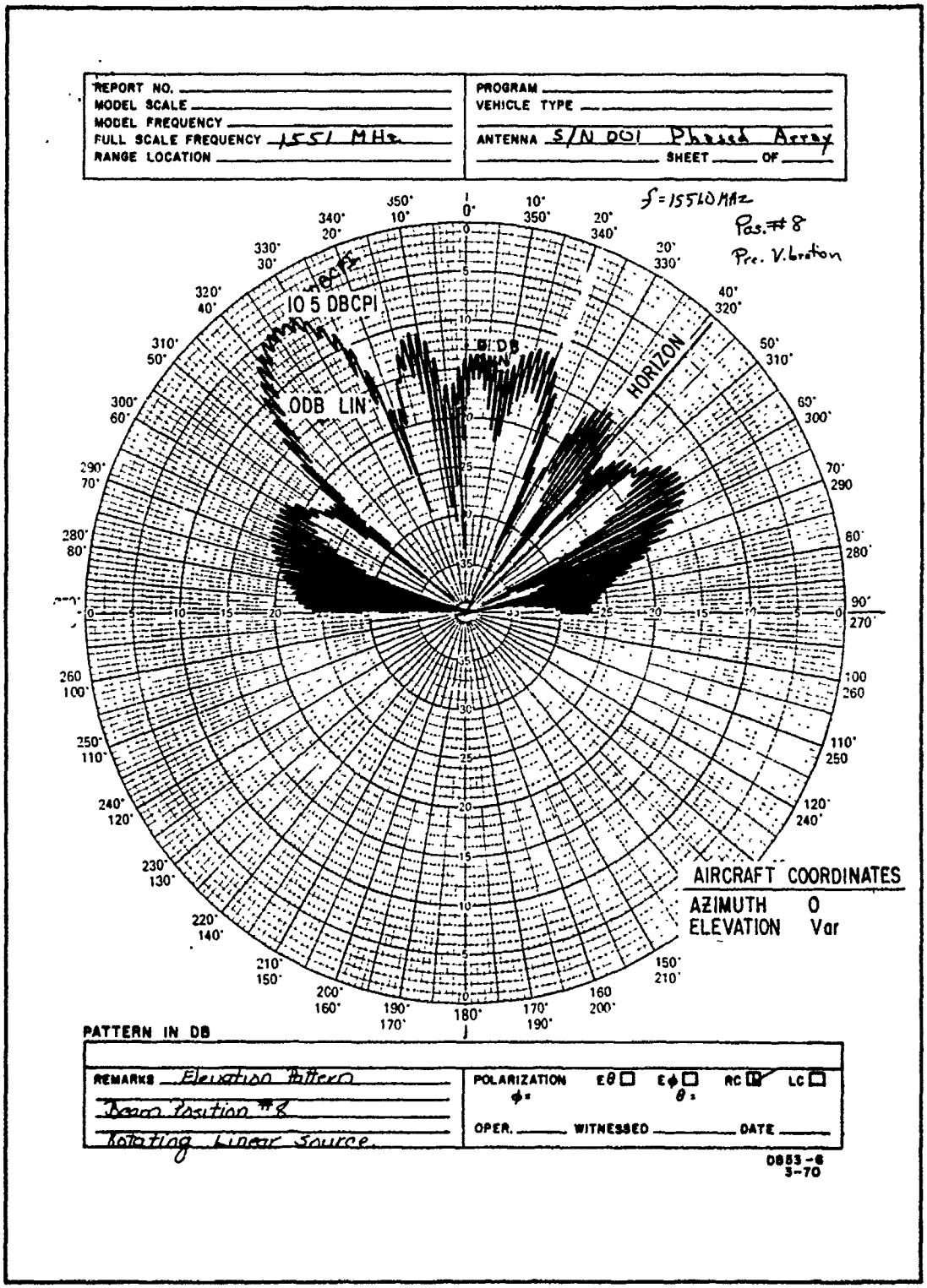

Figure 5-16 Elevation Pattern Beam Position 8 S/N 001

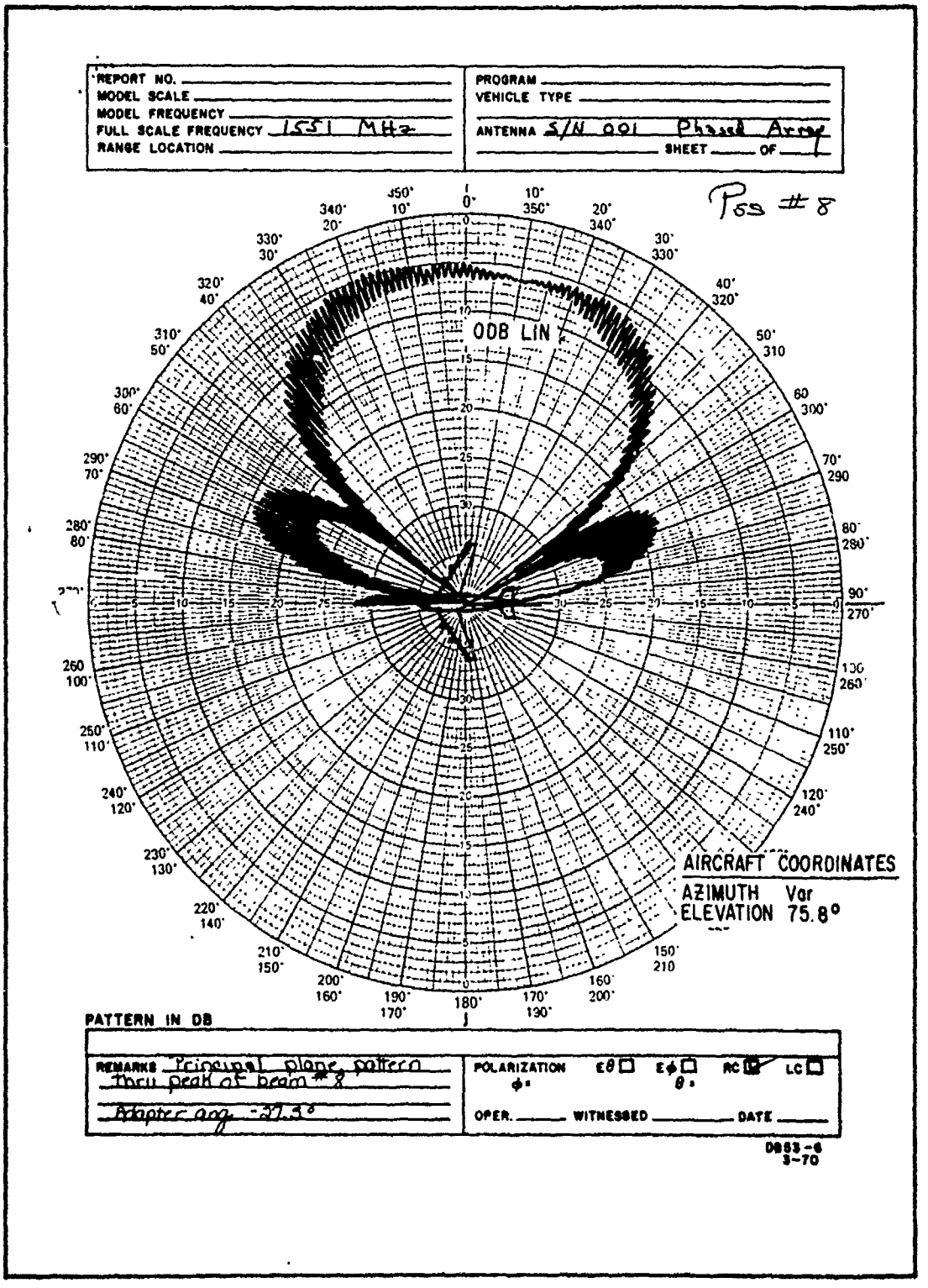

Figure 5-17 Azimuth Pattern Beam Position 8 S/N 001

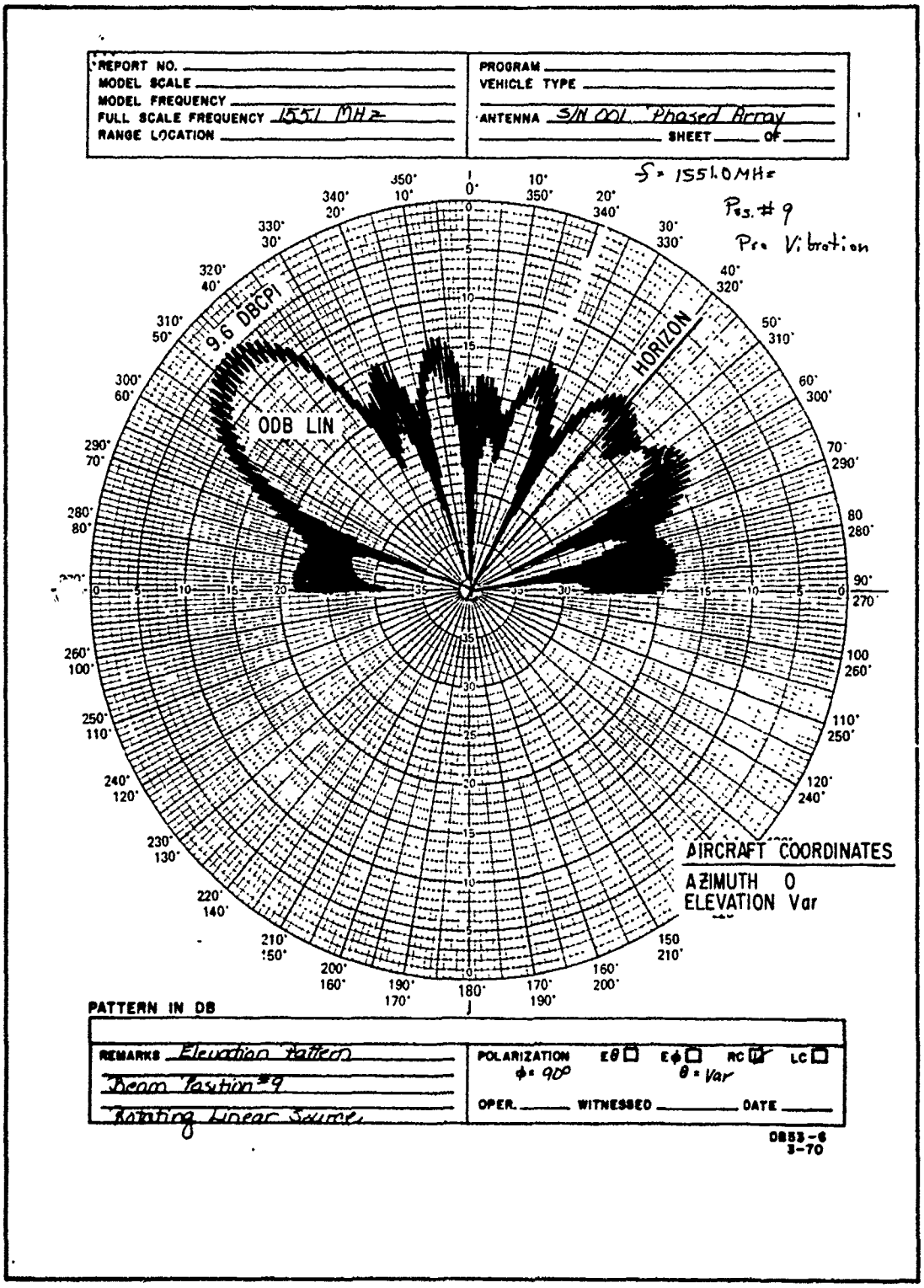

Figure 5-18 Elevation Pattern Beam Position 9 S/N 001

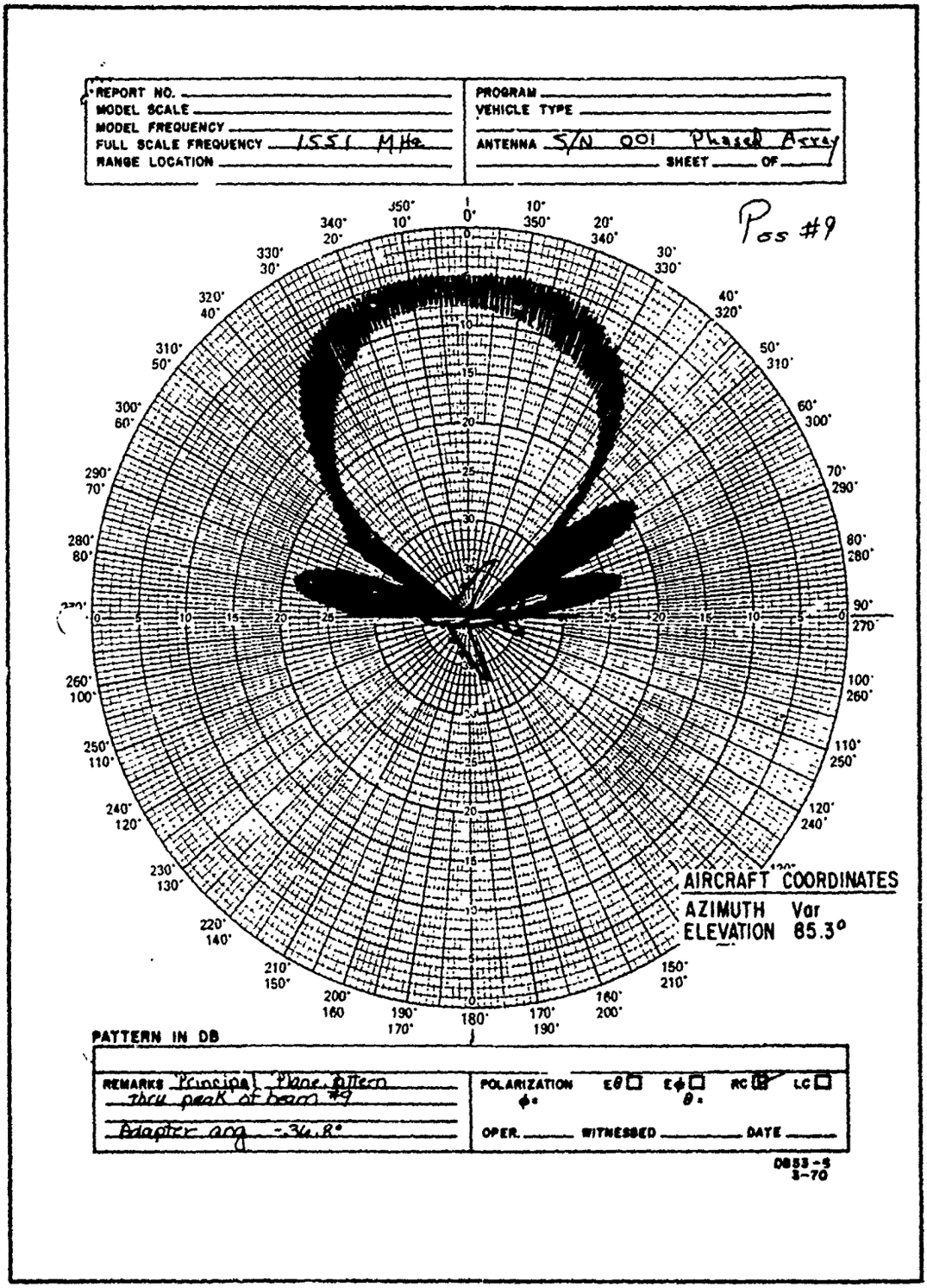

Figure 5-19 Azimuth Pattern Beam Position 9 S/N 001

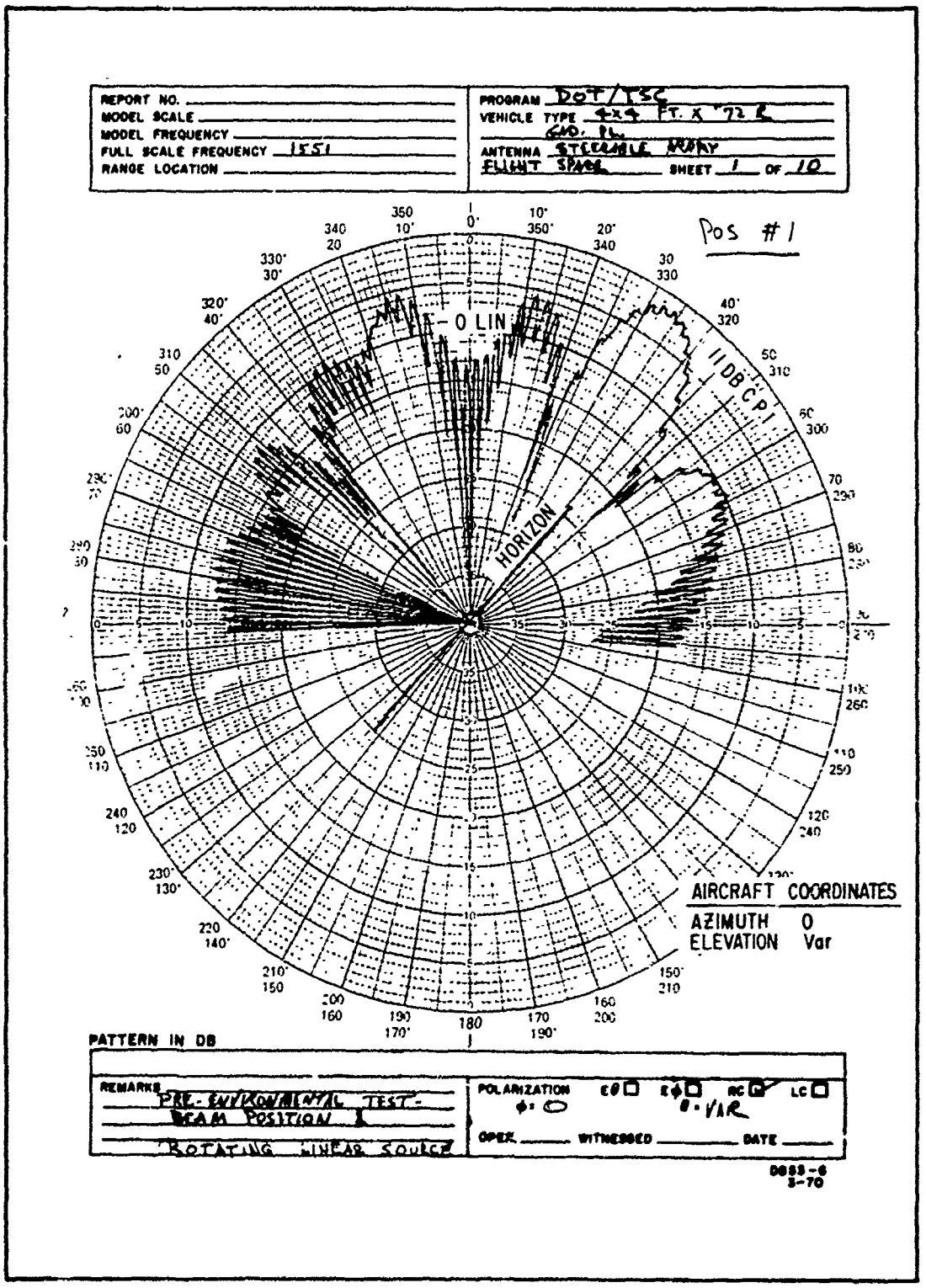

Figure 5-20 Elevation Pattern Beam Position 1 S/N 002

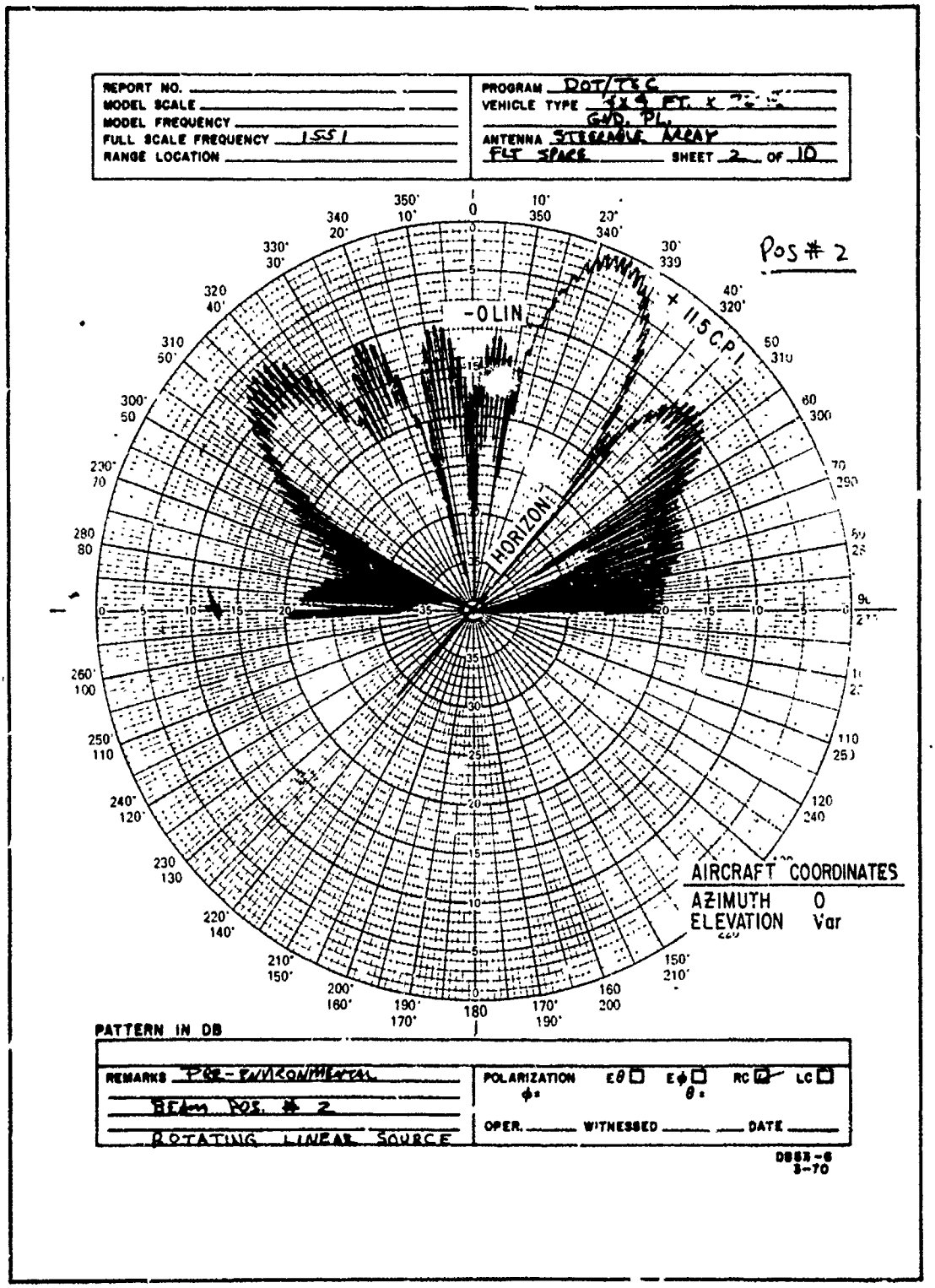

Figure 5-21 Elevation Pattern Beam Position 2 S/N 002

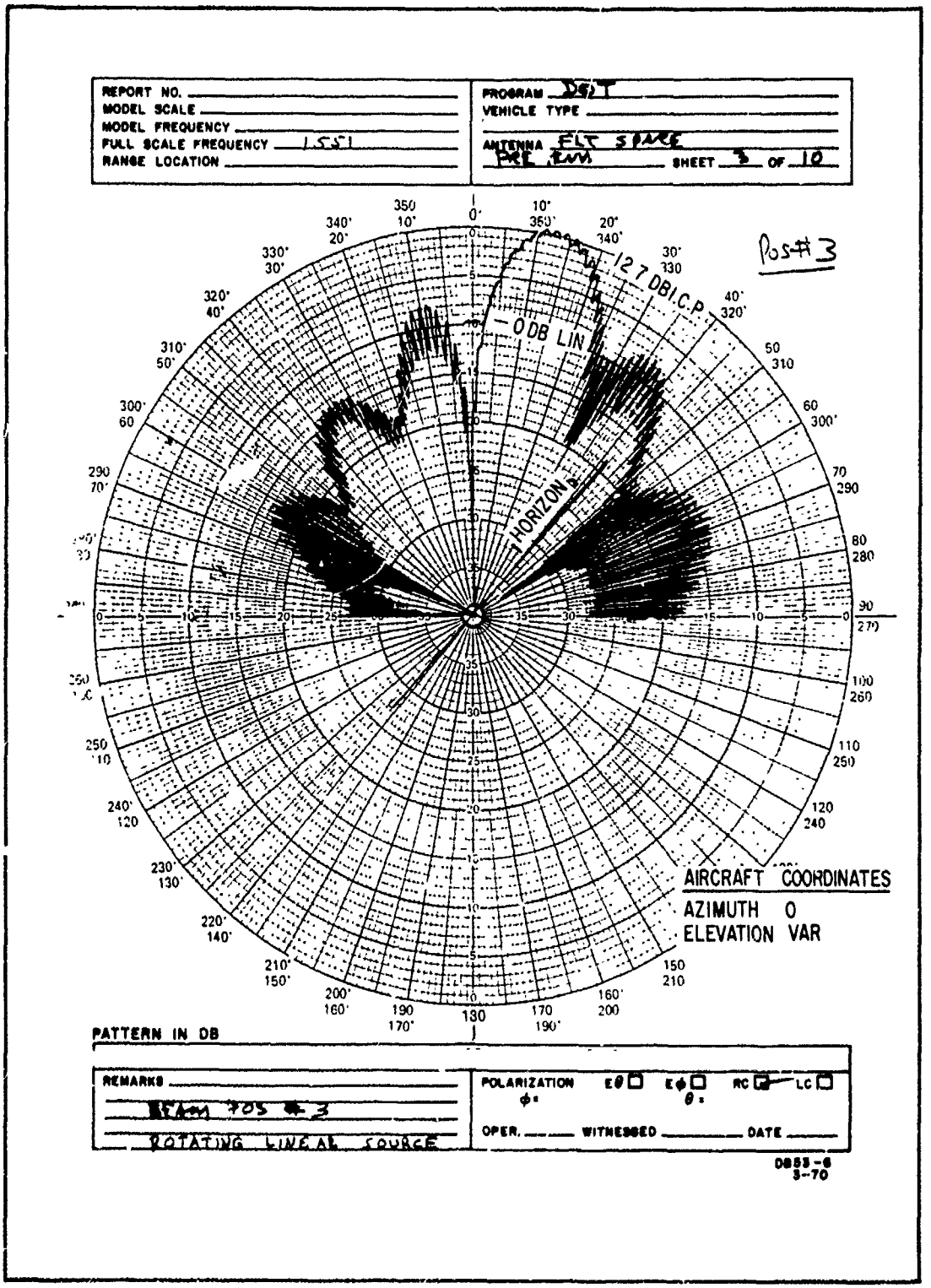

Figure 5-22 Elevation Pattern Beam Position 3 S/N 002

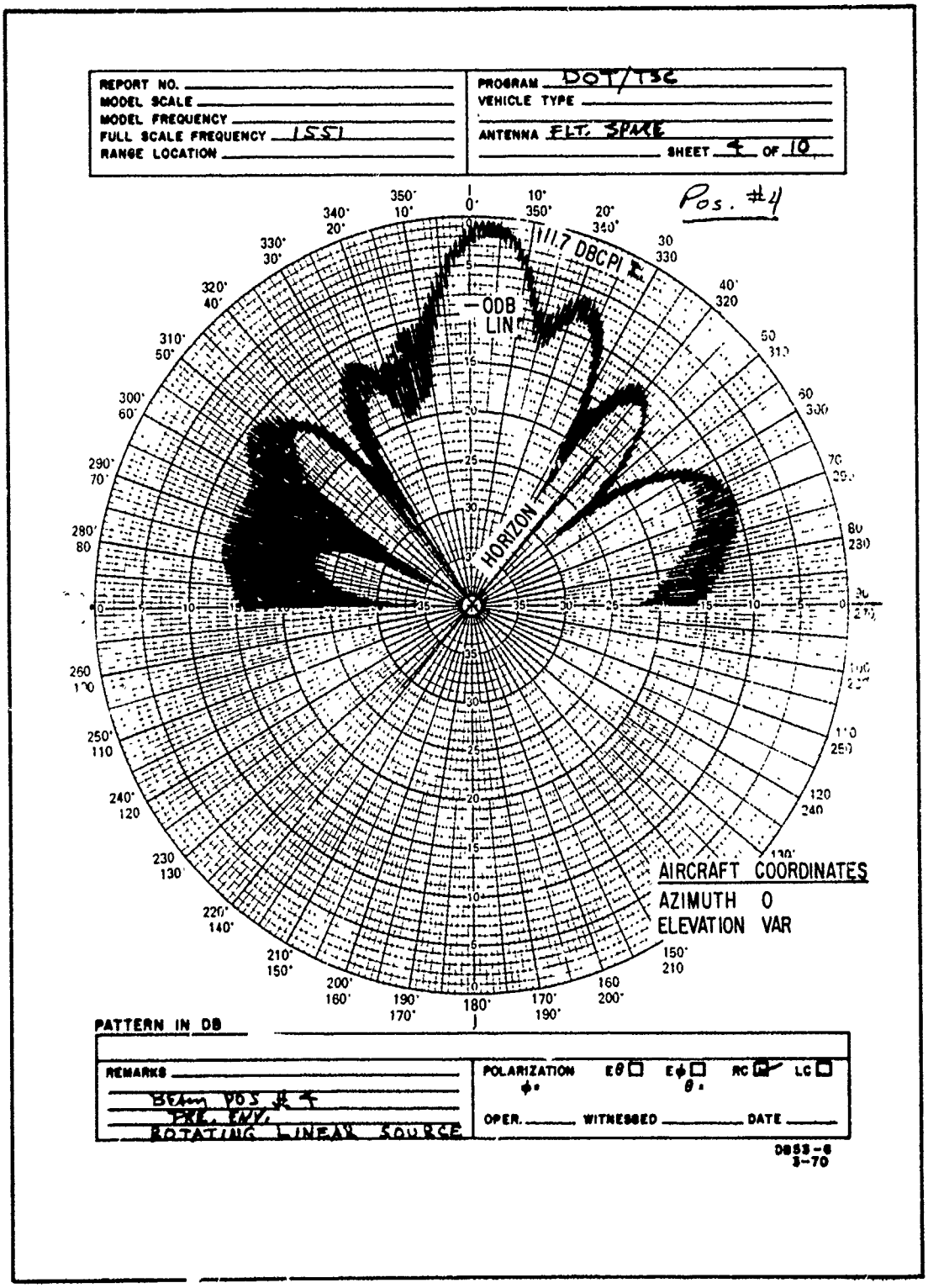

Figure 5-23 Elevation Pattern Beam Position 4 S/N 002

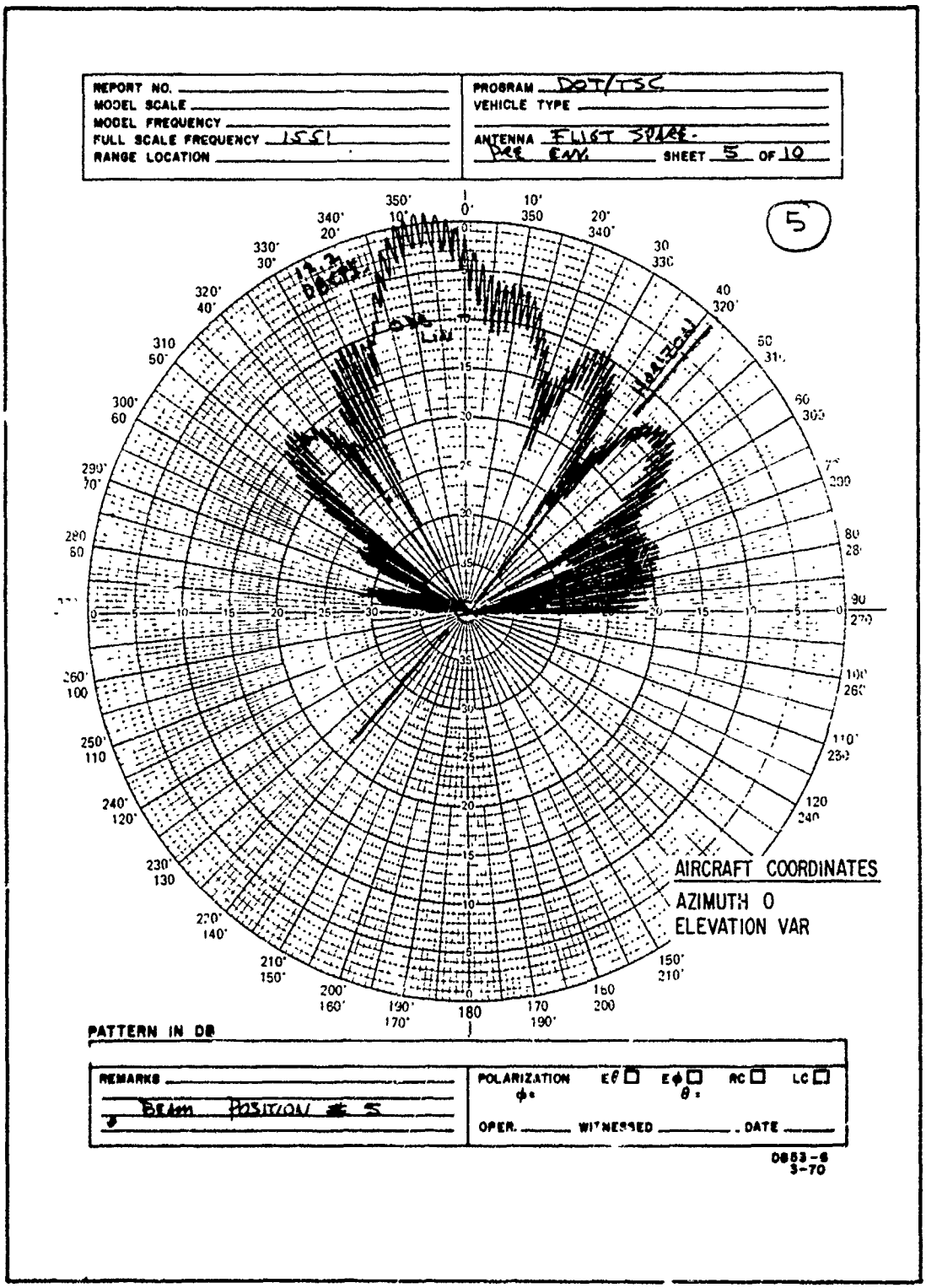

Figure 5-24 Elevation Pattern Beam Position 5 S/N 002

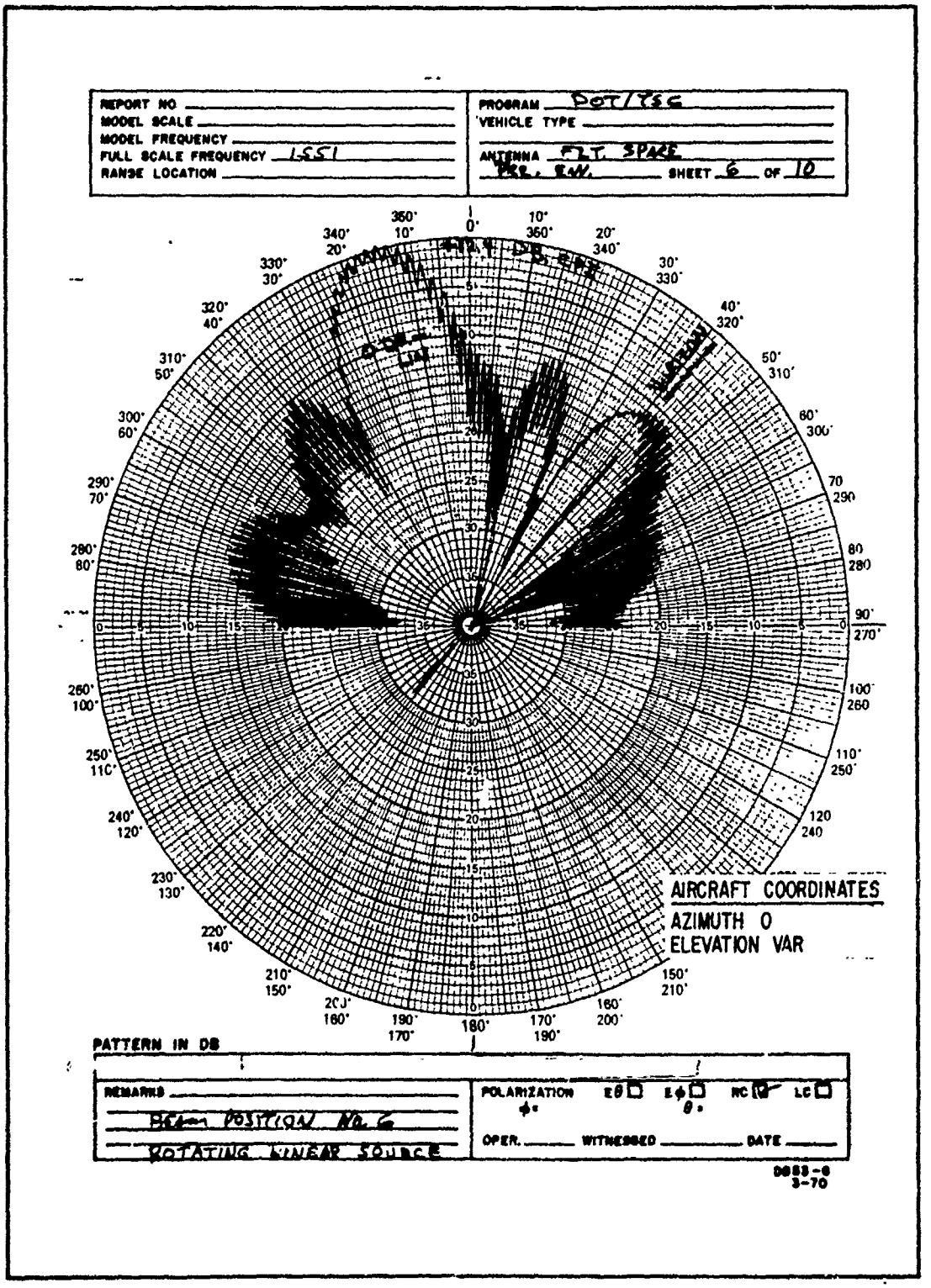

Figure 5-25 Elevation Pattern Beam, Position 6 S/N J02

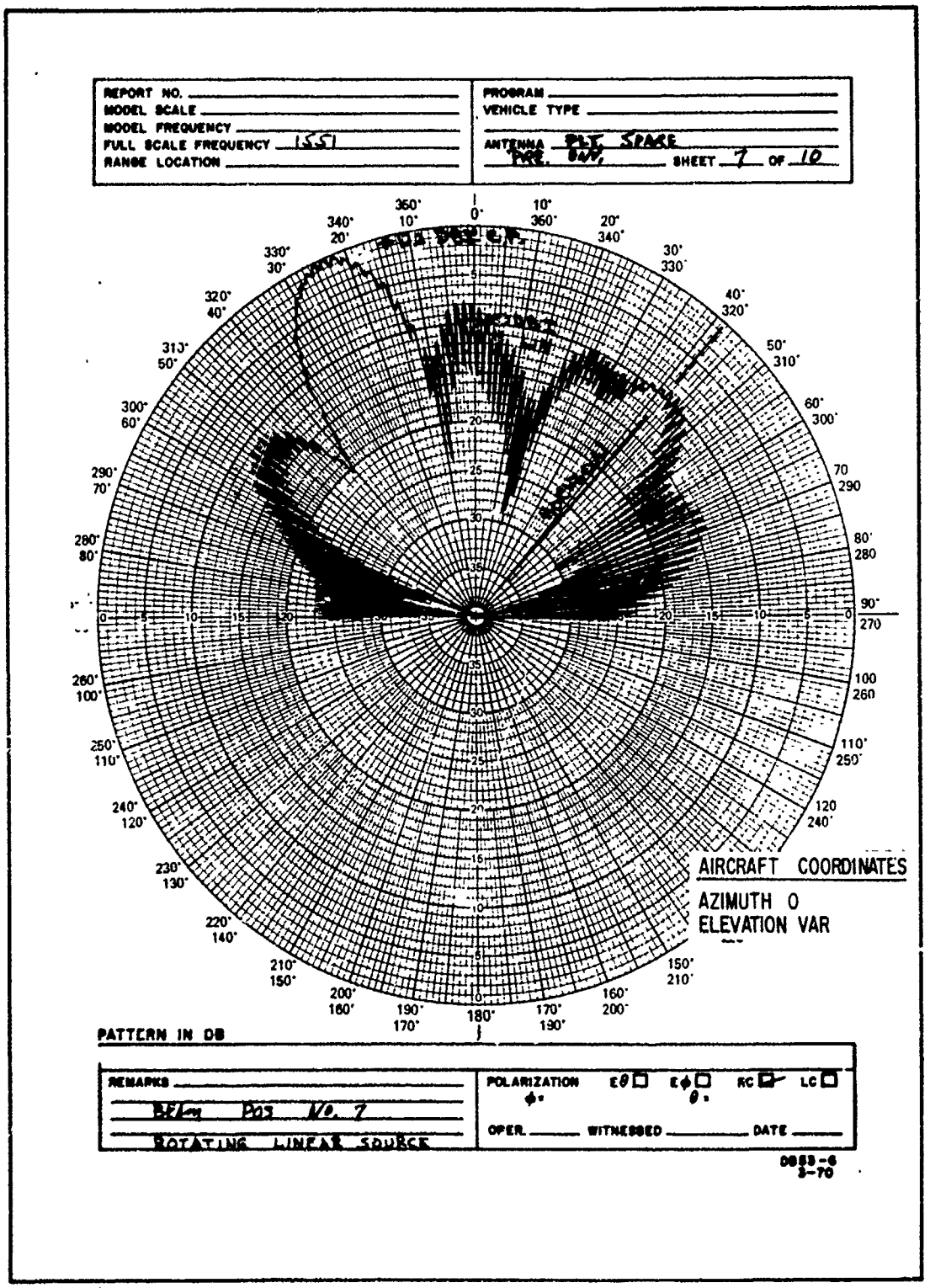

Figure 5-26 Elevation Pattern Beam Position 7 S/N 002

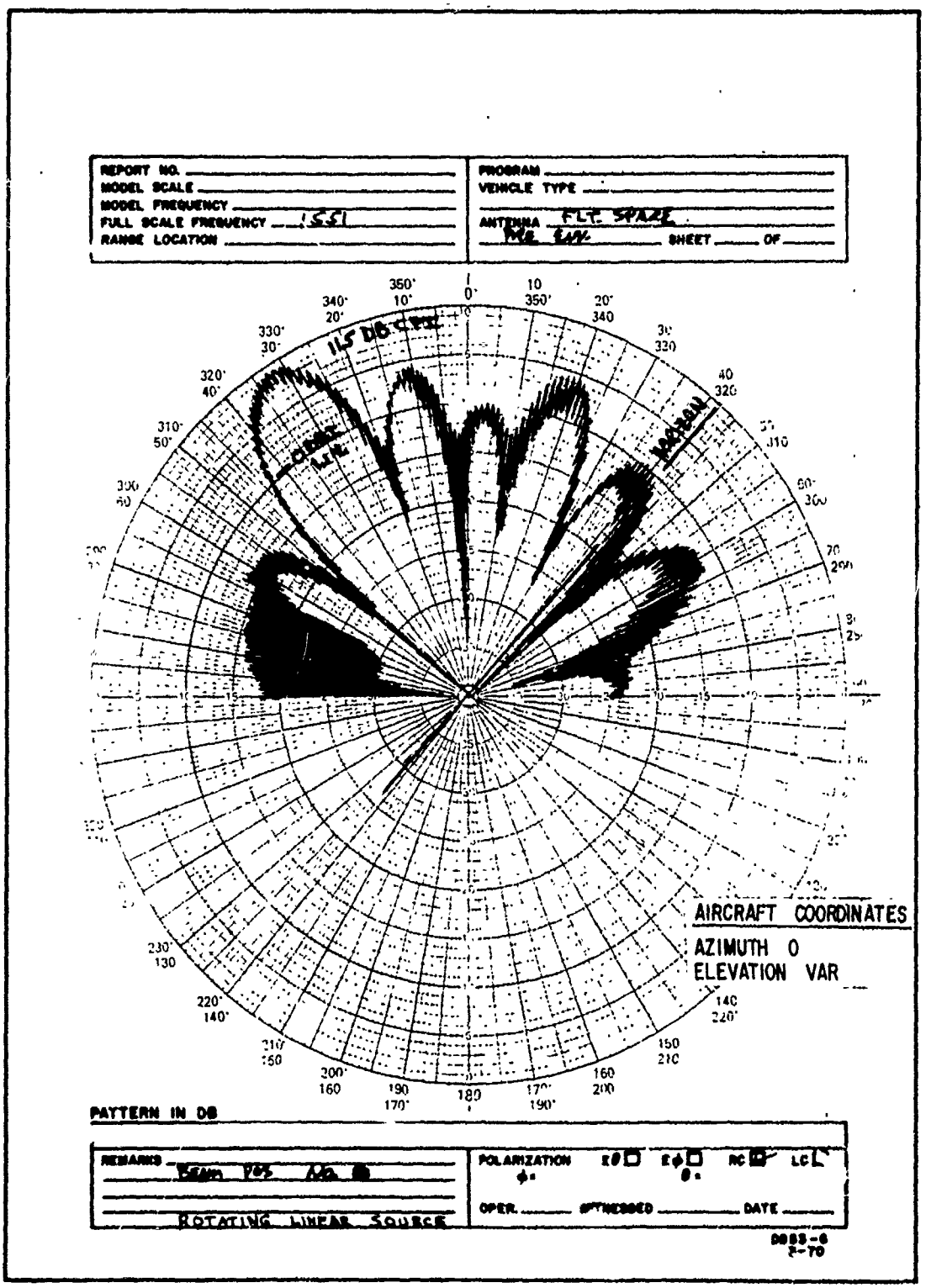

Figure 5-27 Elevation Pattern Beam Position 8 S/N 002

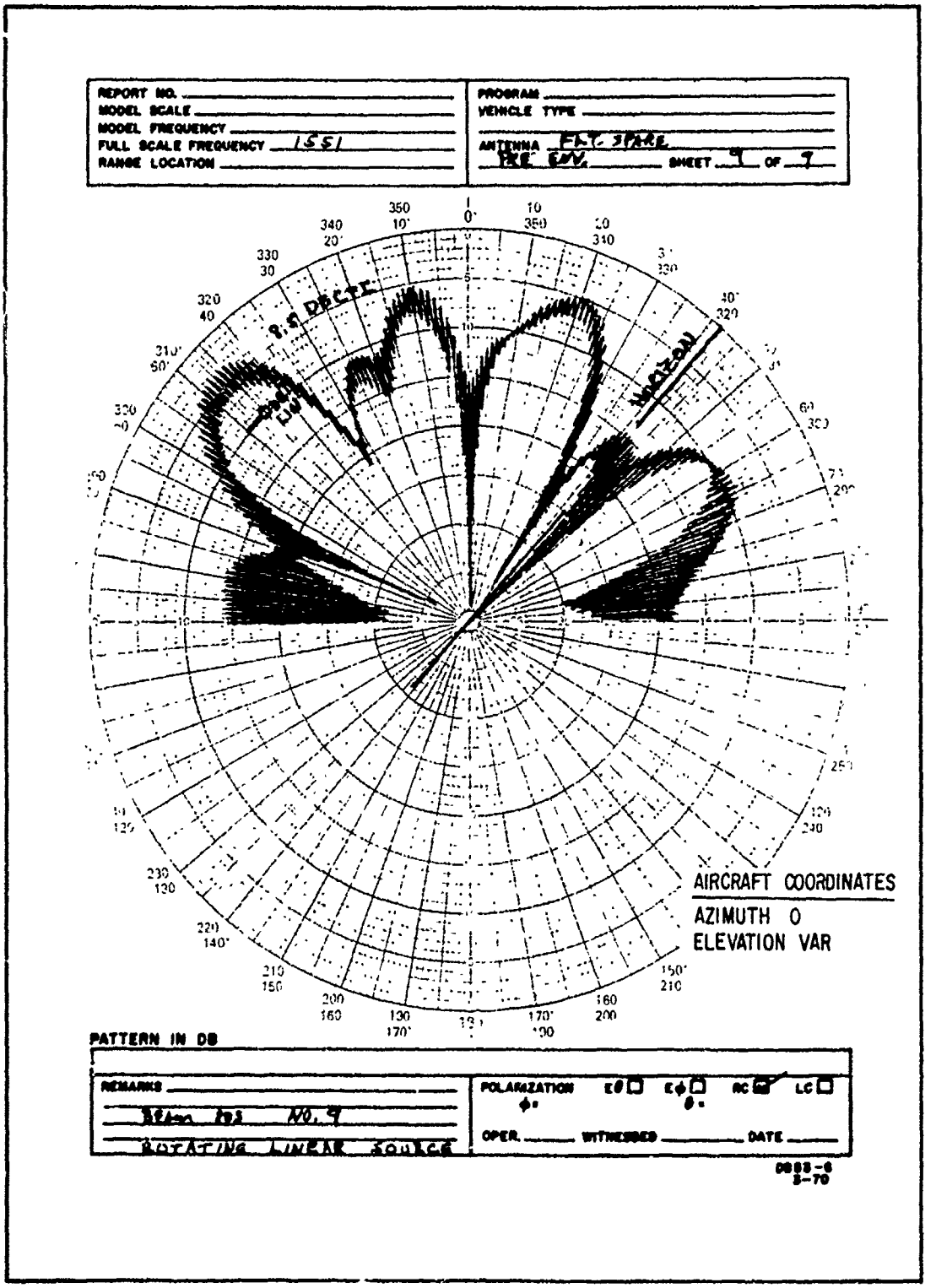

Figure 5-28 Elevation Pattern Beam Position 9 S/N 002

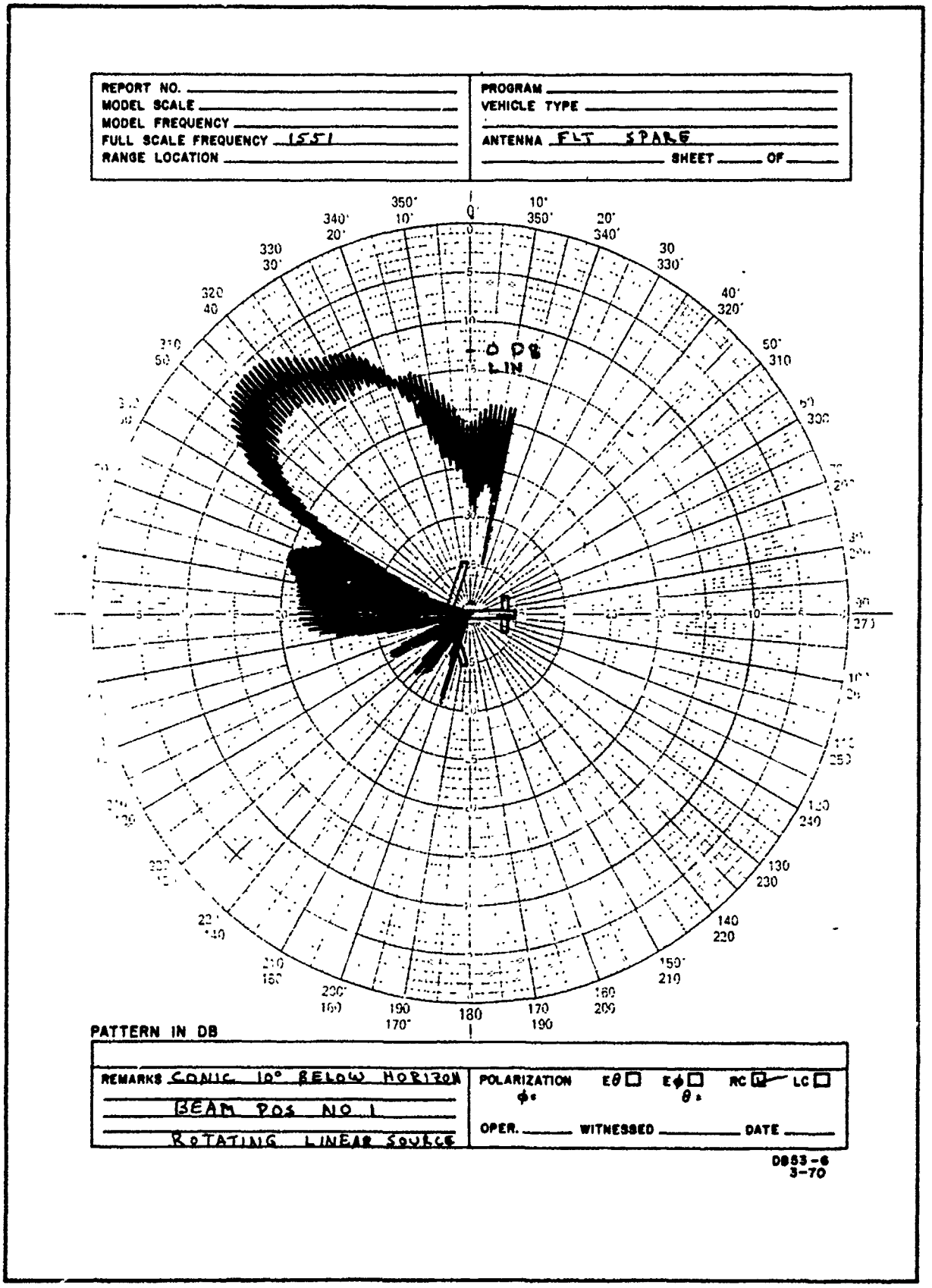

Figure 5-29 -10° Conical Cut Beam Position 1 S/N 002

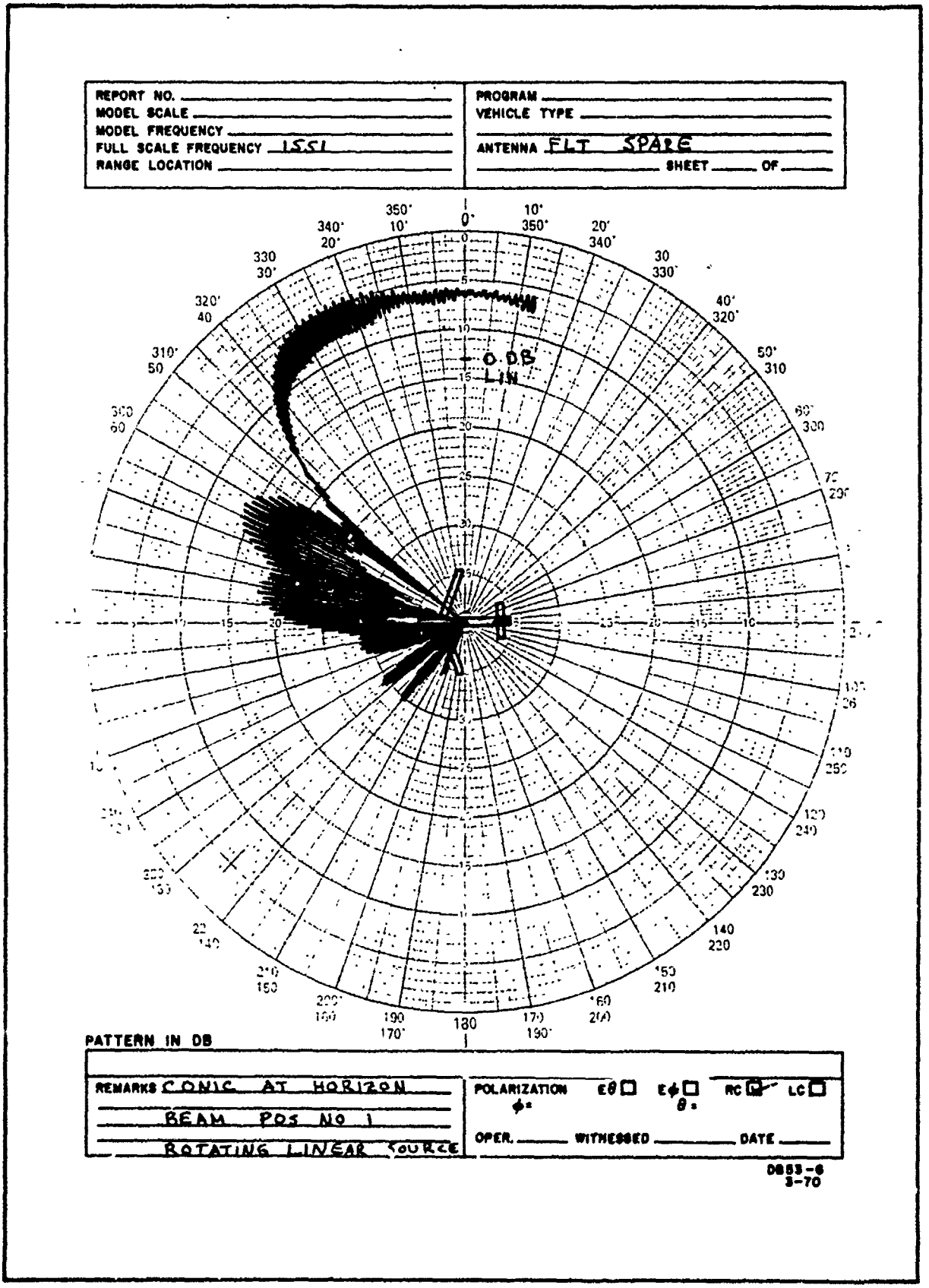

Figure 5-30 +0° Conical Cut Beam Position 1 S/N 002

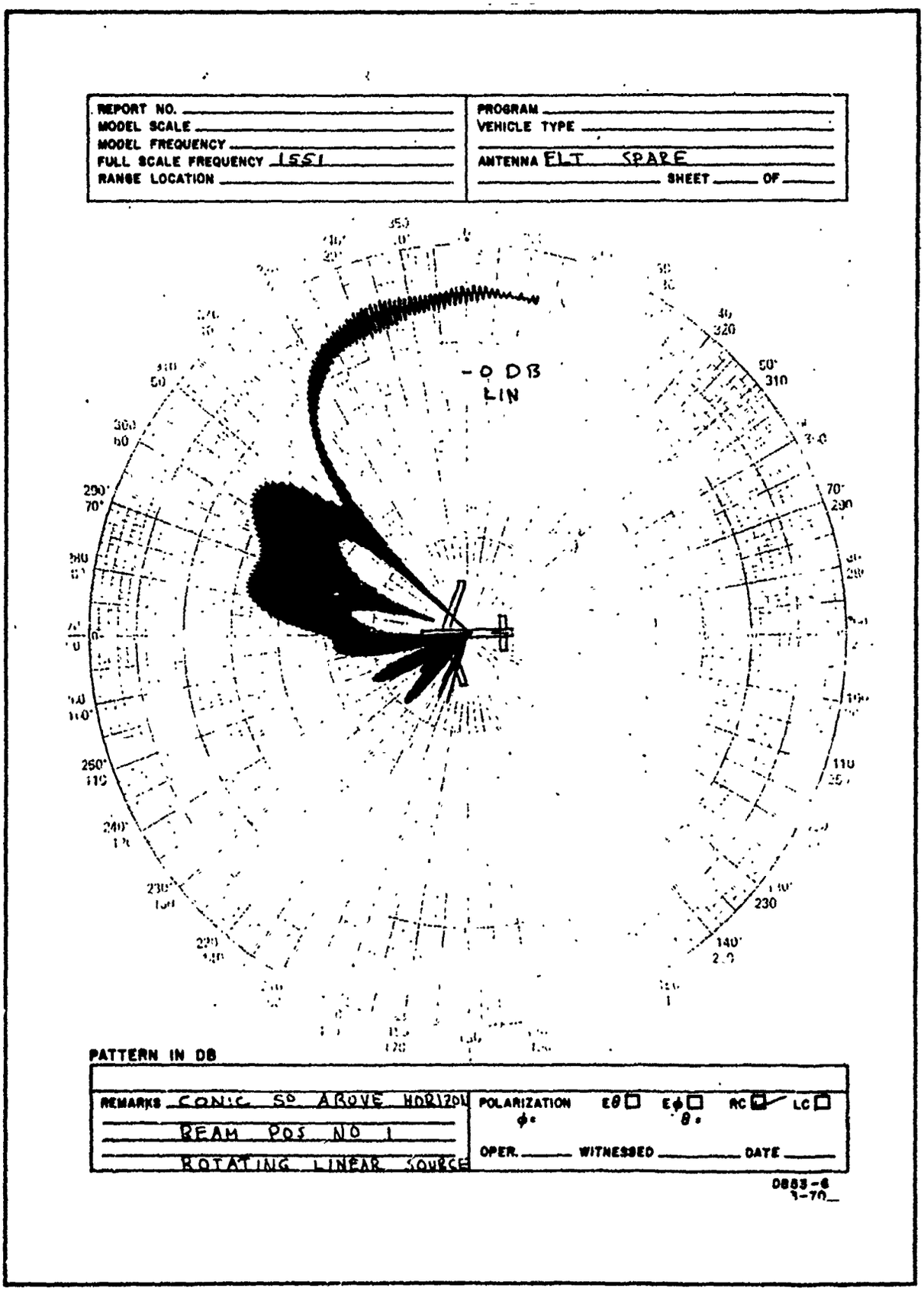

Figure 5-31 +5° Conical Cut Beam Position 1 S/N 002

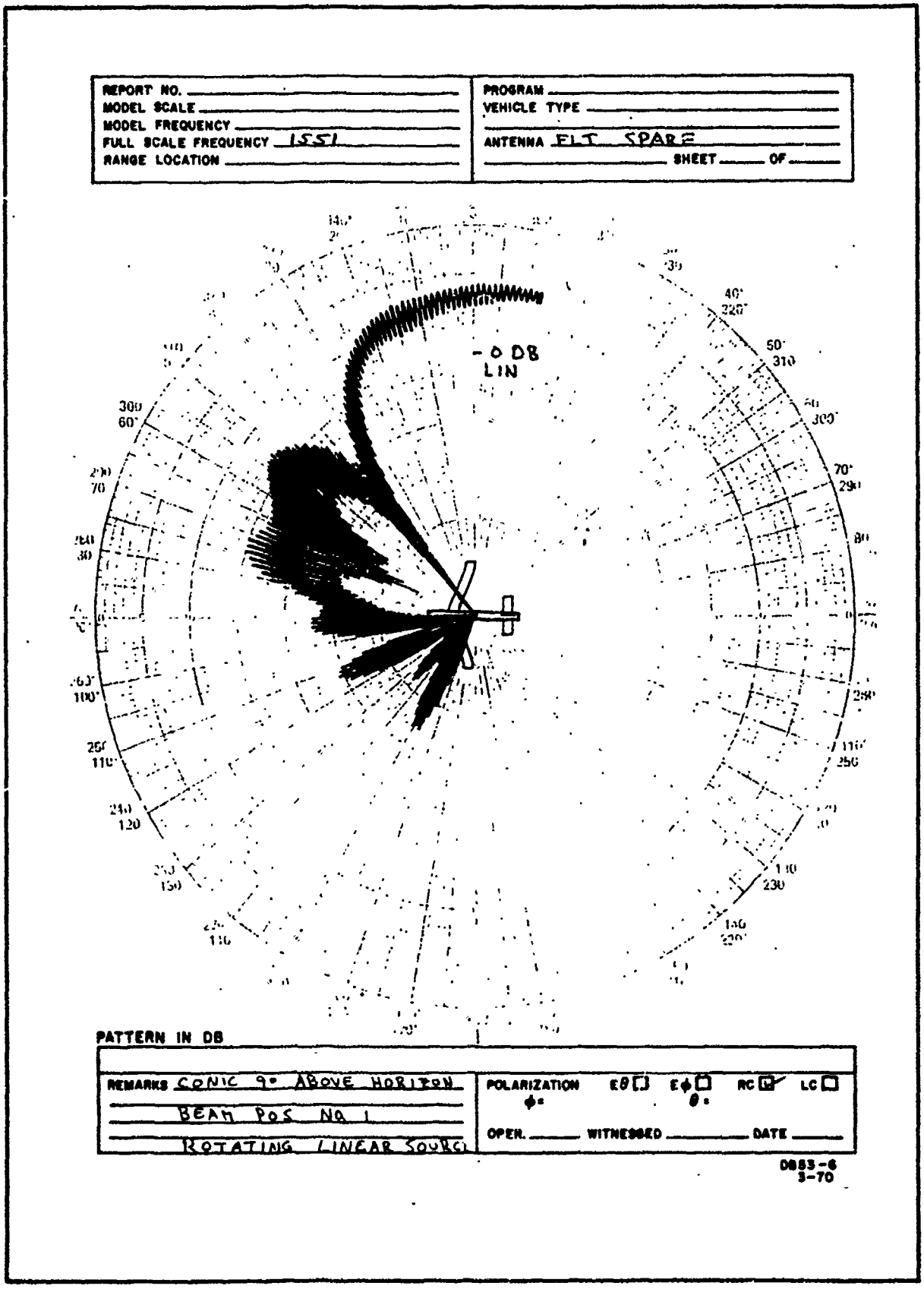

Figure 5-32 +9° Conical Cut Beam Position 1 S/N 002

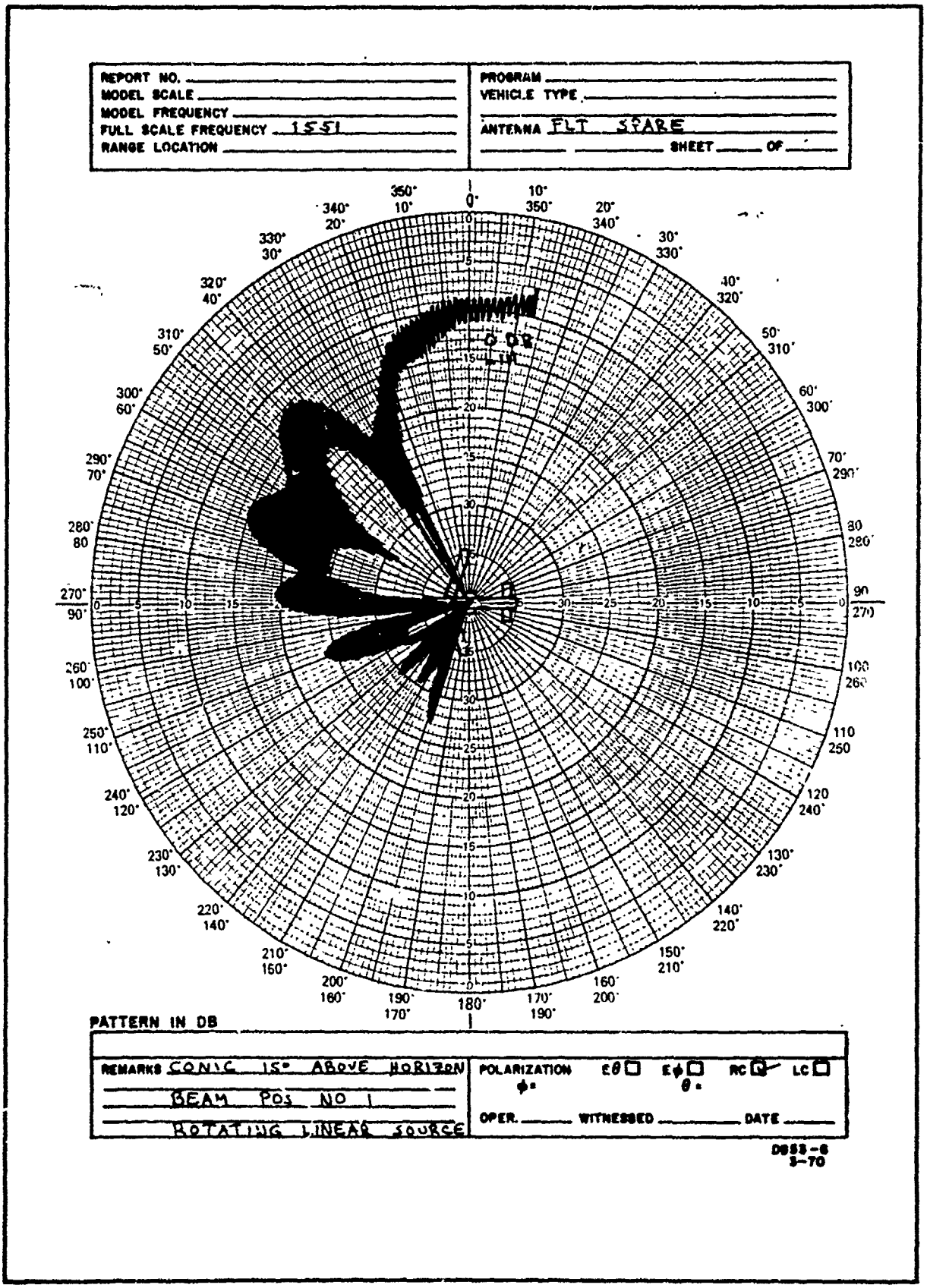

Figure 5-33 +15° Conical Cut Beam Position 1 S/N 002

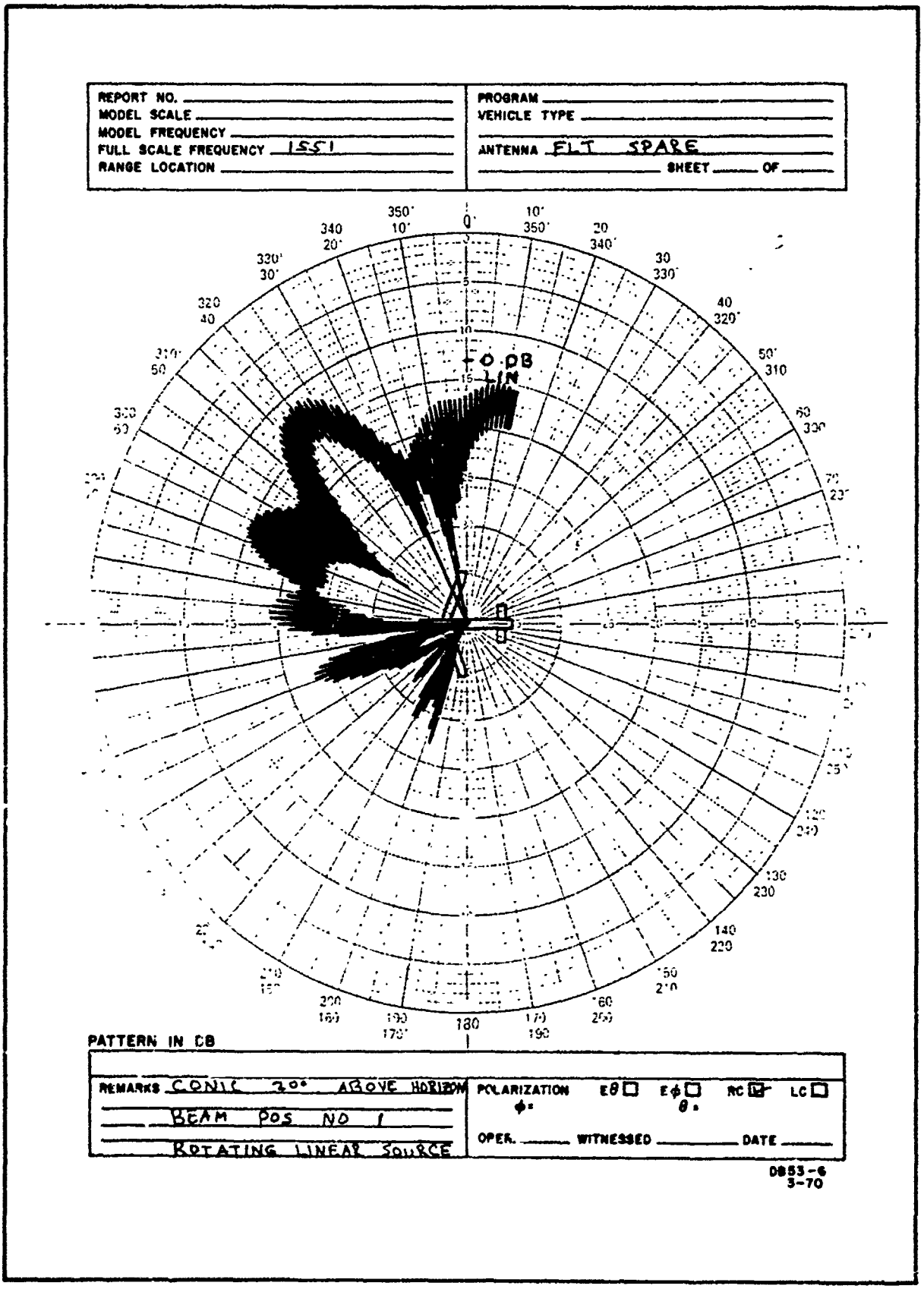

Figure 5-34 +20° Conical Cut Beam Position 1 S/N 002

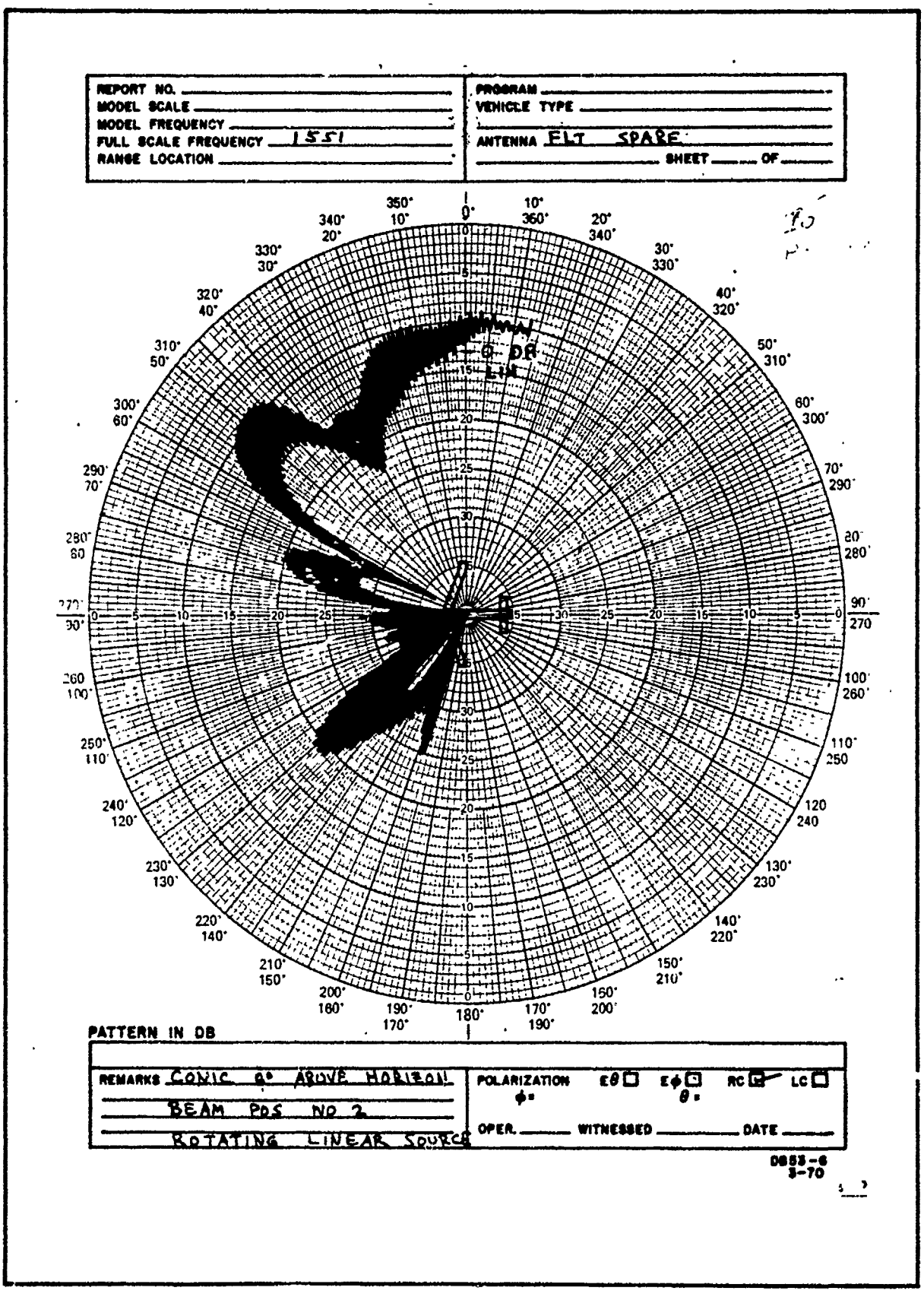

Figure 5-35 +6° Conical Cut Beam Position 2 S/N 002

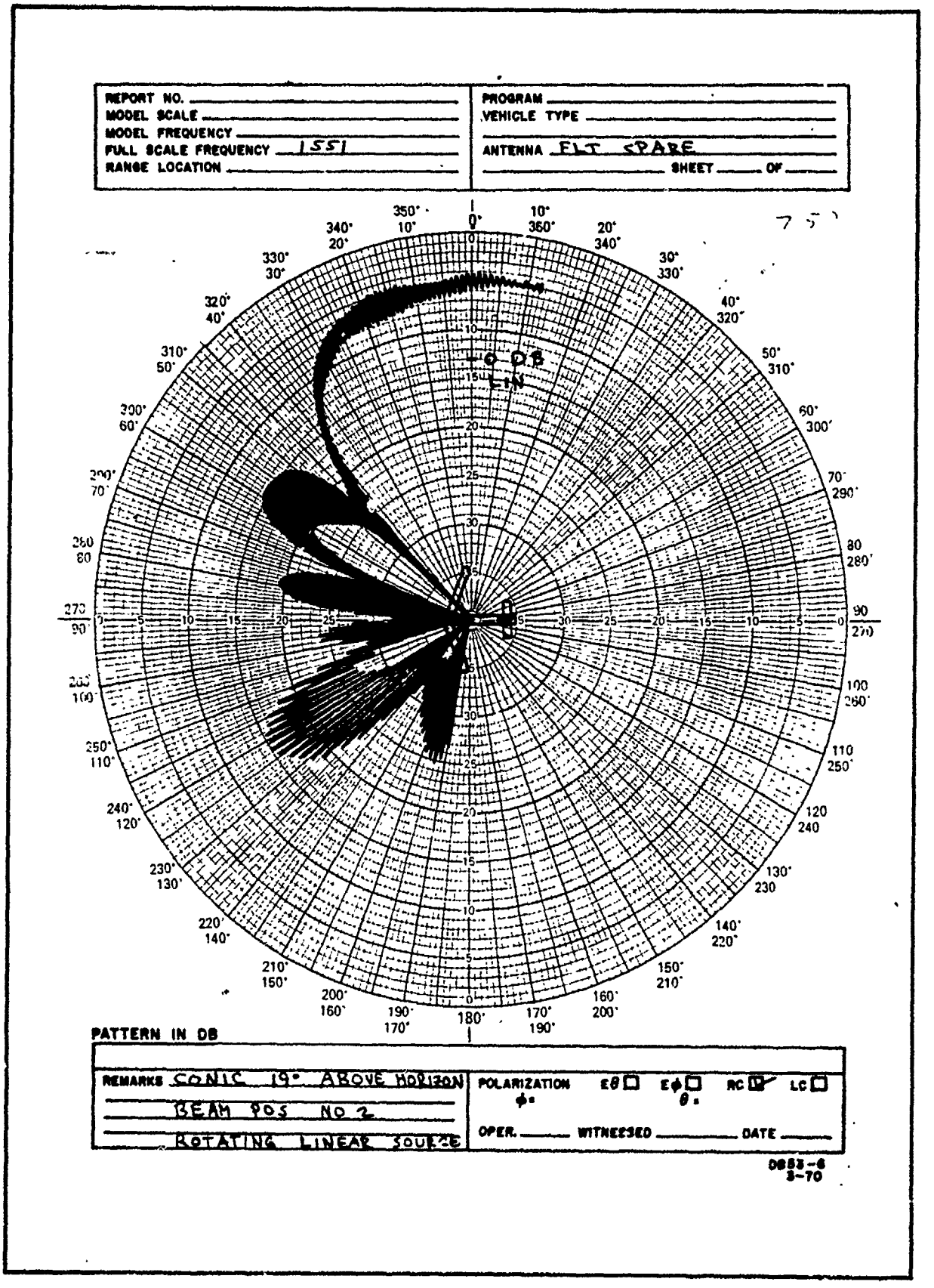

Figure 5-36 +19° Conical Cut Beam Position 2 S/N 002

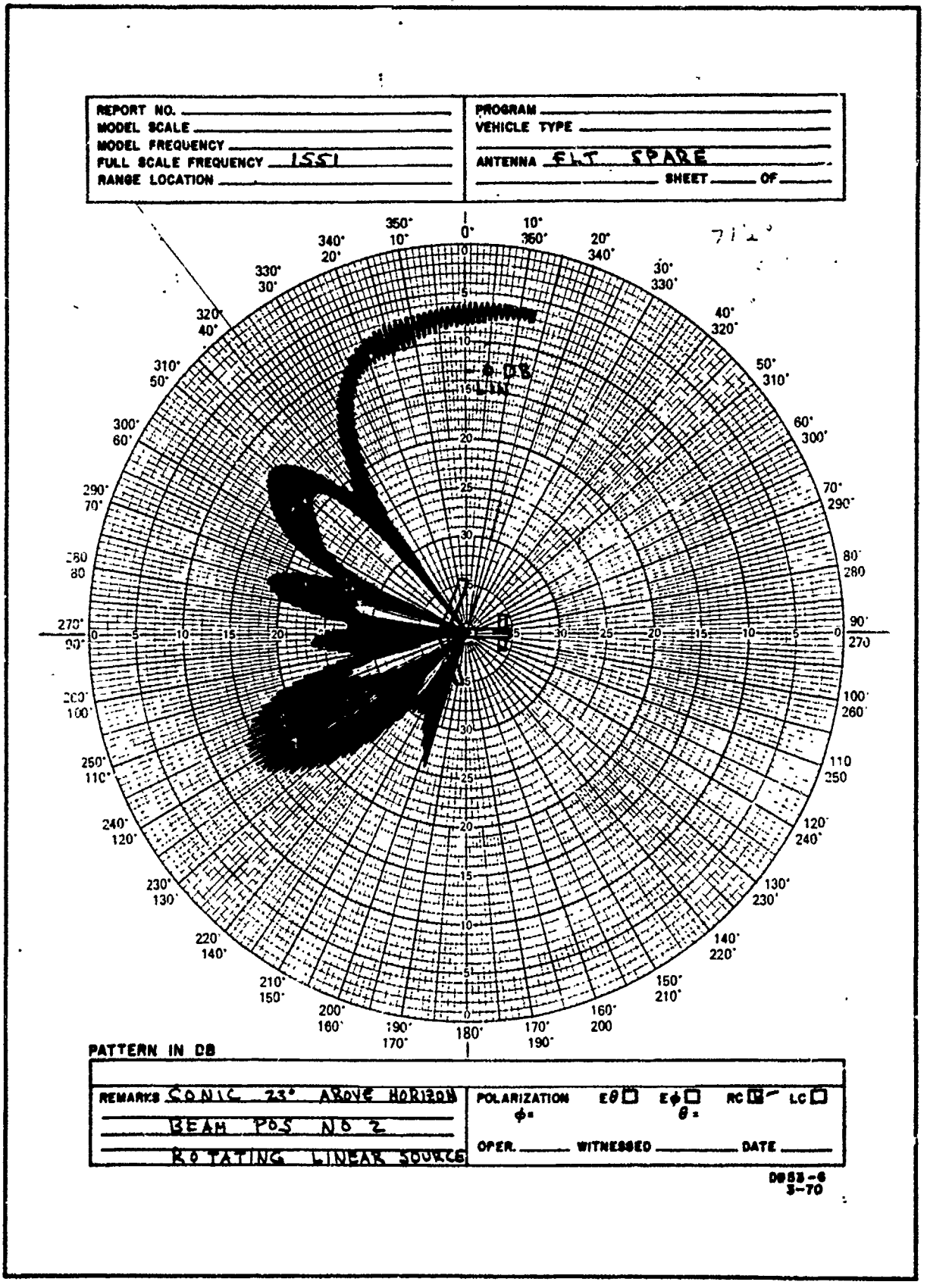

Figure 5-37 +23° Conical Cut Beam Position 2 S/N 002

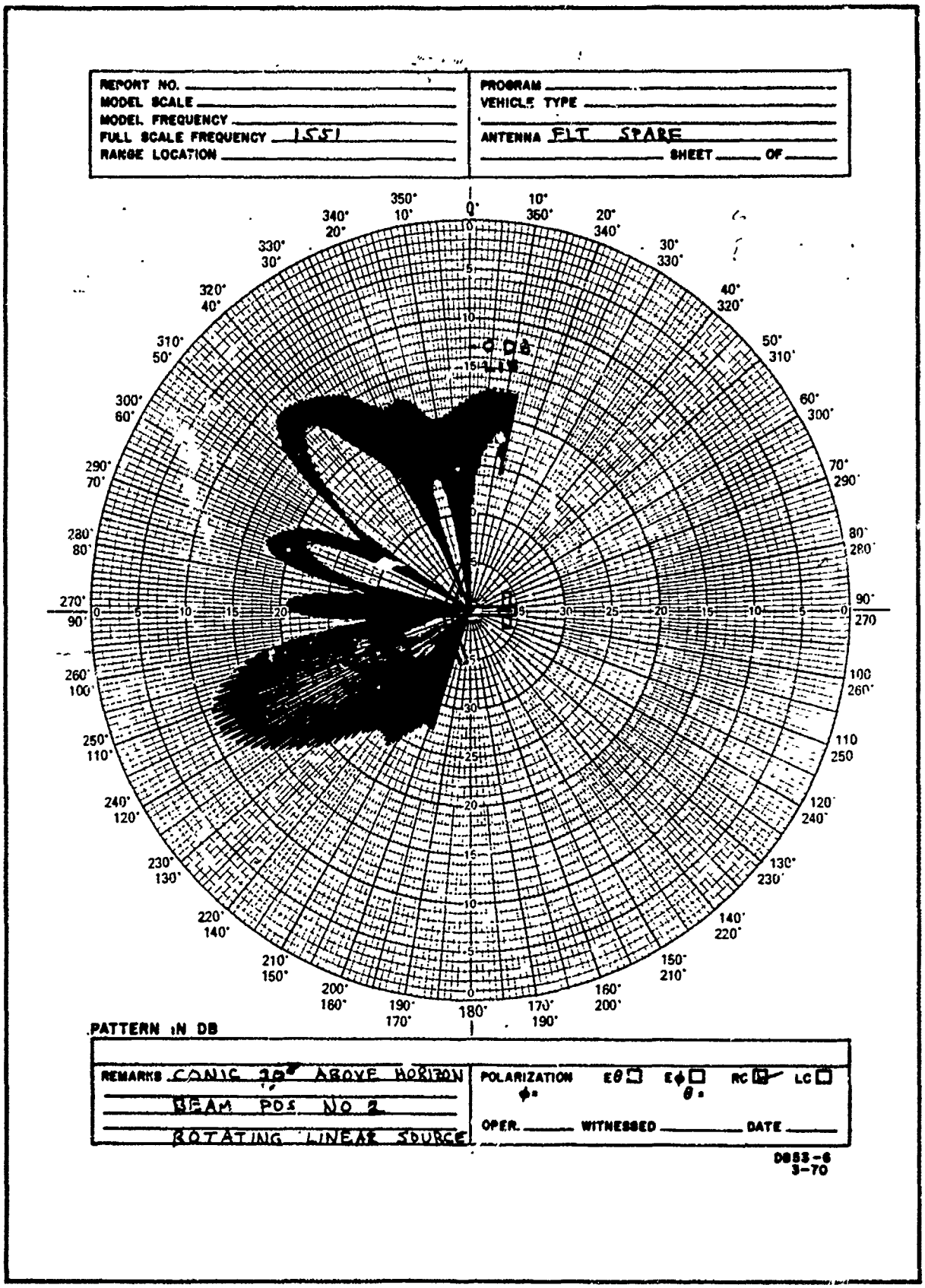

Figure 5-38 +30° Conical Cut Beam Position 2 S/N 002

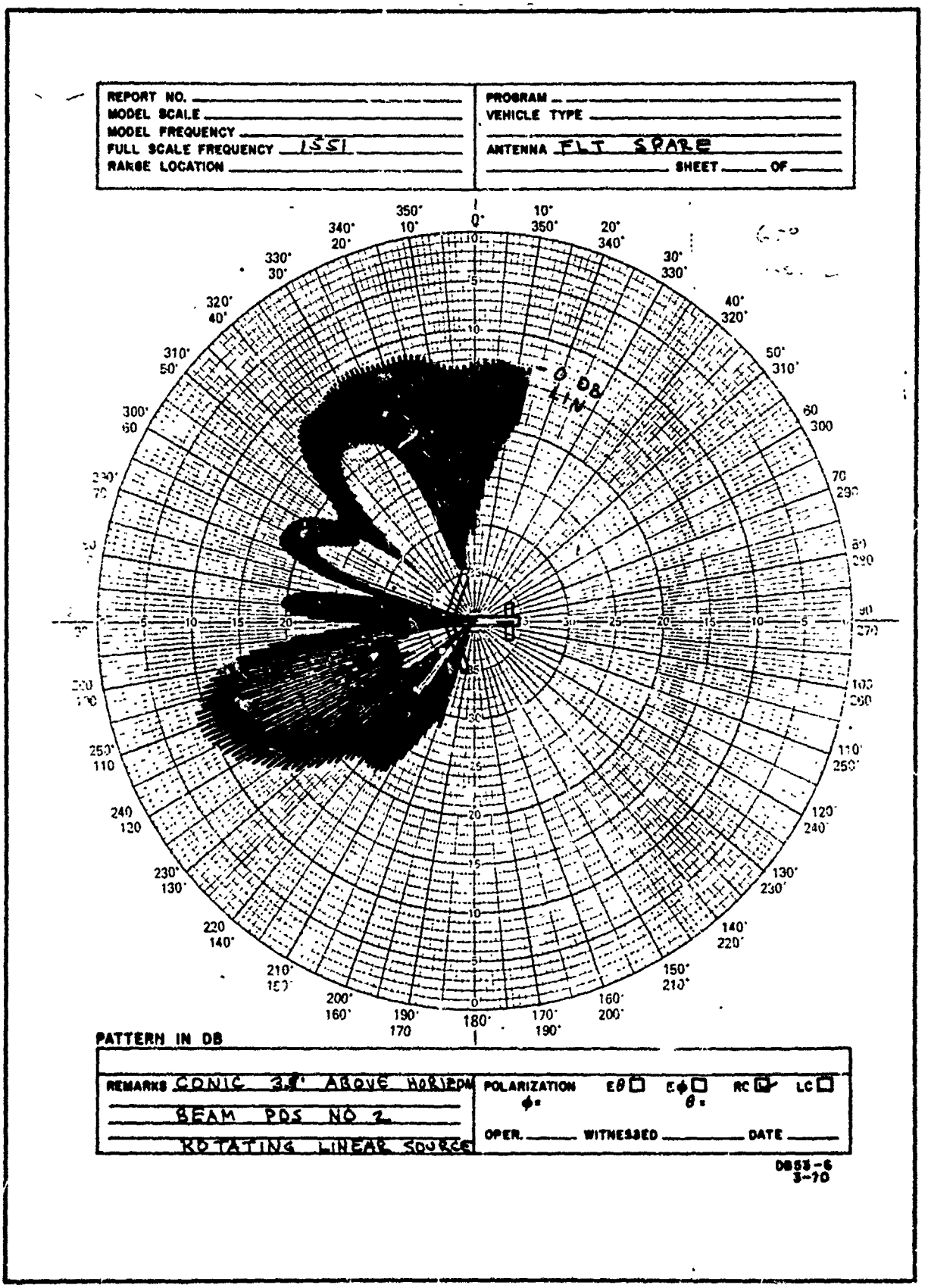

Figure 5-39 +35° Conical Cut Beam Position 2 S/N 002

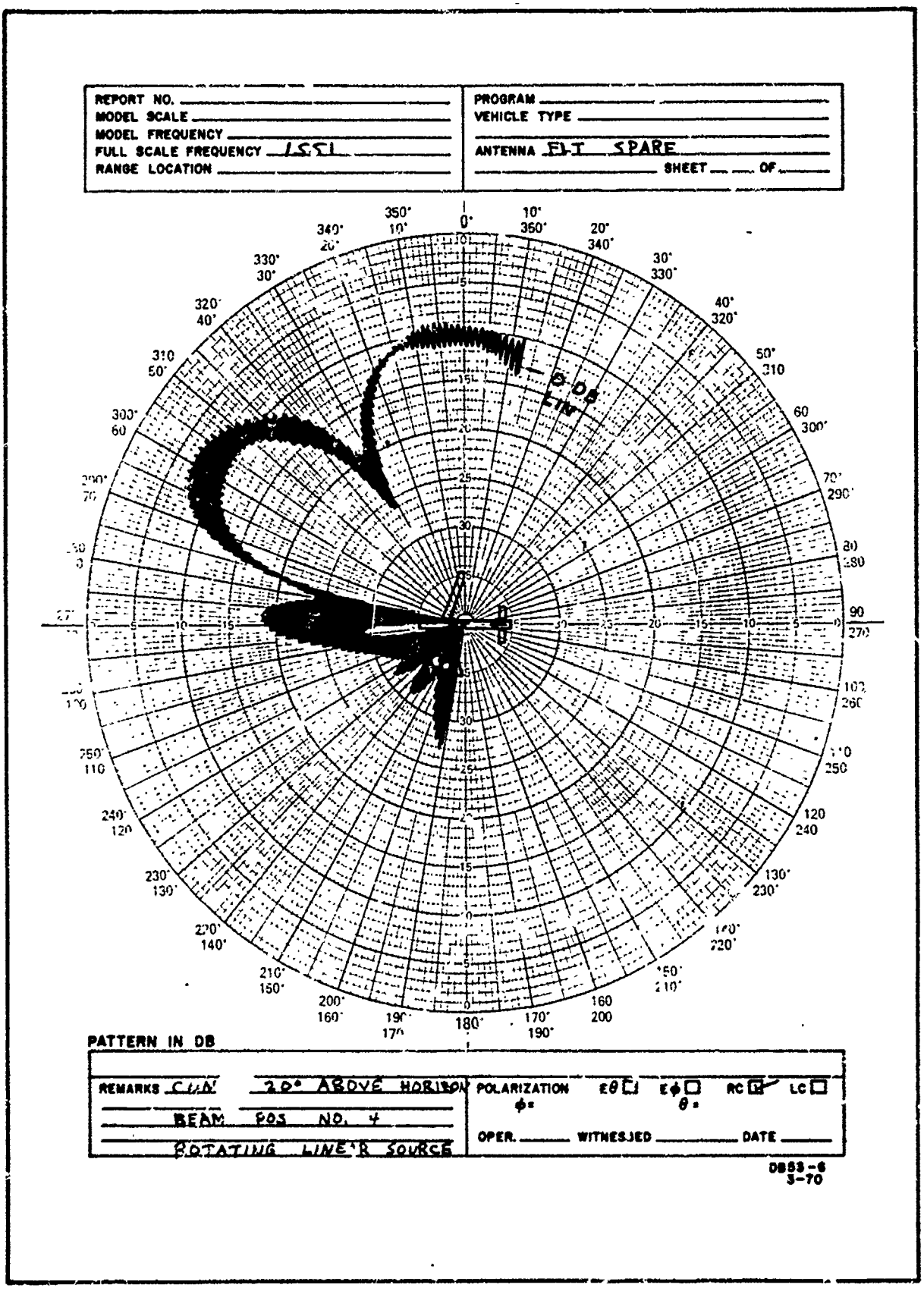

Figure 5-40 +20° Conical Cut Beam Position 4 S/N 002

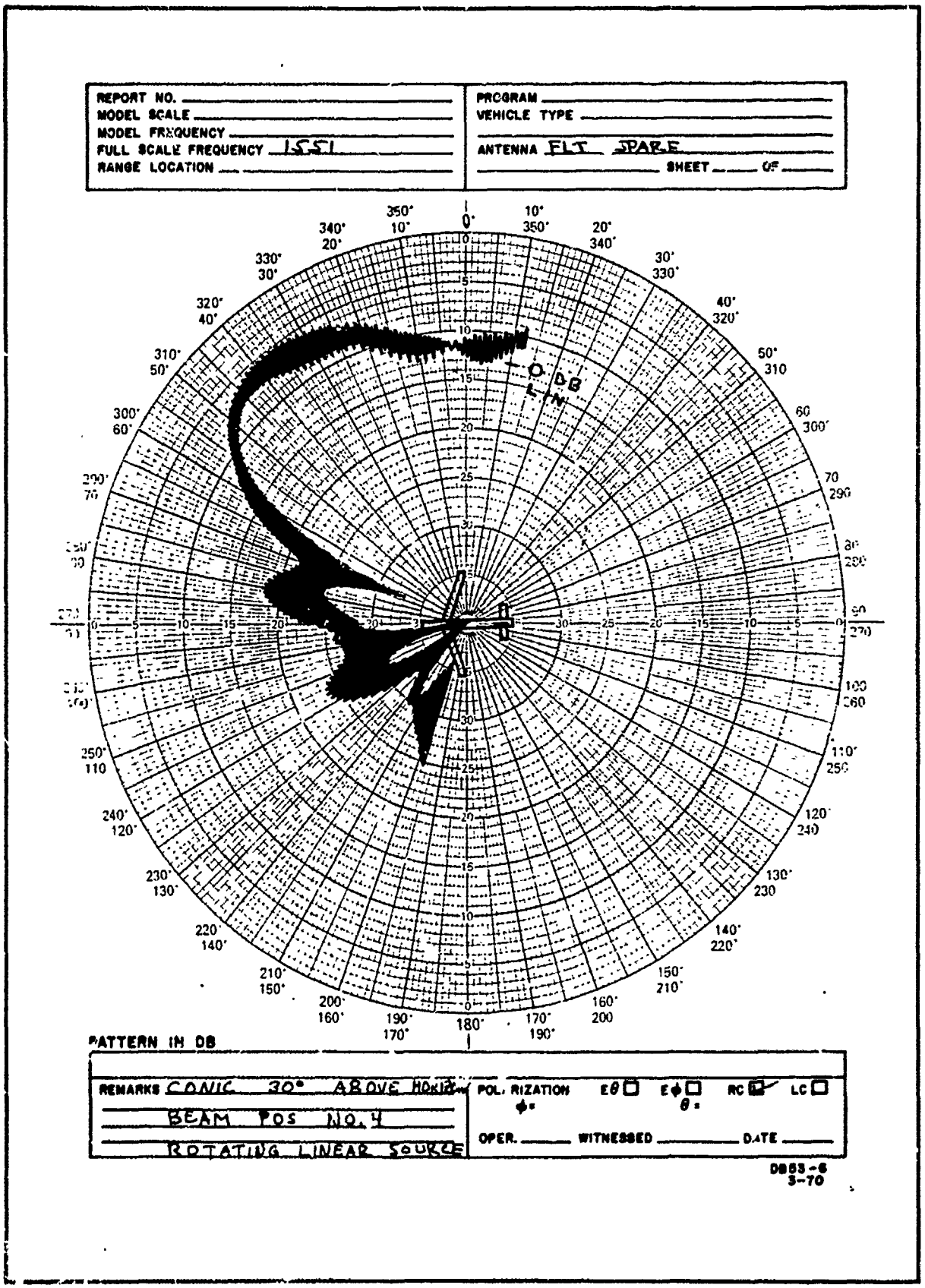

Figure 5-41 +30° Conical Cut Beam Position 4 S/N 002

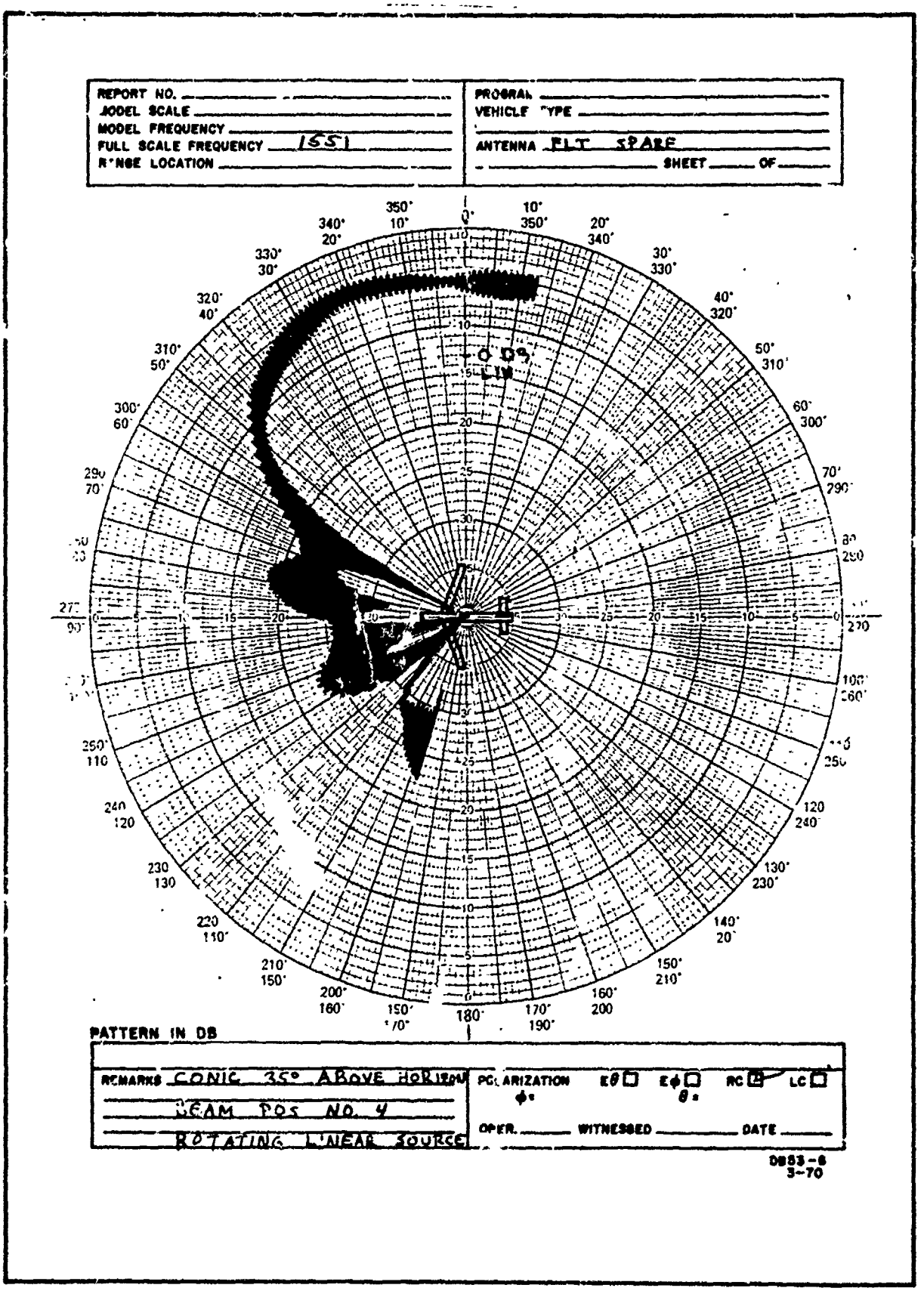

Figure 5-42 +35° Conical Cut Beam Position 4 S/N 002

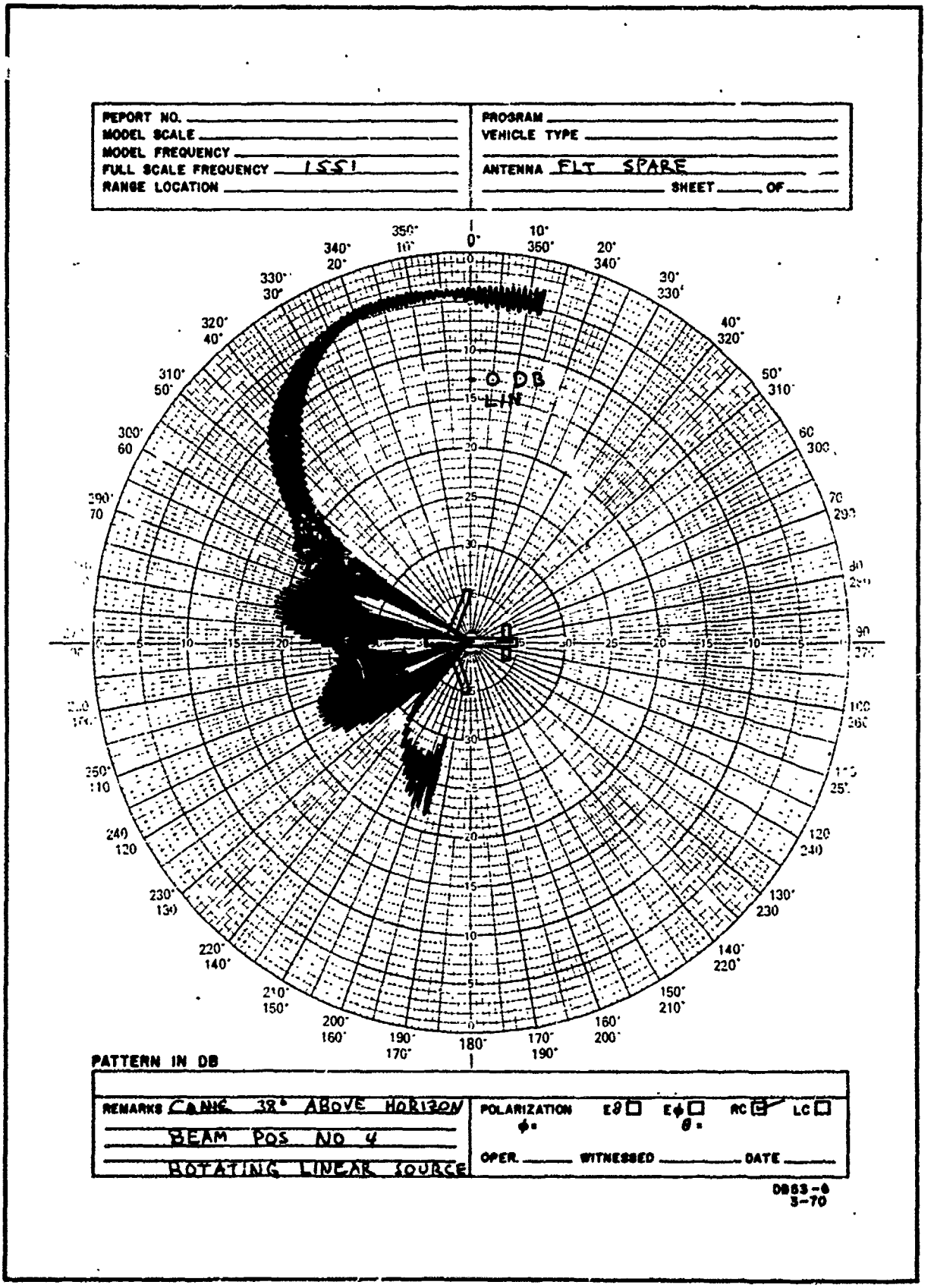

Figure 5-43 +38° Conical Cut Beam Position 4 S/N 002

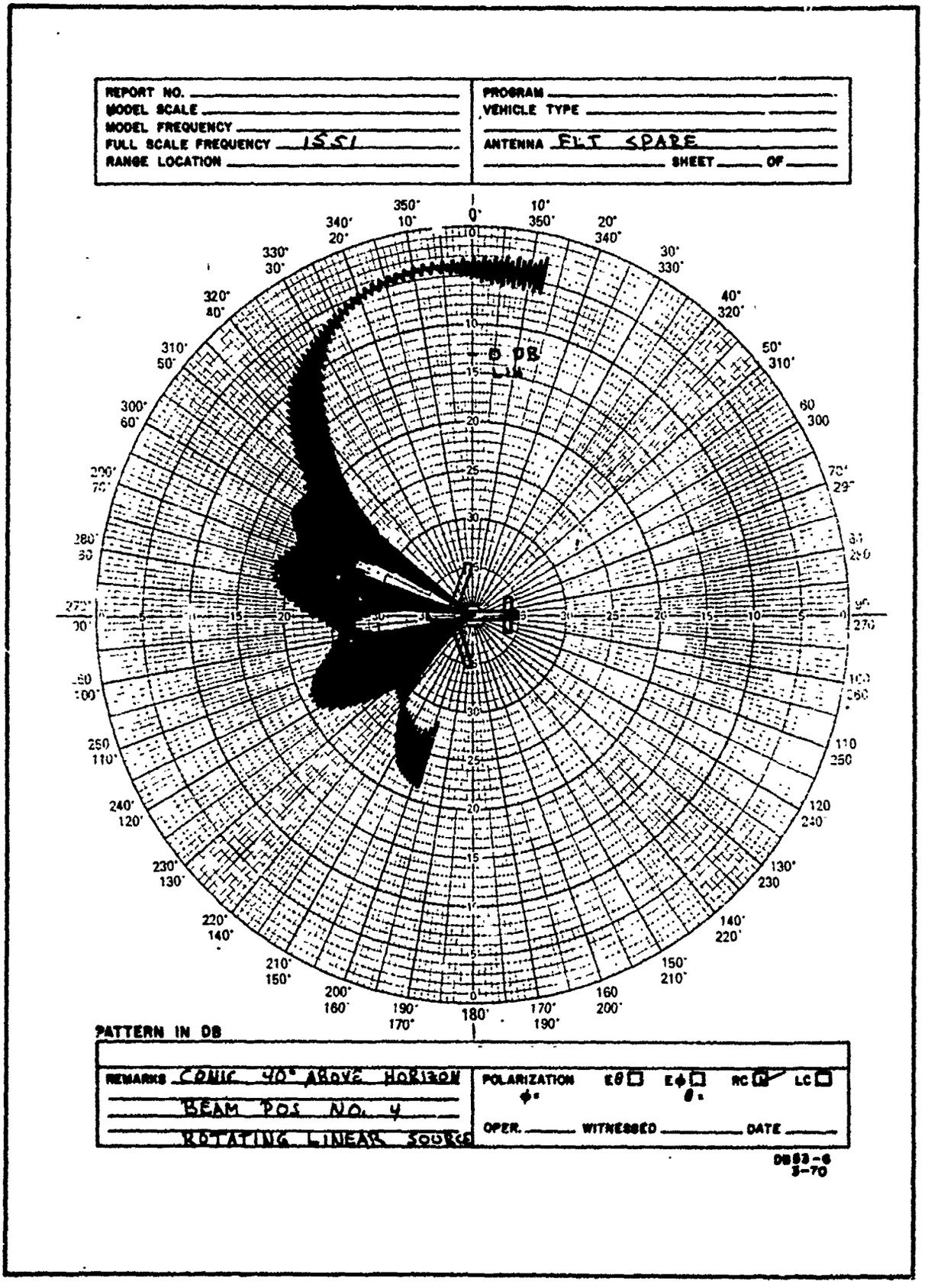

Figure 5-44 +40° Conical Cut Beam Position 4 S/N 002

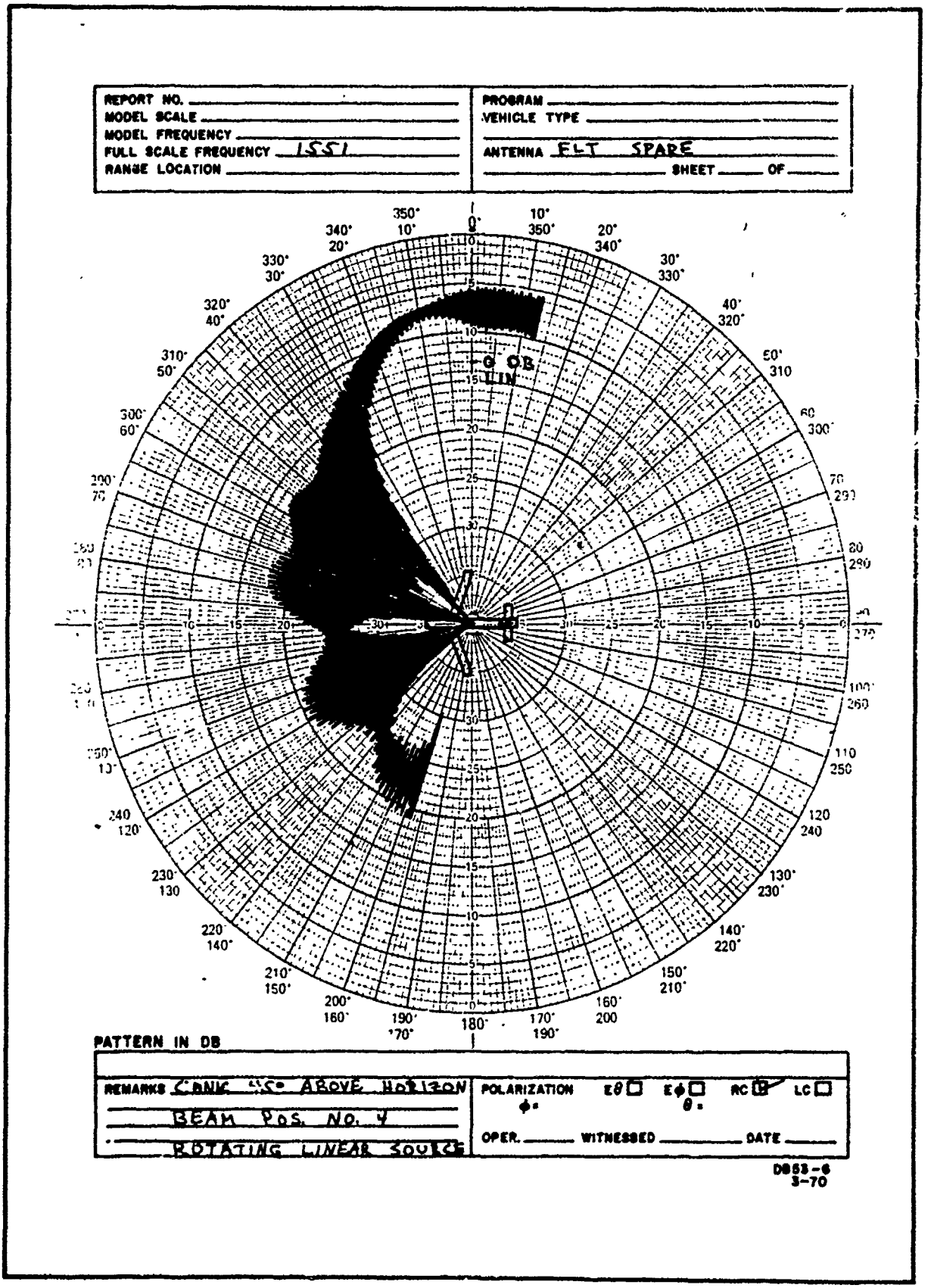

Figure 5-45 +45° Conical Cut Beam Position 4 S/N 002

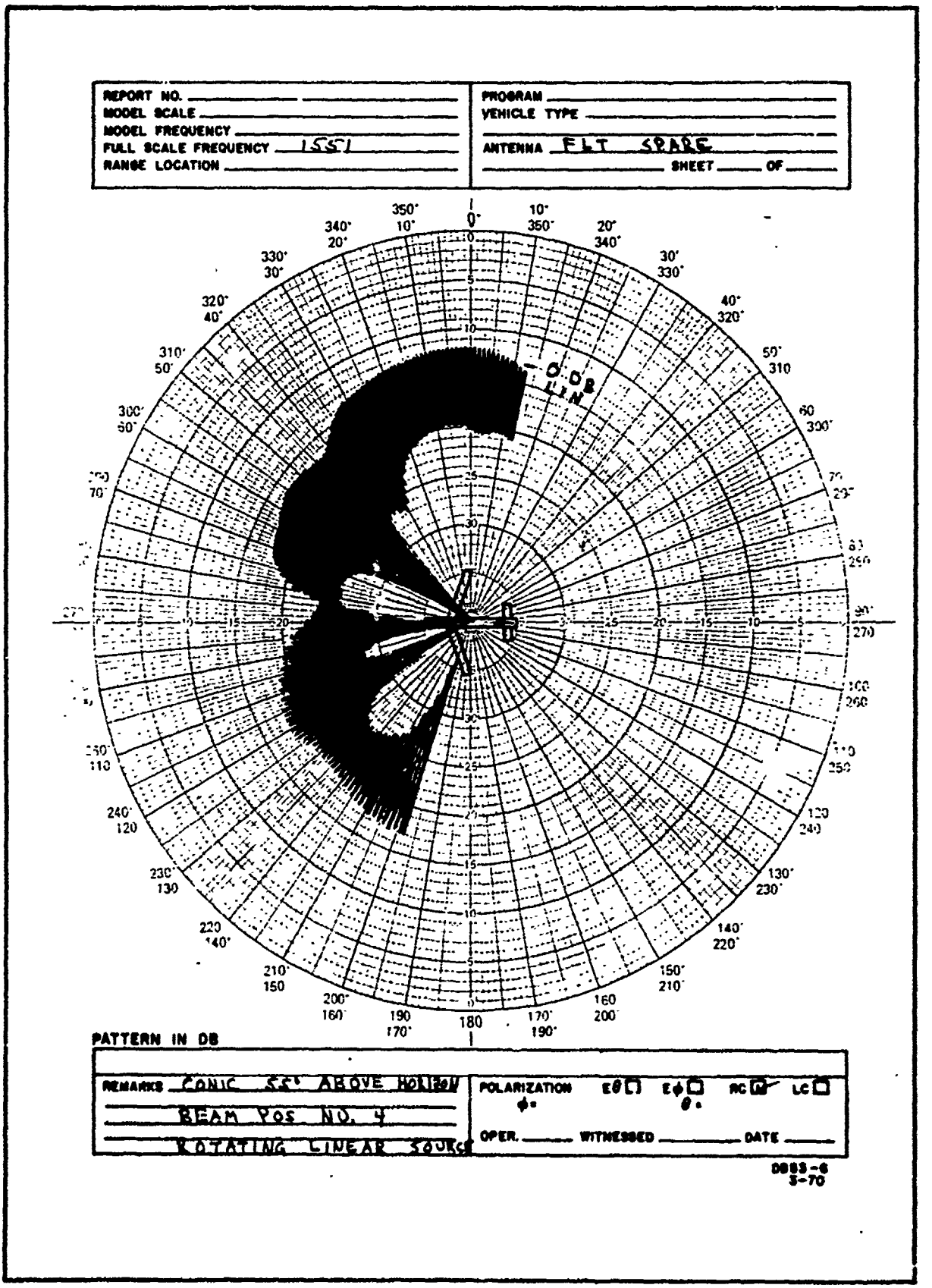

Figure 5-46 +55° Conical Cut Beam Position 4 S/N 002

5.1.2 Impedance

Impedance of the phased array was measured on a network analyzer using a frequency sweep from 1543.5 to 1558.5 MHz. Data for all beam positions were recorded. Figure 5-47 is a composite impedance plot for the nine beam positions of the flight antenna (S/N 001). Figure 5-48 is a similar plot for the flight spare antenna (S/N 002). The differences between the two plots are primarily due to the differences in cover material and diodes.

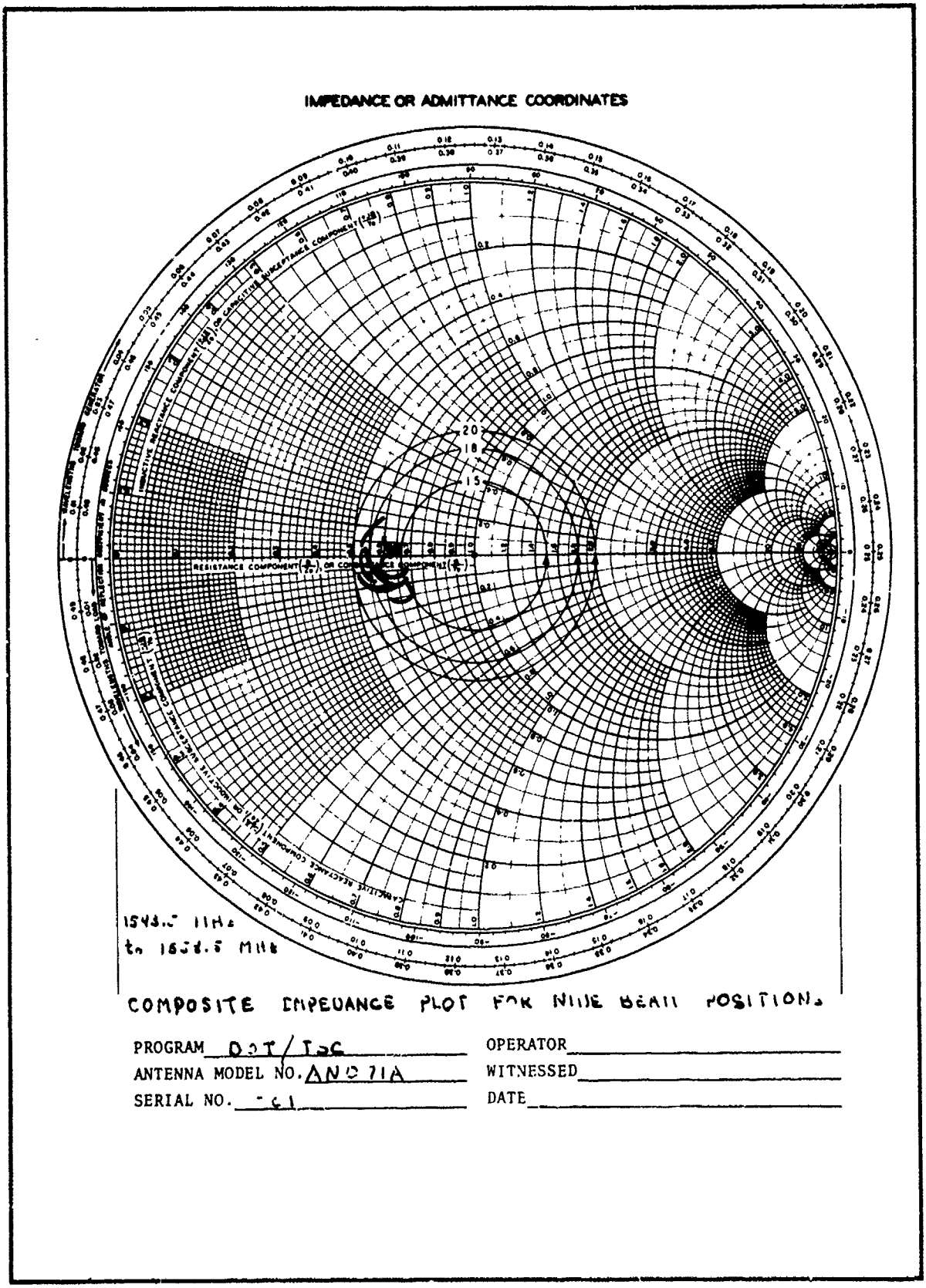

Figure 5-47 Composite Impedance Plot for Nine Beam Positions Antenna S/N 001

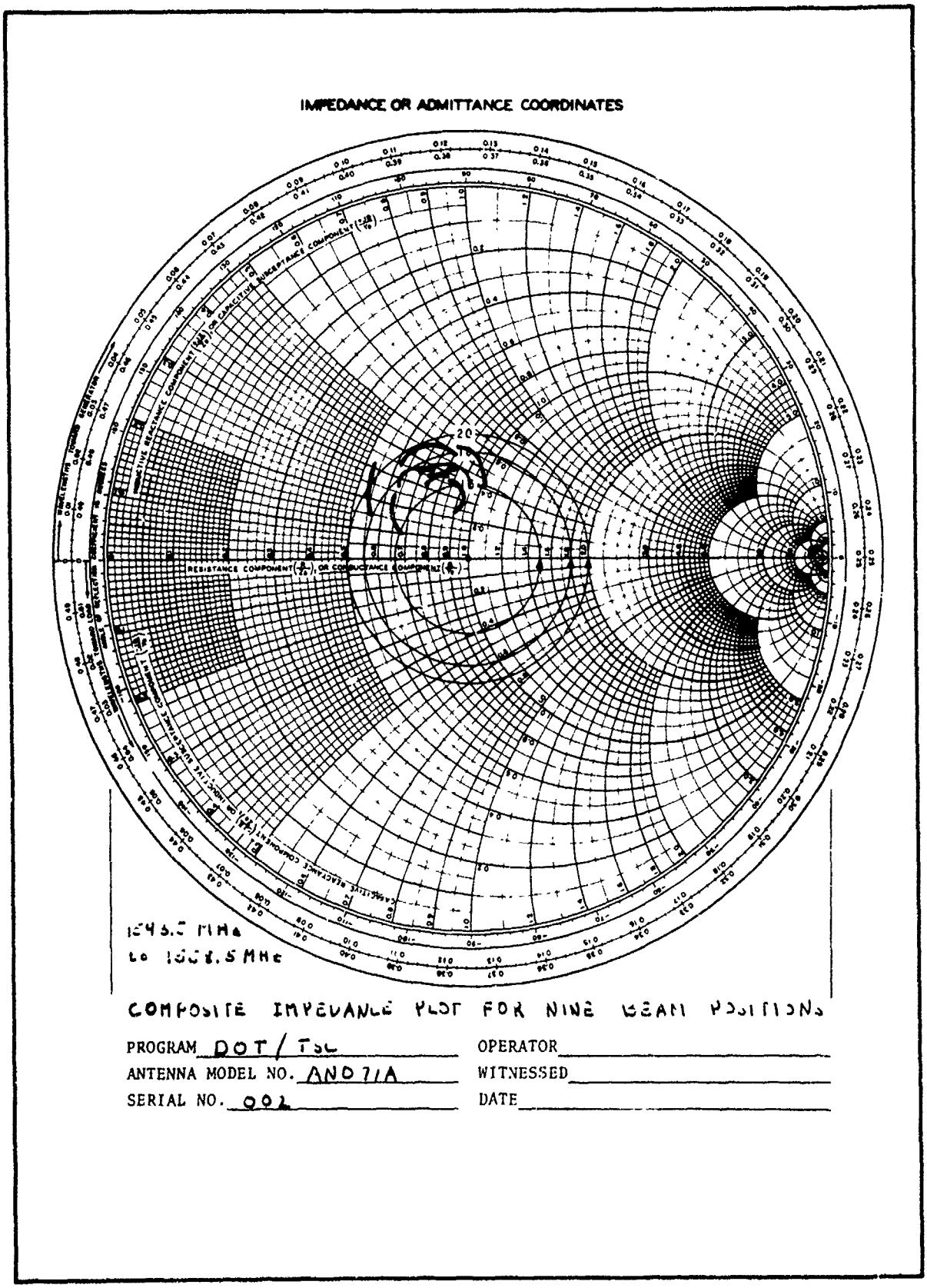

Figure 5-48 Composite Impedance Plot for Nine Beam Positions Antenna S/N 002

5.2 ENVIRONMENTAL TEST PROGRAM

A flow chart of the environmental tests for the array assembly and controller is shown in Figure 5-49. Because of the different environments for the controller and the array, the units were subjected to separate tests. However, insofar as possible the units were operated as a system with the interconnecting cable in place and the units energized to simulate operational conditions.

The vibration levels for the steerable array and controller unit are given in Tables 5-2 and 5-3 and plotted in Figures 5-50 and 5-51. These levels were derived from information given in Boeing Document #D-16046, Vibration Test Requirements for Equipment Installed in Model KC-135 Airplanes. Other environmental limits and durations of the exposure are indicated on the test plan flow chart of Figure 5-46. Vibration fixtures were fabricated for the phased array and the controller. Connector sleeves and cables were also prepared. These components were checked for assembly fit prior to starting the test sequence.

Subsequent to exposure of environmental tests, the steerable array assembly was subjected to final VSWR and elevation pattern measurements while installed on the 4-foot by 4-foot ground plane. At no point during or after the environmental test was a significant change in performance observed. Rather than showing all the post-environmental test results which would simply duplicate the pre-environmental data, Figure 5-52 may be compared with Figure 5-2 to illustrate the minor variations in the radiation pattern.

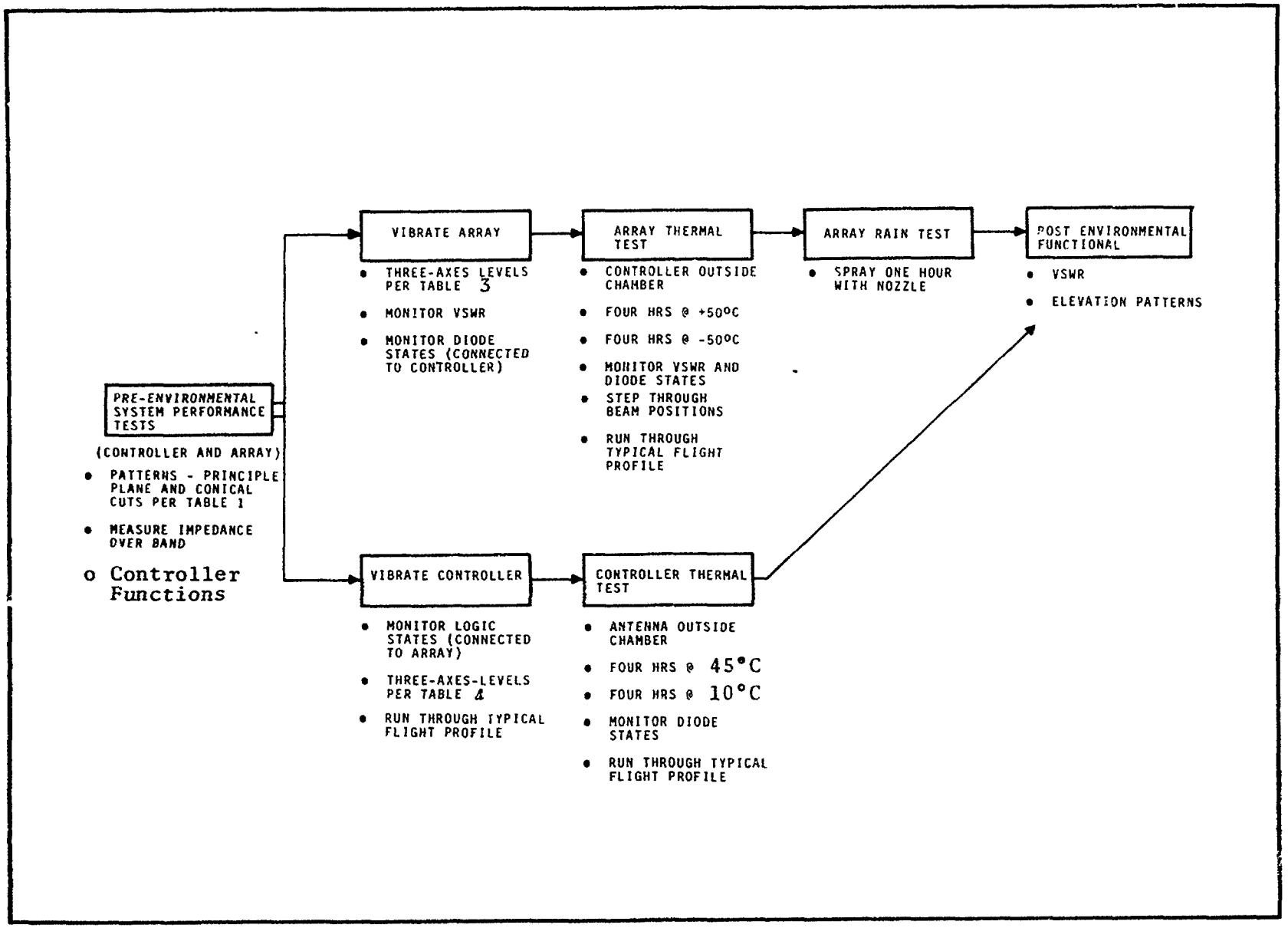

Figure 5-49 Test Plan of DOT/TSC Steerable Beam Antenna

Table 5-2

VIBRATION TEST FOR STEERABLE ARRAY ANTENNA

Test	Frequency	Level	Time	Axis
Frequency Scan	5 - 30 Hz	.02 in. (p-p)	15-minute sweep	All Three
	30 - 200 Hz	1 g		
	200 - 350 Hz	.0005 in. (p-p)		
	350 - 1000 Hz	3 g		
Cycling	Same as Above	Same as Above	15-minute cycle 5-1000-5 Hz for total time of 1 hour	All Three

Table 5-3

VIBRATION TEST FOR STEERABLE ARRAY CONTROLLER

Test	Frequency	Level	Time	Axis
Frequency Scan	5 - 30 Hz	.1 in. (p-p)	15-minute sweep	All Three
	30 - 60 Hz	1 g		
	60 - 1000 Hz	.5 g		
Resonance Endurance	Same as Above	Same as Above	50,000 cycles or 30 minutes whichever first occurs for the principal resonance	All Three
Cycling	Same as Above	Same as Above	15-minute cycle 5-1000-5 Hz for total time of 1 hour	All Three

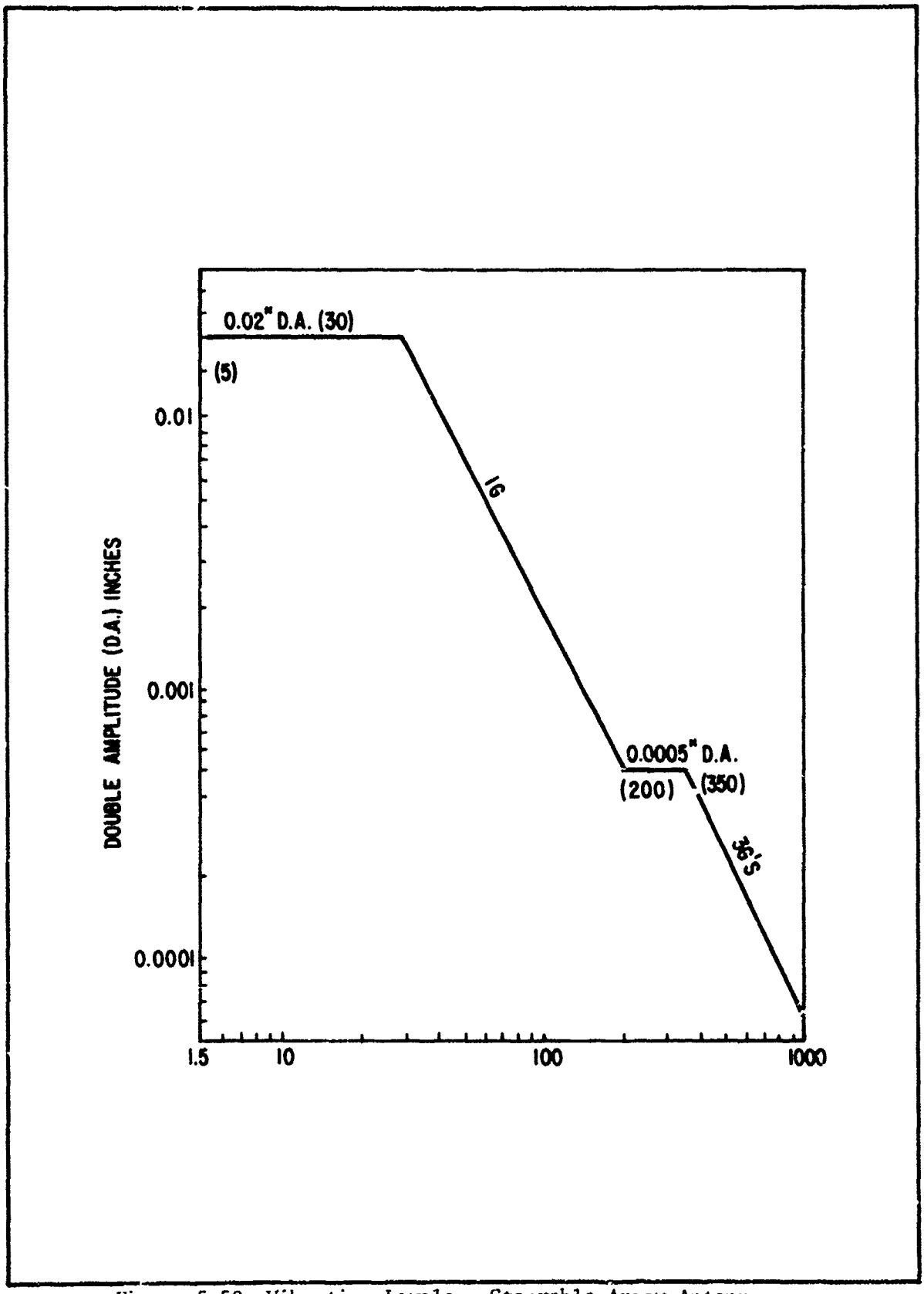

Figure 5-50 Vibration Levels - Steerable Array Antenna
(Group 8, Category A, D-16046)

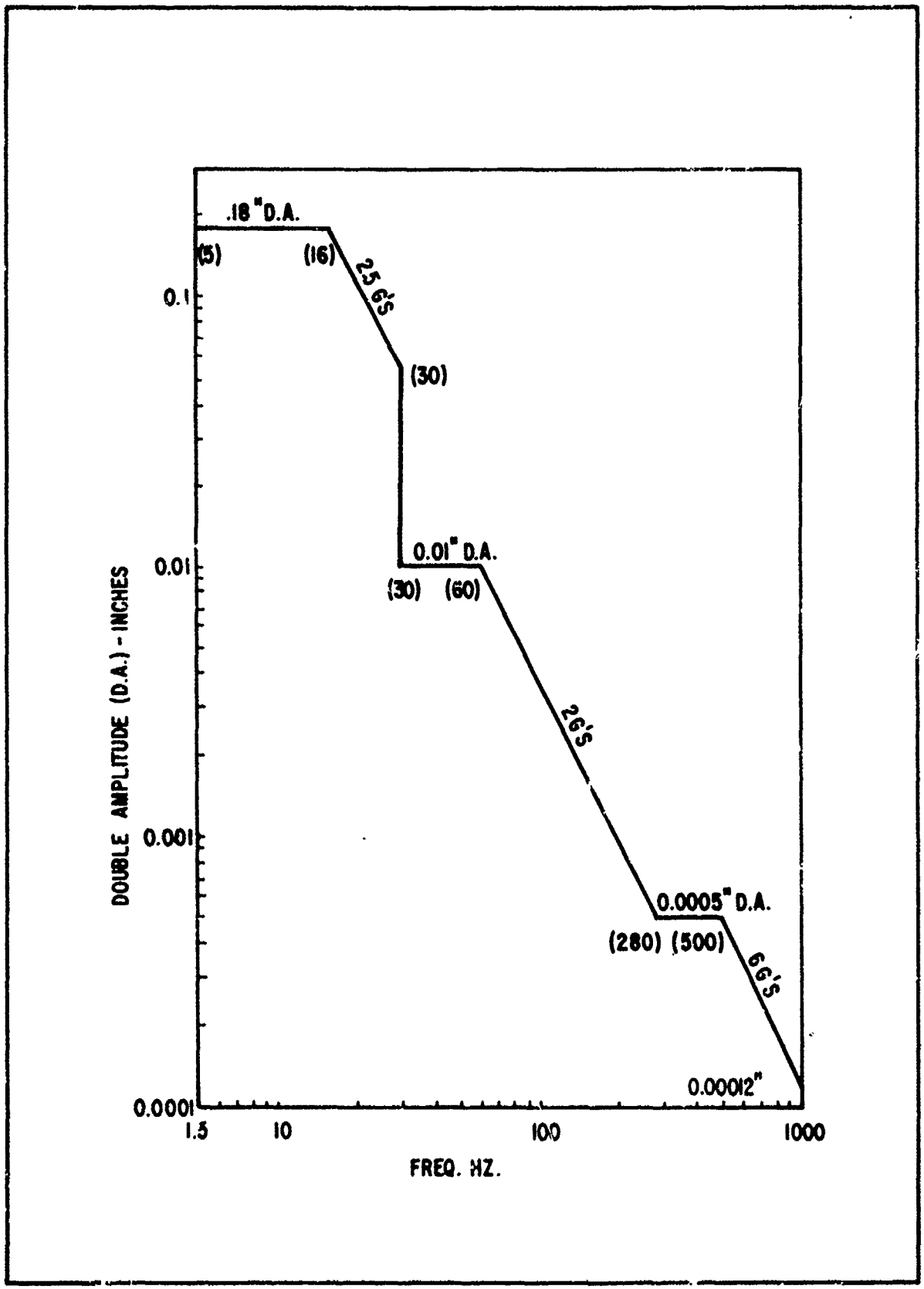

Figure 5-51 Vibration Levels - Steerable Array Controller
(Group 9, Category A, D-16046)

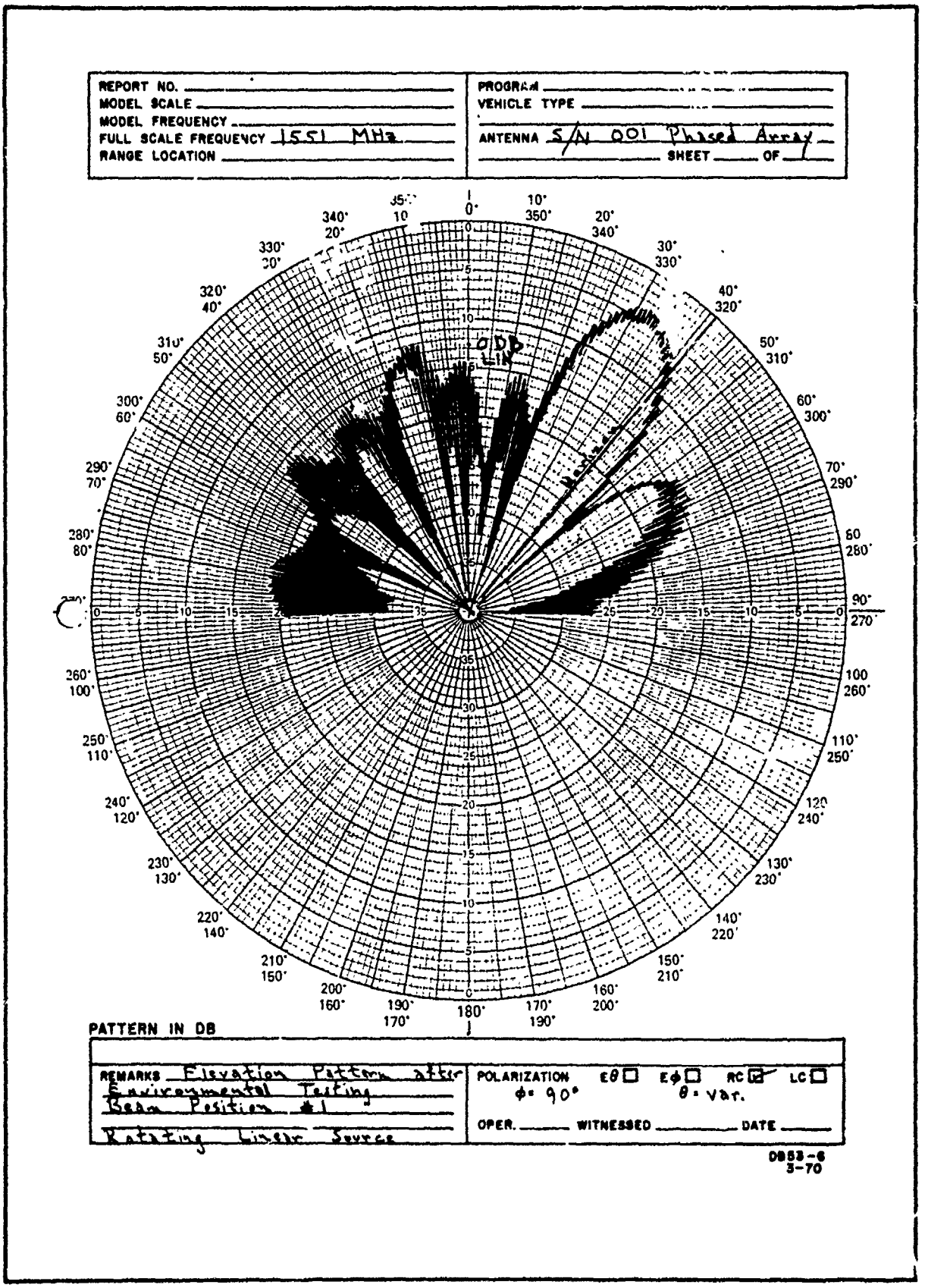

Figure 5-52 Post-Environmental Elevation-Pattern Antenna S/N 001 Beam Position 1

5.3 SCALE-MODEL-TESTING

One-tenth scale antenna units were designed for beam positions 1, 2 and 4. Beam positions 1 and 2 were selected since they are most likely to be affected by the presence of the aircraft wings. Beam position 4 is representative of the higher steering angles and allows comparison of the patterns from the full scale model with those from the tenth scale model for a position not likely to be seriously affected by the presence of the aircraft structure.

Antennas for the tenth scale model were made using etched microstrip circuit board techniques. The radiating elements were scaled directly from the full-sized elements. The feed lines were too narrow to scale and therefore a modified feed circuit was designed and tested for use on the tenth scale model. The elements were combined in a 1 by 8 array with appropriate phasing for the beam position being modeled. The completed model antennas are shown in Figure 5-53.

The scale model antennas were mounted on a tenth scale ground plane using the same coordinates as the full scale ground plane. Elevation and conical patterns were taken for comparison with full scale patterns.

A tenth scale Convair 880 was used to model the aircraft. TSC supplied the model along with a document describing the model and rotator mount. Slight damage occurred to the model during shipment; however, the damage was repaired without impact on the scale model test program. After installation of the antennas on the tenth scale aircraft model, the previously recorded patterns were repeated. The coordinate systems for the tenth scale model aircraft pattern tests is shown in Figure 5-54.

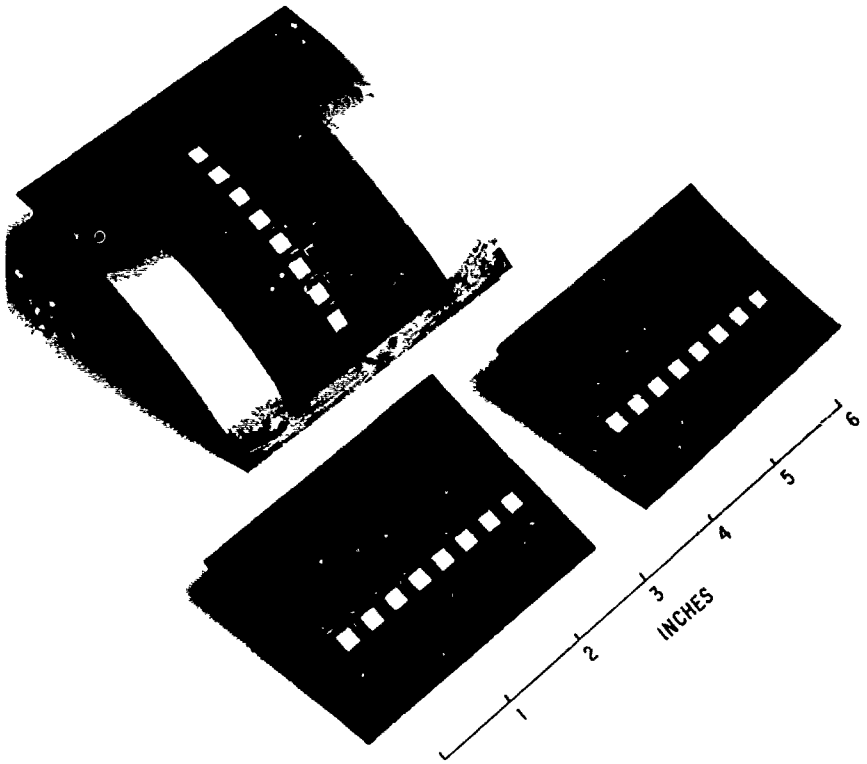

Figure 5-53 Completed Model Antennas

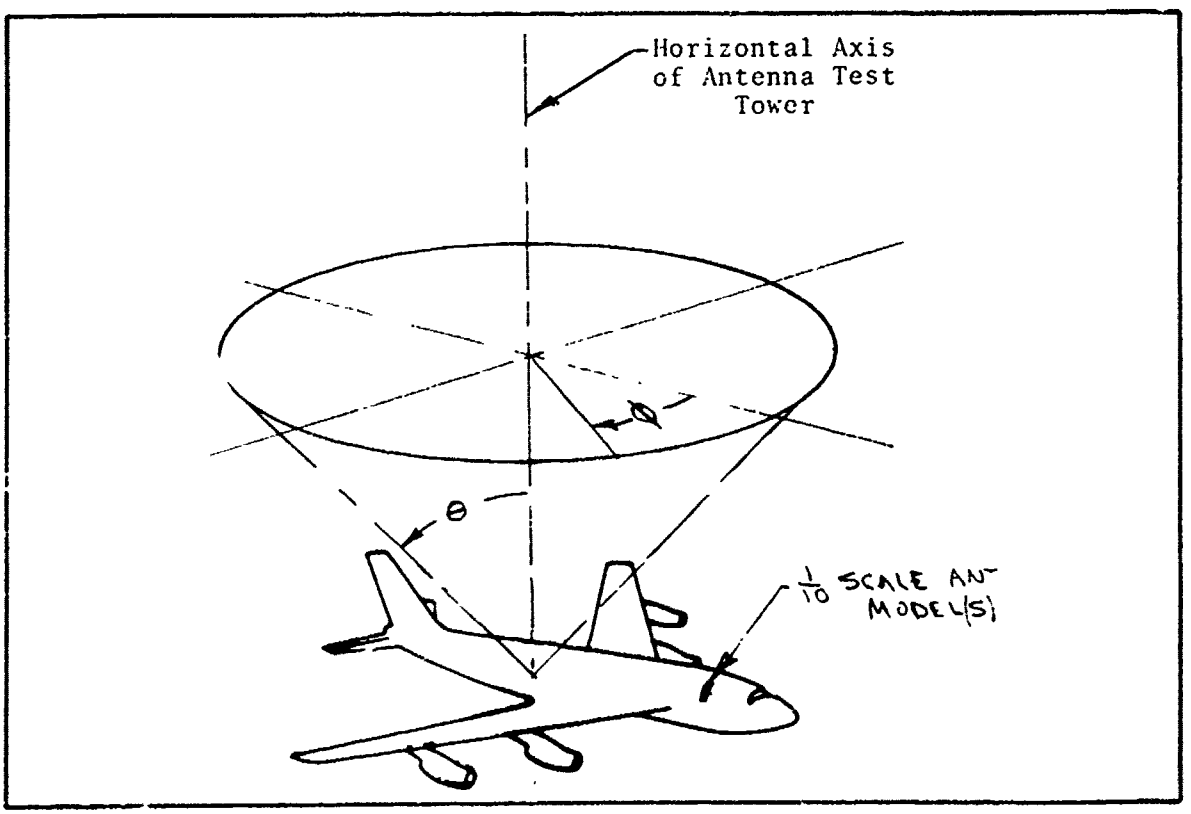

Figure 5-54 Coordinate System - 1/10 Scale Model Aircraft - Pattern Tests

The patterns of the tenth scale antenna on the tenth scale ground plane were not closely matched to the full scale patterns. Time did not permit a good examination of the problem and the results of the scale model work were not conclusive. Figure 5-55 through 5-58 show patterns on the tenth scale airplane compared to the full scale patterns. Since losses at 15 GHz do not scale, the level of the tenth scale aircraft patterns was adjusted for an acceptable comparison level.

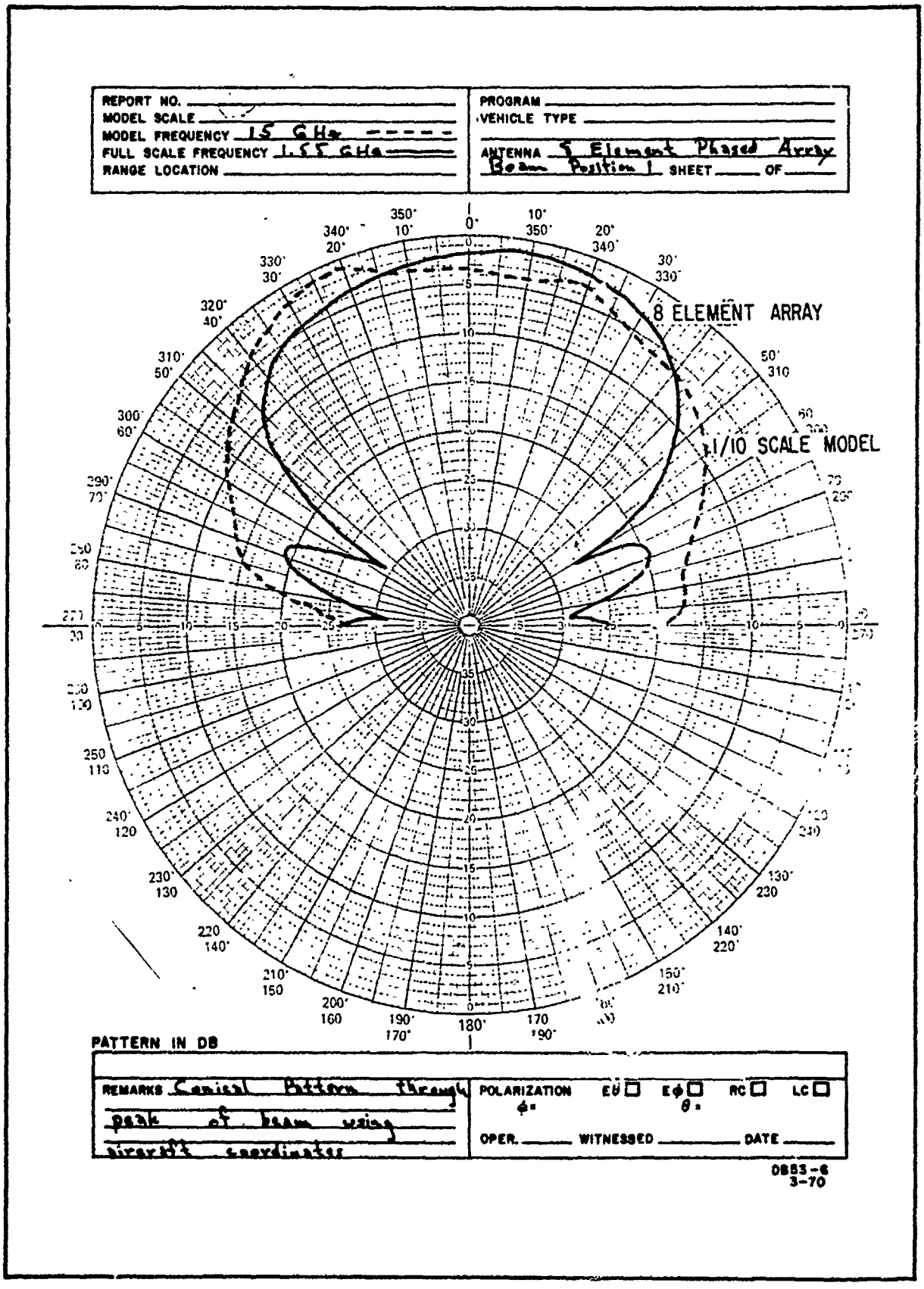

Figure 5-55 Tenth-Scale Model on Model Aircraft and Eight-Element Phased-Array Azimuth Pattern Beam Position 1

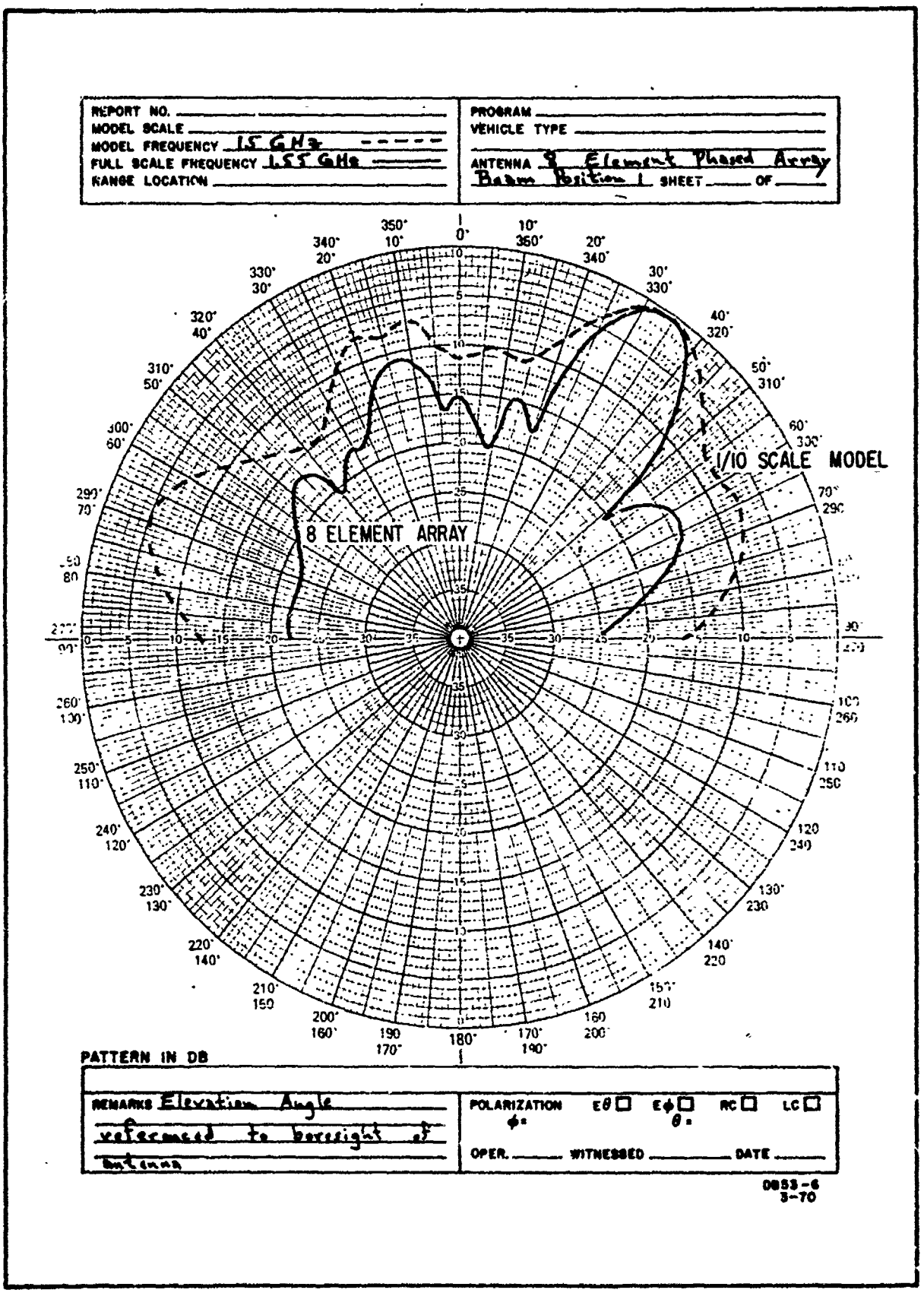

Figure 5-56 Tenth-Scale Model on Model Aircraft and Eight-Element Phased-Array Elevation Pattern Beam Position 1

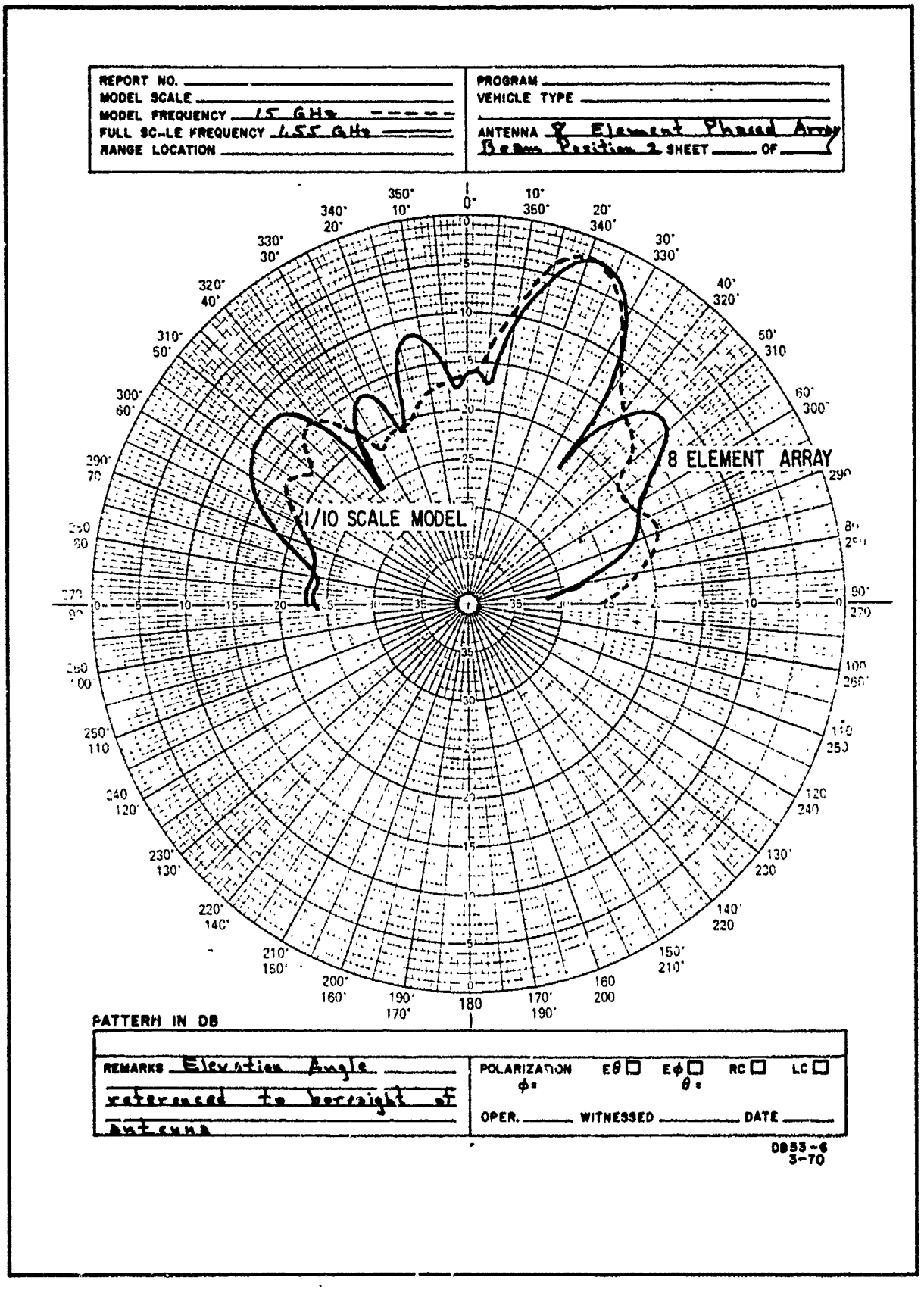

Figure 5-57 Tenth-Scale Model on Model Aircraft and Eight-Element Phased-Array Elevation Pattern Beam Position 2

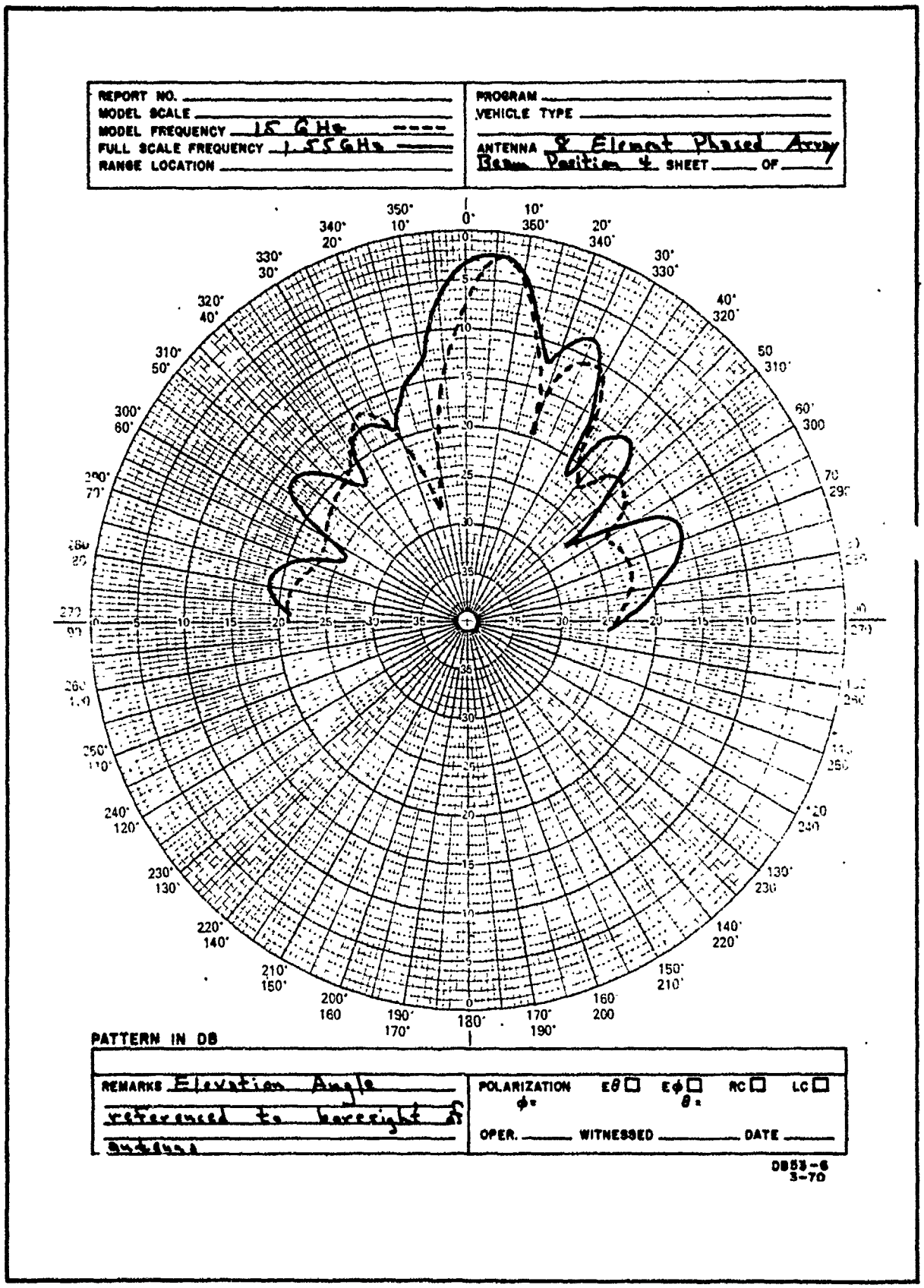

Figure 5-58 Tenth-Scale Model on Model Aircraft and Eight-Element Phased-Array Elevation Pattern Beam Position 4

6. FIELD INSTALLATION

All work involving the FAA test aircraft was coordinated with NAFEC. This included antenna mounting at Oklahoma City and controller installation and final system checkout at NAFEC.

A trip was made to the FAA Aeronautical Center at Oklahoma City, to examine the proposed locations for the antenna and control unit in the aircraft, and confirm the feasibility of the installation. The original location for the steerable array was to have been at Station 390, forward of the cargo door area. This location on the aircraft is at the transition from the constant cross-section to one which has a compound curvature, and it was subsequently decided to move the antenna to Station 410, immediately in front of the cargo door where the cross-section of the aircraft is a constant. Inspection of the aircraft revealed that this location was not practical because of the hydraulic equipment, structural reinforcement, and vent ducts located in that vicinity.

Two other locations were examined which were also not practical. The first was on the opposite side of the airplane at Station 410; this tentative location was eliminated because of the interference with the pressure relief opening in the fuselage. Station at 430 on the right side of the airplane was eliminated because of the presence of fuel tank vent conduits. The most promising location was at Station 450 on the right side of the aircraft.

To enable attachment of the steerable array to the aircraft without the fastening screws interfering with the aircraft stringers, the array angular position was increased from 41 degrees to 41-1/2 degrees above the horizon. The installation drawing for the

antennas was revised and redrawn to reflect the exact location of the aircraft structural elements and confirm the connector locations.

Preparation of the cabling and installation arrangements was accelerated to enable preliminary installation of the antenna cabling and mounting hardware during the second week in June, 1974. Drill templates were prepared for both antennas which enabled positioning the holes accurately, and a cover patch was supplied to simulate the antenna until its actual installation at a later date.

During the period of August 24-28, 1974, antenna installation was conducted in Oklahoma City. The antenna and all its related clamps and cables were put in place on the aircraft. In addition, the antenna electronics control box was set up temporarily and operated. Cabling for the control box was already complete but the equipment racks were not yet mounted. Testing of the controller was conducted in the approximate area in which it would be permanently mounted.

Using the controller to step the antenna through its nine beam positions, preliminary checks were made. A network analyzer was borrowed from the Boeing test crew and the impedances for all beam positions were verified.

During the period of time that the controller was being operated, it persistently blew the fuse in the power line input. It would occur about 50 percent of the time during turn on only. Since final installation was still two weeks away, the controller was returned to BBRC for further checkout.

After returning the controller to BBRC and performing tests to simulate the failure, it was decided that the fuse was blowing because of a transient or noisy power source at Oklahoma City. The power supply manufacturer recommended a "slow-blow" fuse which was then installed.

During the period of September 8-19, 1974, final installation at NAFEC, Atlantic City, N.J., was performed. During installation and checkout, the fuse-blowing problem did not exist, but a problem in the programed sequencing developed. It was traced to a faulty integrated circuit and was corrected. Ventilation in the area provided for the controller was less than expected so a small fan was mounted on the controller itself.

Once the repairs and problems had been corrected, the system was checked from a location outside of the hangar. The aircraft was oriented in such a way that the phased array antenna faced the general direction of the satellite. The received signal strength indicated that the antenna was performing as expected. All signal level data was compared to the Boeing Quad Helix Antenna, since it has a well-known gain level.

A five-hour check flight was flown about 150 miles off the coast of New Jersey. During this flight, the phased array antenna was again compared to the Quad Helix and satisfactory results were obtained. Due to a problem in the Boeing equipment it was not possible during this flight to put the received signal on tape for further analysis.

7. REFERENCES

1. R. E. Munson, "Conformal Microstrip Antennas and Microstrip Phased Arrays", IEEE Transactions on Antennas and Propagation, Vol. AP-22, No. 1, January 1974, pp. 74-78.

2. G. Sanford and L. Klein, "Development and Test of a Conformal Microstrip Airborne Phased Array for Use with the ATS-6 Satellite", IEE Conference Publication No. 128, 1975.

3. G. Sanford, "Conformal Microstrip Phased Array for Aircraft Tests with ATS-6", Proceedings of the National Electronics Conference, Vol. XXIX, 1974, pp. 252-257.

4. "Air Traffic Control Experimentation and Evaluation with the NASA ATS-6 Satellite", ATS-6 Final Report, Vol. VII, Report No. FAA-RD-75-173-7, April 1976.

APPENDIX A

CONFORMAL MICROSTRIP AIRBORNE PHASED-ARRAY TEST

This appendix is an excerpt from "Development and Test of a Conformal Microstrip Airborne Phased Array for Use with the ATS-6 Satellite" G. Sanford and L. Klein, presented at the International Conference for Aircraft and Spacecraft, June 3-5, 1975, in London, England. This paper presents flight test results which were obtained with the antenna mounted on a KC-135 aircraft.

FLIGHT TEST RESULTS

Antenna Configuration on Test Aircraft

Several antenna types were installed aboard the FAA KC-135 aircraft and were tested by the test support contractor, Boeing Commercial Airplane Company, as part of a comprehensive experimental program conducted for the FAA under direction of the Transportation Systems Center. The following antennas were installed and are shown in Figure A-1.

Steerable Quad Helix Array. This mechanically steerable antenna is mounted in the fairings at the junction of the fuselage and vertical stabilizer. The Quad-Helix gain is 15.5 dB at the L-band test frequency, and over much of its range of motion the antenna has negligible interaction with the aircraft structure. It is used as a gain reference for comparison purposes.

Single Element Slot-Dipoles. These elements are mounted in the right and left wing-root fairings and on the zenith line.

Single Element Microstrip Element. This is mounted on the zenith line towards the cockpit, approximately at Station 270, and is used for forward coverage fill.

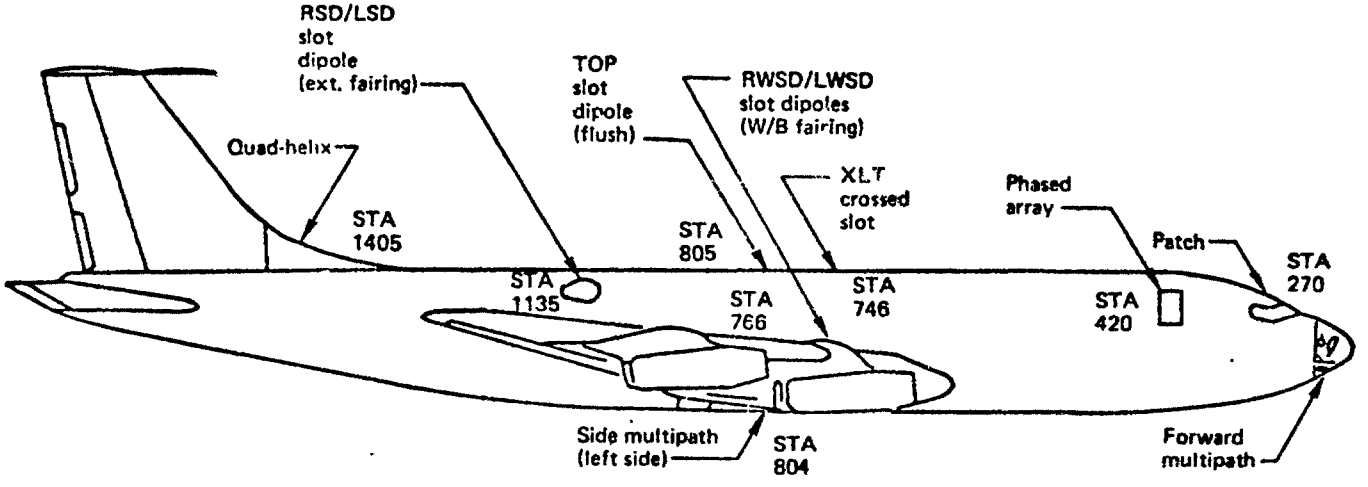

Figure A-1-*KC-135 Antenna Locations*

Eight Element Microstrip Array. The phased array was mounted on the starboard side of the aircraft at approximately Station 420, well forward of the wing. This location minimized antenna interaction with the aircraft structure.

The single elements were tested to gain experience appropriate to experimentation with developmental satellite systems. The microstrip array was tested to gather data about gain, multipath performance and ability of an advanced experimental design to withstand the rigorous environment of the aircraft surface location.

Test Flight Parameters

Test flights took place over the Atlantic in the vicinity of Atlantic City, New Jersey, the Azores and on ferry flights. Data was acquired at elevation angles to the satellite of approximately 10 degrees, 15 degrees and 40 degrees. A summary of planned and completed January 1975 antenna flight tests is shown in Table 1. Weather conditions were responsible for several flight cancellations but data was collected on the runway for one of these by taxiing the aircraft so that the aircraft axis/satellite angle was varied in accordance with the original experiment plan.

Table A-1

JANUARY 1975 ANTENNA FLIGHT TEST SUMMARY

Date	Satellite Elevation Angle	Test Time (Hours) Planned	Completed
1-21	40°	1.9	2.1
1-22	9°	0.5	0.5
1-27	15° to 18°	1.53	1.53
1-29 (1)	11° to 15°	1.53	Zero
11-1 (2)	9°	0.5	Zero
		5.96	4.13

(1) Flight cancelled due to bad weather.
(2) Test cancelled due to fuel reserve consideration.

For a typical flight profile, the aircraft flew seven straight line segments, the seventh segment parallel to the first but in the reverse direction. This flight path was an alternative to a circular path which was found to present difficulties because of aircraft roll during the turn. The substantial roll encountered in fact invalidated some phased array data.

RF Test Configuration

A simplified, typical RF test configuration is shown in Figure A-1. The conformal phased array is connected through a calibrated variable RF attenuator and preamplifier to an L-band receiver designated as the FAA receiver. The Quad Helix and Right Wing Slot Dipole (RWSD) are switch-selectable and connected through a calibrated variable RF attenuator and preamplifier to the NASA PLACE receiver. An additional 10 dB IF pad is used when the Quad Helix is selected, because of its higher gain. Thus, by adjustment of the attenuators, approximately constant signals are fed to the carrier detector unit. A multiplexer switches between the two receiver chains with a three-second switching period. The gains and noise figures of the RF preamplifiers have been calibrated, and the cable losses between antenna inputs and preamplifier inputs have also been accurately determined.

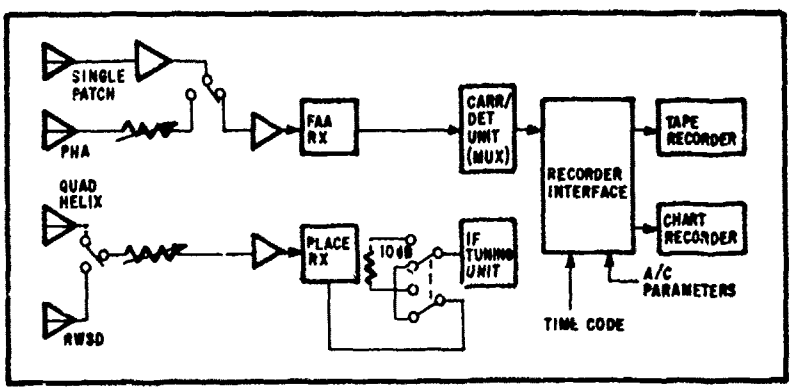

Figure A-2 Simplified Typical R-F Test Configuration

Real Time Measurement Data

Since the gain of the Quad Helix has previously been measured accurately, determination of the gain of the phased array and RWSD antennas is made simply by comparison of received power levels at the carrier detector unit and measurement of the noise spectral density. These are referred to as real-time, manual measurements, as distinguished from computer-analyzed test data. A series of such manual measurements, in addition to automatic large scale data collection for later computer reduction, was taken by the KC-135 experiment crew. A summary of the available data pertinent to the microstrip array, all obtained from the January 1975 test flights, is shown in Table A-2. The data of 21 January was taken by positioning the aircraft on the runway at different headings to the satellite. The aircraft was unable to take off on this date due to weather conditions at Atlantic City. To determine the maximum gain beam position, the antenna beam was switched manually, and the beam with the highest signal strength was used for the measurement. The selected PHA beam is indicated in parenthesis.

The Preliminary results show that the array gain is well maintained at low elevation angles, and also indicate that the azimuth gain (perpendicular to the array axis) falls off faster than the slot-dipole gain.

Computer Analyzed Antenna Data

The real-time, manual measurements described above give no information about side-lobe behavior of the antennas as tested on the aircraft. The side lobe structure of the antenna is important for this application since, along with placement of the antenna on the aircraft, it determines the rejection of oceanic multipath achievable with a given design.

Table A-2

ANTENNA TEST DATA DERIVED FROM REAL-TIME MEASUREMENTS

Date	Satellite Bearing EL (Degrees)	Satellite Bearing AZ (Degrees)	Antenna Tested	Normalized ATS-6 Signal (-dBW)	Antenna Gain (dB) QH	RWSD	PHA
I-21-75	40	16	QH	139.5	15.5		
			RWSD	148.9		6.1	
Runway			PHA (7)	149.6			5.4
		30	QH	138.9	15.5		
			RWSD	147.6		6.8	
			PHA (6)	147.4			7.0
		60	RWSD	147.7		6.7	
			PHA (5)	145.3			9.1
		89	RWSD	145.5		8.9	
			PHA (4)	144.5			9.9
		124	RWSD	145.5		8.9	
			PHA (3)	144.6			9.8
		150	RWSD	148.3		6.1	
			PHA (6)	148.0			6.4
		164	RWSD	149.7		4.7	
			PHA (7)	150.4			4.0
I-22-75	9	90	QH	138.0			
			RWSD	150.2		3.3	
			PHA (1)	142.0			11.5
		45	QH	140.3			
			RWSD	155.0		0.8	
			PHA (2)	145.5			10.3
		135	RWSD	148.0		7.8	
			PHA (3)	148.7			7.1
I-27-75	17	44	QH	143.9	15.5		
			RWSD	152.2		7.2	
			PHA (2)	149.5			9.9
	18	78	QH	136.8	15.5		
			RWSD	148.6		3.7	
			PHA (2)	142.5			9.8
	17	111	RWSD	144.8		7.5	
			PHA (2)	140.7			11.6
	16	145	RWSD	144.8		7.5	
			PHA (3)	144.6			7.7

A measure of this rejection is the signal-to-interference (S/I) ratio. The S/I for a given antenna can be determined by computer analysis of the carrier detector unit output. The method is based on an examination of the spectrum of the received signal. Because the multipath signal is Doppler shifted with respect to the direct path, it is possible to separate their two signals spectrally and estimate the power in each component. The noise density may also be inferred by this method.

Computer-reduced data for the flights of I-22 and 27, 1975, are shown in Table A-3. The data show that the S/I achieved for the phased array and the right wing-root slot dipole is greater than 20 dB for the satellite elevation and bearing angles considered. The gains calculated by the computer method are in good agreement with the real-time measurements for the same test segments. Excellent multipath rejection has been achieved by the phased array without use of the structure of the aircraft for shadowing, and the phased array gain is well maintained at low angles. A complete presentation of data from the ATS-6 flight tests is found in the ATS-6 Final Report (Reference 7-1 Section 7)

Table A-3

COMPUTER ANALYZED ANTENNA TEST DATA

Date	Bearing to ATS-6 EL (Degrees)	Bearing to ATS-6 AZ (Degrees)	Antenna Tested	Normalized ATS-6 Signal (dBW)	Gain (dB)	S/I dB
1-27-75	18	78	RWSD	-148.8	4.0	> 22
			PHA (2)	-143.5	9.3	> 24
			QH	-137.3	15.5	
	17	44	RWSD	-152.7	7.1	> 20
			PHA (2)	-149.8	10.0	> 20
			QH	-144.3	15.5	
1-22-75	9	45	RWSD	-155.8	Zero	> 20
			PHA (2)	-146.0	9.8	> 20
			QH	-140.3	15.5	
	9	90	RWSD	-149.7	4.2	> 20
			PHA (1)	-141.7	12.?	> 20
			QH	-138.4	15.5	

Conclusions

A conformal airborne phased array has been developed which has been successfully tested during the current ATS-6 test series and which has potential as a practical antenna for use in future operational systems. Antenna gain and side lobe performance have been verified by measurements taken on board the test aircraft. Gain and multipath rejection capability are both well maintained at low elevation angles for the side-mounted array. The array has operated over a wide, rapidly changing temperature range during the extensive KC-135 test program with no indication of failure or degradation in electrical performance or mechanical integrity. The practicality of the array antenna for commercial aircraft application is attributed to the use of advanced, low-cost microstrip technology, in which all critical RF components are etched in a single manufacturing step. The microstrip approach to phased array design should prove advantageous in other applications where cost or conformality are important considerations.

APPENDIX B

REPORT OF INVENTIONS

Work performed under this contract has significantly advanced the state-of-the-art in conformal antenna design. A list of accomplishments would include the following:

first microstrip phased array to fly on an aircraft

largest microstrip phased array to date

active circuits designed to function outside of the aircraft skin

completely integrated phased array design.

Nevertheless, a diligent review of the work has revealed no innovation, discovery, improvement or invention, other than those previously patented.